UDC 622

ISSN 2334-8836 (Štampano izdanje)
ISSN 2406-1395 (Online)

Mining and Metallurgy Engineering Bor

3-4/2020

Published by: Mining and Metallurgy Institute Bor

Mining and Metallurgy Engineering Bor

3 - 4/2020

MINING AND METALLURGY ENGINEERING BOR is a journal based on the rich tradition of expert and scientific work from the field of mining, underground and open-pit mining, mineral processing, geology, mineralogy, petrology, geomechanics, metallurgy, materials, technology, as well as related fields of science. Since 2001, published twice a year, and since 2011 four times a year.

Editor-in-chief

Academic Dr Milenko Ljubojev,
Principal Research Fellow
Mining and Metallurgy Institute Bor
Full member of EAS
E-mail: milenko.ljubojev@irmbor.co.rs
Phone: +38130/454-109, 435-164

Editor

Vesna Marjanović, B.Eng.

English Translation

Nevenka Vukašinović, prof.

Technical Editor

Suzana Cvetković

Preprinting

Vesna Simić

Printed in: Grafomedtrade Bor

Circulation: 200 copies

Web site

www.irmbor.co.rs

Journal is financially supported by

The Ministry of Education, Science and Technological Development of the Republic Serbia
Mining and Metallurgy Institute Bor

ISSN 2334-8836 (Printed edition)

ISSN 2406-1395 (Online)

Journal indexing in SCIndex and ISI.

Published by

Mining and Metallurgy Institute Bor
19210 Bor, Zeleni bulevar 35
E-mail: milenko.ljubojev@irmbor.co.rs
Phone: +38130/454-110

Scientific – Technical Cooperation with the Engineering Academy of Serbia

CONTENS

SADRŽAJ

ISSN: 2334-8836 (Štampano izdanje)
ISSN: 2406-1395 (Online)

UDK: 552.3(045)=111
DOI: 10.5937/mmeb2004 001M

Aleksej Milošević, Boško Vuković**, Miodrag Čelebić**

FORMATION ANALYSIS OF MAGLAJCI – MOŠTANICA OPHIOLYTIC ZONES IN THE NORTH OF KOZARA FOR THE USE OF ROCKS IN CONSTRUCTION

Abstract

Based on the field work and laboratory research, the basic geological characteristics of the ophiolitic melange of northern Kozara are presented, with an emphasis on the Maglajci ophiolitic block. Criteria for separations of formations were established and then applied in the analysis, especially those geologically directly recognizable in the field and outcrops, so one ore formation with two ore subformations was separated in the Maglajci block. In the central zone of block, the basalt outflows and diabase are dominant, while in the south of the block it is an outflow basaltic sequence of the ocean floor with the acidic differences of rhyolites and keratophyres. The second subformation also includes the Moštanica and Vojkova Bloc as a whole. The ore bearing formation is evaluated as a medium to low perspective formation, while parts of the Maglajci block with a massive to brecciated outflow are highly perspective terrain. There are rocks of good physical-mechanical characteristics and they meet the most requesting standards for road building. The results of formation analysis have denied a prior prognosis of ore bearing characteristics of this area, because it was thought that the ophiolitic blocks was built almost exclusively of diabase, and that the fields with those blocks are equally and good perspective for researching the deposits of construction stone.

Keywords*: diabase, ophiolitic melange, ore bearing formations, technical-construction stone, Kozara*

1 INTRODUCTION

In the area of northern Kozara the ophiolites are represented by several blocks such as: Trnava, Vojskova, Balj, Mrakodol, Moštanica and Maglajci (Fig. 1). They are an integral part of the ore bearing formation of ophiolites „Ophiolitic melange of the north Kozara", defined according to its dominant member, applying the criterion of paragenetic formation analysis.

Specifically developed parts of the ore formations are the ore subformations. During defining of their specificities follo-wing criteria have been used: level of magma solidification, manner of rock occurrence with different participation, mineralogical and structural - texture characteristics, post-magmatic processes and hydro-thermal alteration, tectonic reshaping, etc.).

When the qualitative - quantitative indicators (basic technical characteristics of rocks and possible application, possibility of exploitation and stone processing, recovery, reserves, etc.) are included to the mentioned geological parameters, possibilities for extraction a wide spectra of subformations and its ranking based on geological and economic significance can be revealed. Criteria and indicators were also used to determine the potentiality of surfaces on which ophiolites appear as rocks used as the technical building stone.

* *Faculty of Mining Prijedor, University in Banja Luka, e –mail: aleksej.milosevic@rf.unibl.org*
** *Mine and TPP Gacko, Industrial zone bb, e –mail:bosko.vukovic@ritegacko.com*

2 OPHIOLITIC MELANGE OF THE NORTH KOZARA (ORE BEARING FORMATION OPHIOLITES)

Unlike the southern area, where the ophiolitic melange (diabase-chert formation) is of Jurassic age [1], northern Kozara includes a similar but younger formation defined as the Cretaceous (tectonic) "ophiolitic melange" or "ophiolitic complex" [2]. The formation consists of a sedimentary matrix and blocks of different composition and dimensions. The more prominent magmatic bodies, most often in a tectonic contact with the surrounding formations, rarely the contacts are the tectonic olistolytic. These larger bodies account for about 80% of the surface distribution of formation [3]. In the northern Kozara, the Trnava and Vojkova blocks are highlighted, then the Moštanica block, Mrakodol block and Maglajci block - the subject of this paper (Fig. 1).

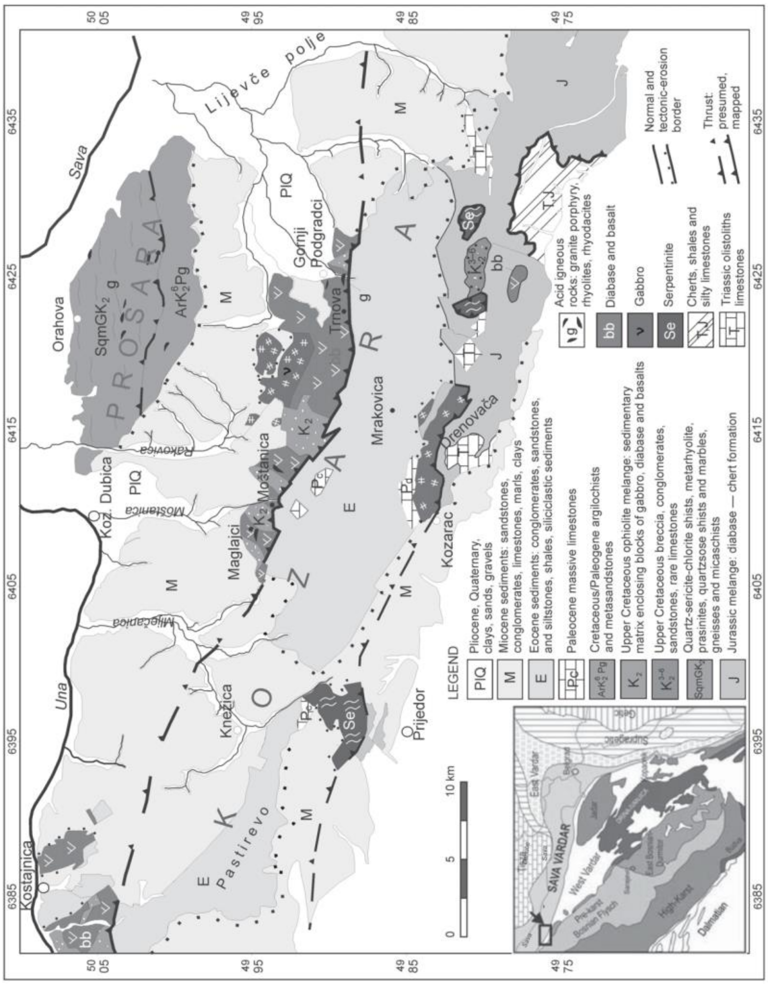

Figure 1 *Geological map of the Kozara compiled from sheets the Basic Geological Map of SFR Yugoslavia, changed and supplemented [2, 9]*

Igneous rocks are represented by gabrro, dolerite and diabase dikes and their systems, then basalts, acidic rock dikes and their volcanics. The variety in mineralogical and chemical composition is the result of bimodal intra-oceanic magmatism. Unlike the southern diabase-chert formation, no ultramafits have been identified here.

It is a typical melange of tectonic origin. It is genetically related to the finite, spatially narrowed substantially narrowed parts of the Dinaric part of Tethys, when the process of its closure or collision begins. Based on the results of research on a "chaotic formation" in the western Serbia and Kosmet [4], considering the similarities in the properties of blocks and time of their occurrence with those in northern Kozara, as well as the fact that they belong to the same regional geological unit the genesis of ophiolitic melange is interpreted partly by tectonic, and partly by olistostromic [2].

The Cretaceous age of these formations was assumed by Pamić and Jelaska [5], based on the limestone fragments with calpionella and globotruncans in the melange, and it has been proven by Grubic et al. recent provisions of globotruncans in red limestones ”Scaglia Rossa“, which were intercalated by pillows – lava [6, 7]. The mentioned biostratigraphic data are in accordance with the U-Pb ages obtained on zircons from the dolerites of the Vojskova block of 81.6 and 81.4 Ma, and also agree well with the K-Ar ages of 79 and 82 Ma, obtained from the "whole rock" dolerite from the Trnova diabase complexes [8].

2.1 Maglajci – Moštanica ophiolitic zone (ophiolitic ore formation)

In the north of Kozara, the creations diabase - basalt - spilite - keratophyre association rocks were selected that build several ophiolitic blocks, out of which the largest is the Vojskova block (Fig. 3). The rocks occur as fresh, altered and fractured - intensely altered in the form of effusions of magma, pillow–lavas and dikes and alternate on short distances. Basaltic effusions are usually solid with little dikes them break through. Basalts rarely contain phenocrysts of plagioclass surrounded by volcanic glass [9]. The formation matrix consists of alevrolites, sandstones, marls and limestones with all transitions between the last two members.

The Maglajci – Moštanica of ophiolitic zone is built by three ophiolite blocks with different geological and petrographic characteristics. Therefore, the magmatic rocks of this zone are also classified into two ore subformations. The first smaller Basaltic effusions of northern Kozara builds the western parts of the Maglajci block, while the other with the most acidic rock differentiators belong to the other igneous rocks.

2.1.1 Basaltic effusions of northern Kozara (ophiolitic ore subformation)

The ophiolitic block Maglajci is located on the northern slopes of Kozara, south of Kozarska Dubica and north of Prijedor. Border of blocks to the south make flysh sediments of the Lower and Middle Eocene represented by conglomerates, sandstones and marls ($E_{1,2}$), and the northern sides are sediments of the terrigenous-carbonate formation of the Lower and Middle Miocene and Sarmatian.

The block is suitable for geological observations on the Maglajci deposit where, on the open profile about 50 m long and about 20 m high diabases, the lava effusions occur, subordinate to wire, and in higher parts dominated by the ellipsoidal pillow bodies (Figs. 2 and 5). During magma cooling, the predisposed sputtering directions are created and a plate-like appearance of the basalt mass is formed. At the base of profile, diabase occurs in a form of massive to brechiated basin effusion (Fig. 4). The rock here is not altered, dark gray to greenish-gray in color. The structure, individual fragments and appearance of the rock resemble pillow–lava, however, with more detailed observations, were found to be the pseudo pillow–lavas. "Chillded margins" occur in them as a result of the rapid lava cooling. The described rock corresponds to the variety “unaltered diabase”, whose thickness on the open profile of deposit ranges from 10 to 12 m.

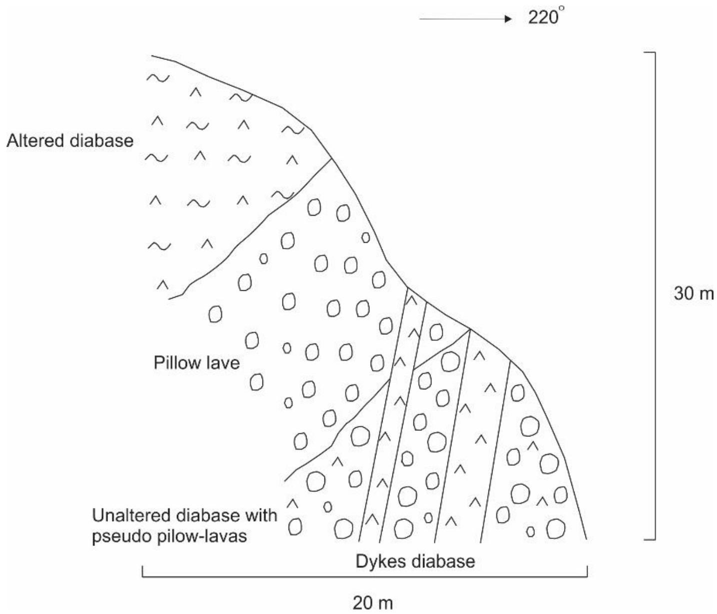

Figure 2 *An open profile on the southern part of the Maglajci ophiolitic block*

The contact of lava, massive diabase from the described open profile zone and pillow–lavas from the upper levels, is marked with a hyaloclastic material. It is a volcanic glass that is finely splashed in contact with water as it forms and easily alters. The thickness of this clearly visible contact zone is 0.5 m. In the southwestern part of profile base, a dike of keratophyre was mapped, representing the impulse of acidic magma through the basaltic effusion (Fig. 3). The rock is light green with a thickness of 0.6 m. Basaltic effusion are mostly brecciated, so they are penetrated by diabases and keratophyres.

In the upper levels, above the massive basaltic effusion lava, pillow–lavas with a diameter of about 30 cm are represented (Fig. 5). These are pillowy and ellipsoidal bodies formed by the rapid cooling of lava in an interaction with water. They are densely arranged and connected by a hyaloclastic matrix which is somewhere solider, when it is silenced. "Chillded margins" and intensely altered crust are observed along their edges. Their interior, unlike the edges, is solider with a rarely seen ophitic structure. The thickness of this zone is up to 7 m. The rock has worse physical-mechanical properties, although some zones look solid.

Although this is a small detected area described relative to the surface of the block western part, however, it can be stated that its geological column generally corresponds to the described local one, which was confirmed by drilling and laboratory testing.

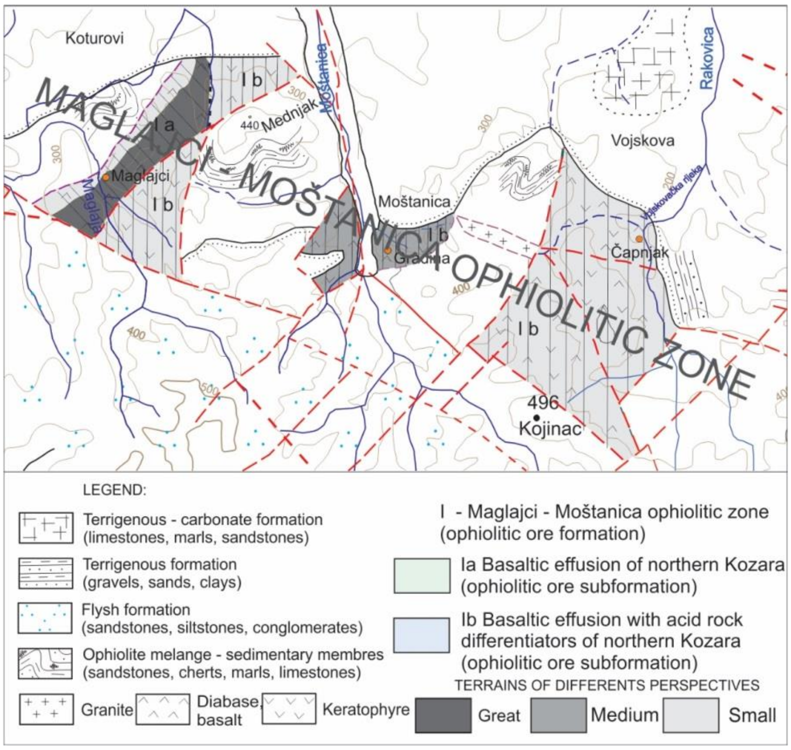

Figure 3 *Formation draft of the Maglajci ophiolitic block*

The rocks of this part of the block and subformation are ophitic and porphyritic structures and of homogeneous and fluid textures, and hypocrystalline and vitrophyric structures are represented. The geological structure of block and structural characteristics of diabase and basalt are closely related to the genesis, that is, to the sudden outflow and cooling of magma in the marine environment, and with exogenous processes related to the crust of decaying diabase masses. So, this is a surface facies of the basic magma, and in the Maglajci block belongs to the volcanic level. Basaltic effusions are massive or brecciated when penetrated by diabases and keratophyres dykes. Massive outflow is not suitable for the process of embossed. Embossed individual dykes, especially acidic ones, not favorably have effect on the quality of rock mass, and thus the potential of ore formations that contain them.

The described creations of the western part of ophiolitic block of the Maglajci are of a great potentiality. They have relatively low distribution and are excavated on the deposit of Maglajci. The highly promising part is primarily marked by a massive to slightly brecciated basaltic outflow. The rocks are unaltered, solid with the good physical and mechanical characteristics: hardness to pressure 151.94 MPa; friction wear "Los Angeles" test (gradation B) 9,2 %; friction wear by the Böhme: 11.01 $cm^3/50\ cm^2$; water absorption 0.65% [10]. The crust of decay is variable and ranges from 14 m to 27 m. The areas of low perspective are classified as the areas of boundary part of the fog block where the diabase is decayed, dilapidated, tectonically processed and hydrothermally altered.

2.1.2 Basaltic effusions with acidic rock differentiators of northern Kozara (ophiolitic ore subformation)

On the southern part of described profile of the block Maglajci, the pillow–lavas are pierced with several diabase polygonal appearance up to 2 m thick. It is not possible to determine exactly whether the dike broke through the entire mass or breakthrough stopped at the observation site. The dike represents a channel through which magma penetrated and was eventually filled with igneous materials. To the south, acidic differentiators dominate - quartz diabase, spilites, and keratophyres (Figs. 3 and 7).

Apart from the southern part of Maglajaci block, subformation belongs to the Moštanica block in which with diabase and basalt represented keratophyres and granites. These are leucocratic rocks of massive texture with a hypidiomorphic granular structure. The most common occurrence of rocks are slabs of different thickness, less than 1 m to several meters. Diabases appear as the rocks of ophitic structure, but porphyritic varieties with large plagioclasses are also significantly represented. There are often mandolas with interspaces filled with the secondary material. The ophiolitic block is of medium perspective with the good qualitative characteristics: hardness to pressure 123.68 MPa; friction wear "Los Angeles" test 19.22 %; friction wear by the Böhme: 10.76 $cm^3/50\ cm^2$; water absorption 0.14%.

The Vojskova block with numerous fault zones, crushing zones, etc. also belongs to the subformation. In these zones, the rocks are the most damaged, with the most of expressed alteration processes. Pillow–lavas have been discovered at multiple sites and build mostly peripheral sections of the block. A sample of basalt-andesite from the northeast part of block was tested for chemical composition on major and trace elements by the ’’whole rock’’ method, as well as determination the absolute age of zirconia from dolerite by the U – Pb method [8]. The obtained age of dolerite on zircons by the U – Pb method is 81.4 Ma and fits well with the paleontological and other radiometric determinations from the entire ore formation. The Vojskova block is of a small prospect, due to a large share of keratophyres in the entire rock mass, and then due to a strong tectonic damage that caused wear and tear and decay. This also resulted in a decrease in hardness to pressure, increased friction wear and water absorption, and poor resistance to frost.

Fig. 4 *Brecciated basaltic effusions of the deposit Maglajci have been pierced by the dyke keratophyres*

Fig. 5 *Pillow–lavas with core and hyaloclastic material of the Maglajci block*

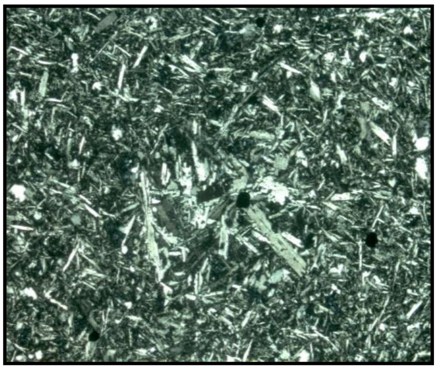

Fig. 6 *Crossing plagioclasses in diabase of the Maglajci block*

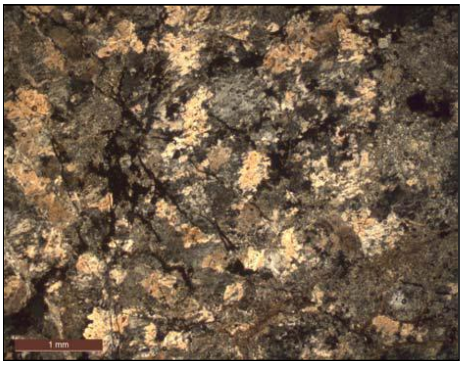

Fig. 7 *Micropiolytic strtucture in rhyolite*

3 CONCLUSIONS

- In the northwest of Bosnia and Herzegovina as a part of the regional tectonic unit "Vardar zone western belt", the ore bearing formation ophiolites ”Ophiolitic Mélange of the north Kozara” is separated. The formation consists of a sedimentary matrix and blocks of different composition, origin and dimensions. The more prominent magmatic bodies, most often in tectonic contact with the surrounding formations.
- Each of the ophiolitic blocks, by itself or with blocks of similar genetic characteristics, represents a certain ore formation of technical building stone. Specifically developed parts of the ore formations are the ore subformations separated based on their geological and petrological parameters. These parameters, along with the qualitative - quantitative indicators, mark potential surfaces for finding the new deposits.
- The Maglajci – Moštanica ophiolitic zone is built by three ophiolitic blocks and two ore subformations with different geological and petrographic characteristics. The first smaller "Basaltic effusions of northern Kozara" builds the western parts of the Maglajci block, while the other "”Basaltic effusions with acidic rock differentiators of northern Kozara” belongs to the other magmatic rocks.
- Basaltic effusions of the Maglajci block represent the ore subformation great prospects for the central parts with highly promising fields for expansion the raw materials, whose central parts are highly potential for expanding the raw material base and finding the new deposits. There are rocks with the good physical-mechanical characteristics, and a wide domain of application in construction.

REFERENCES

[1] Jovanović Č., Magaš N., 1986: Explanatory Book for the Basic Geological Map SFRY 1:100.000, Sheet Kostajnica. Federal Geological Survey, Belgrade.

[2] Grubić A., Milošević A., Cvijić R., (2018): Geology of the Mountains Kozara and Prosara. Monographs, Department of Natural – Mathematical

and Technical Sciences, Book 37. Academy of Sciences and Arts of the Republic of Srpska. Banja Luka, pp. 241.

[3] Milošević, A., (2013): Ophiolitic Mélange of the North Kozara and Schistes Lustres of Prosara (Geology and Minerogeny). Doctoral Dissertation, Natural Mathematics Faculty in Banja Luka. pp. 131. Banja Luka.

[4] Radoičić, R., (1997): On the Chaotic Formation of Rujevac and Veliki Majdan (Western Serbia). Ibid, Book 47, pp. 53–61. Belgrade.

[5] Pamić, J., Jelaska, V., (1975): Occurrences of the Volcano-Sedimentary Creations of the Upper Cretaceous and Ophiolitic Mélange in the North Bosnia and their Importance in the Geological Composition of the Internal Dinarides. Proceedings of the II Annual Scientific Conference JAZU, pp. 109–117. Zagreb.

[6] Grubić, A., Radoičić, R., Knežević, M., Cvijić, R. (2009): Occurrence of the Upper Cretaceous Pelagic Carbonates within the Ophiolite-Related Pillow Basalts in the Mt. Kozara Area of the Vardar Zone Western Belt, Northern Bosnia. Lithos, Vol. 108, Nos. 1–4, pp. 126–130. Elsevier. Amsterdam.

[7] Grubić, A., Ercegovac, M., Cvijić, R. & Milošević, A., (2010): The Age of Ophiolite Melange and Turbidites in the North-Bosnian Zone. Bulletin, CXL, Academie Serbe des Sciences et des Arts, Classe des Sciences Mathematiques et Naturelles, Sciences Naturelles, No. 46, pp. 41–56. Belgrade

[8] Ustaszewski K., Schmidt S. M., Lugović B., Schuster R., Schaltegger U., Bernoulli, D., Hottinger, L., Kounov, A., Fuegenschuh, B. & Schefer, S., (2009): Late Cretaceous Intra-Oceanic Magmatism in the Internal Dinarides (Northern Bosnia and Herzegovina): Implications for the Collision of the Adriatic and Europoean Plate. Lithos, Vol. 108, Nos. 1–4, pp. 106–125. Elsevier. Amsterdam.

[9] Cvetković, V., Šarić, K., Grubić, A., Cvijić, R., Milošević, A., (2014): The Upper Cretaceous Ophiolite of North Kozara – Remnants of an Anomalous Mid-Ocean Ridge Segment of the Neotethys. Geologica Carpathica, Vol. 65, No.2, pp. 117–130. Bratislava.

[10] Milošević, A, (2020): Elaborate on Classification, Categorization and Calculation the Reserves of Technical Building Stone - Diabase on the Maglajci Deposit near Kozarska Dubica. Fund for Professional Documentation of the Faculty of Mining Prijedor.

MINING AND METALLURGY INSTITUTE BOR
UDK: 622

ISSN: 2334-8836 (Štampano izdanje)
ISSN: 2406-1395 (Online)

UDK: 681.325:622.33(045)=111

DOI: 10.5937/mmeb2004009V

Nenad Vušović[*], *Milica Vlahović*[**], *Milenko Ljubojev*[***], *Daniel Kržanović*[***]

STOCHASTIC MODEL AND GIS SPATIAL ANALYSIS OF THE COAL MINE SUBSIDENCE[****]

Abstract

The occurrence of subsidence caused by the underground coal mining may be a complex process that causes damage to the environment. In the last century, there was a significant development in prediction methods for calculating the surface subsidence. In this paper, a new prediction method has been developed to calculate subsidence by combining a stochastic model of the ground movements and Geographical Information System (GIS). All the subsidence calculations are implemented by an original program package MITSOUKO, where the components of the GIS are used to fulfil the spatial analysis. This subsidence prediction technique has been applied to calculate the ground movements resulting from excavating 21 mining panels that are mined successively in the coal mine "Rembas"-Resavica, Serbia. Details of movement were sequentially predicted and simulated in terms of years exploitation. Predictive calculation of the undermined terrain displacement parameters by the stochastic method and integration into the GIS is a powerful risk management tool.

Keywords*: underground coal mining; stochastic prediction method; GIS; spatial analysis*

1 INTRODUCTION

The underground coal mining is accompanied by a ground subsidence which presents a pressing issue and needs attention in order to avoid its harmful effect on the surface and subsurface structures. Therefore, prediction of subsidence using the reliable methods is of a great importance. With the aim to predict subsidence induced by the underground coal mining, the scientists from all parts of the world applied various methods, such as [1]:

Empirical methods are the most numerous group based on the results of systematic measurements in the local conditions of a coal basin. The values of subsidence in the main cross sections by the seam strike and dip were obtained on the basis of type curves. They are the result of approximation and averaging of curves obtained by the measurements or theoretical assumptions. The analytical form of type curves, depending on the author, can vary (Averšin 1950; Kolbenkov 1961; Müller et al. 1965; N.C.B. 1963; Anon 1975; Peng et al. 1981, 1993; Kratzsch 1983; Hood et al. 1983; Kapp 1985; Whittaker and Reddish 1989; Kay 1991; Holla 1997; Holla and Barclay 2000; Seedsman 2001, 2004, 2006; Gale 2008).

[*] *University of Belgrade, Technical Faculty in Bor, Vojske Jugoslavije 12, Bor, Serbia, E-mail: nvusovic@tfbor.bg.ac.rs*

[**] *University of Belgrade, Institute of Chemistry, Technology and Metallurgy, Karnegijeva 4, Belgrade, Serbia*

[***] *Mining and Metallurgy Institute Bor, Zeleni bulevar 35, Bor, Serbia*

[****] *This work was financially supported by the Ministry of Education, Science and Technological Development of the Republic of Serbia (Grant Nos. 451-03-68/2020-14/200131, 451-03-68/2020-14/200026 and 451-03-68/2020-14/200052).*

Profile function methods are based on application the influence function of the elementary excavated volume on the ground surface subsidence. They originate and were mostly applied in Germany, and their authors are: Schmitz 1923; Keinhorst 1925; Bals 1931; Flaschentrager 1938; Perz 1945; Sann 1949; Hoffman 1964; Daemen and Hood 1981; Peng and Chyan 1981; Kumar et al. 1983; Karmis et al. 1984; Alejano et al. 1999; Díez and Álvarez 2000; Torano et al. 2003; Asadi et al. 2004; Zhao et al. 2004; Asadi and Shakhriar 2014.

Influence Function Methods was first proposed by Bals in 1931. In Poland, since 1950 two influence function methods have been developed based on appying distribution of impacts using the Gaussian normal distribution curve (Budyk-Knothe 1953, 2005) as well as method by Kochmansky's (1959) based on the distribution of impacts on a specified derived curve. Using these methods, a subsidence calculation can be performed for horizontal and slightly inclined coal seams (Zenc 1969; Brauner 1973; Marr 1975; Ren et al. 1987; Karmis et al.1990; Lin et al. 1992; Sheorey et al. 2000; Álvarez-Fernández et al. 2005; Luo and Cheng 2009; Luo 2015; Polanin 2015; Nie et al. 2017; Malinowska et al. 2020). *Stochastic Influence Function Methods* start from the assumption that the massif is layered, divided by a series of cracks into a large number of rock blocks whose movements have a random character. The displacement of a rock massif, as the sum of the movements of a large number of clastic elements, obeys the laws of mathematical statistics (Pokrovsky 1929; Litwiniszyn 1957, 1974, 2014; Liu Bao-chen 1965; Pataric and Stojanovic 1994; Vulkov 2001; Meng et al. 2014; Borela 2016; Cai et al. 2016; Malinowska et al. 2020).

Numerical models. Theories of rock mechanics and mathematics are the base of numerical models for subsidence prediction. In mathematical modeling, the mechanisms of rock deformations are approximated to the components that can be definied and quantified since this view means understanding the physical behavior of attacked rocks. A reliable model is formed on the basis of defined mutual interactions of components. Many theoretical studies and mathematical modeling of the underground mining-induced surface deformations are performed applying the methods that rely on numerical models. The most important methods are: the *elastic methods* and *visco-elastic method*. Numerical models include usage of the *finite-element methods-FEM* (e.g. Reddish 1984; Najjar and Zaman 1993; Yin et al. 2008; Migliazza et al. 2009; Zhu et al. 2016; Liu et al. 2017), *boundary element method* and *distinct element method* in predicting the ground subsidence and deformations. In addition, the numerical methods were used for the subsidence modeling and calculating the movement of rock strata (Yao et al. 1989; Alejano et al. 1999; Zhao et al. 2004, Keilich et al. 2006; Shabanimashcool and Li 2012; Zhang and Xia 2013; Unlua et al. 2013; Zhu et al. 2016; Zhang et al. 2017).

Values of in situ rock mass parameters are neccessary for all numerical models. All subsidence phenomena such as the decay of rock, detachment, sliding, and rotation of seam cannot be quantified in laboratory tests or incorporated into numerical models. The reliability of the prognosis depends on the number and degree of approximations of the real conditions that are always involved in the subsidence modeling. Manipulating certain parameters is usually necessary for obtaining a model which approaches the measured subsidence profile results very closely.

The shape and position of subsidence trough in relation to the excavated area depend on the geological and technological conditions of the underground exploitation. For the horizontal coal seams, a subsidence trough is symmetrical in relation to the excavated area, while it becomes asymmetrical for the sloped coal seams.

Surface subsidence due to the underground mining and evaluation the subsidence-induced damages of objects are nowadays growing problems in the Serbian coal mines with the underground exploitation. The sloped seams, with a thickness of 10-20 m at small and medium depths and an extremely steep relief as well as not large population of the mine area, are specific for Serbia. Material costs and psychological responses have forced the underground coal mining companies in Serbia to start resolving these problems by the subsidence prediction methods that minimize damages instead of previous repairing the buildings or compensating their owners.

The stochastic method proposed by the authors Pataric and Stojanovic [2] has been applied for almost four decades in predictive calculations the subsidence at most brown coal mines with the underground exploitation in Serbia. The results of long-term measurements at these mines with different naturally-geological and mining-technological conditions of exploitation indicated a correlation between the elements related to the cause- excavation of the coal seam and elements related to the consequence - subsidence on the ground surface. By comparison the calculated and measured values, it was revealed that using this stochastic method the extent of change on the ground surface can be successfully predicted, thus indicating the expected damage level of objects due to the subsidence above the mining works [3]. This confirmed the possibility of applying the stochastic Pataric-Stojanovic method for a reliable subsidence prediction.

Modern geoinformation technologies provided the use of progressive systems for the management of spatial data with their integration in the Geographic Information System-GIS. By general definition, the GIS represents a "…computerized database management system for capture, storage, retrieval, manipulation, analysis and display of spatial (i.e. locationally defined) data" [4]. Computer-based analytical methods that realistically simulate spatially distributed, time-dependent subsidence processes are desirable for the reliable design of mining layout to minimize the impact of underground excavation on the ground surface. GIS is designed to support the integrative modeling, perform an interactive spatial analysis and comprehend different processes. Furthermore, based on the simulation of complex subsidence processes that are spatially distributed and progressive in time, it is possible to create the innovative thematic maps containing the land-surface properties [5-8]. The stochastic calculation model for the mine subsidence without GIS would be time-consuming and very complicated in cases of a large number of excavation areas [9-12].

The aim of this paper is to present a new approach for subsidence prediction, based on the stochastic Pataric-Stojanovic method with integration into GIS, applied to the exploitation of the "Strmosten" pit in the underground coal mine "Rembas"-Resavica (Serbia) for the period from 2018-2038. The subsidence calculations are implemented by the original program package MITSOUKO, created by professor Vusovic, based on the Pataric- Stojanovic stochastic method. Spatial analysis in GIS is based on the integration of the subsidence prediction results using MITSOUKO software and data processing in the ArcGIS computer program [13].

2 STOCHASTIC METHOD FOR THE MINE SUBSIDENCE PREDICTION

Ground movements, caused by the underground coal mining, are very complex and therefore difficult for modeling due to the complicated behavior of the overlying rock mass and land profiles. In the mid-twentieth century, for the mining-subsidence prediction, several idealized media were used. Since the behavior of overlying strata is complicated due to numerous known and unknown factors that affect and conduct moving of the rock mass, the sto chastic theory of ground moving was used in these models for the mine subsidence prediction [14,15]. Generally, it is easier to predict the definite subsidence than the movements caused by the sequential and complicated mining processes. Therefore, the stochastic theory can be a universal method for the mine-subsidence prediction [16-20].

2.1 The stochastic theory model

The idea of the stochastic theory model was introduced by Pokrovsky (1929) and further was applied and developed by the other authors of stochastic methods [2, 14, 21, 22] . During studying the pressure variation with a depth due to the concentrated force on the surface, Pokrovsky concluded that the pressure change at the horizontal plane can be represented by the standard Gaussian distribution curve. The massif movement, which is a sum of movements a large number of clastic elements, obeys the laws of mathematical statistics. Litwiniszyn (1957) proposed the stochastic subsidence model presuming the ground mass as a discontinuous medium where element movement towards a collapsing cavity is considered as the Markovian process [19]. According to the stochastic theory, moving of the rock mass above the excavated element might happen randomly with a certain likeliness [22]. Numerous solutions of rock movement computing in various geological and mining conditions have been realized based on this stochastic method. This method proved to be effective allowing to find the theoretical solutions to many problems [17]. Liu and Liao (1960) established a stochastic method named the Stochastic Medium Theory Model (SMTM), a profile function based on the statistic medium algorithm method, for prognosis the underground mining-induced surface movement, which is the most commonly used method in China [23]. Nowadays, SMTM is also used for calculating the ground movement caused by a tunnel construction. The Stochastic Medium Theory Model arose into Probability Integral Method-PIM, based on the statistical theory which is more reliable and easier to use for subsidence and deformations prediction in the entire excavation field [24].

2.2 Stochastic method by Pataric and Stojanovic

The Pataric-Stojanovic stochastic method presents a model based on the original mathematical formulas [2]. This method applies the mathematical statistics and starts from the assumption of Litwiniszyn that the massif is a multi-layered, divided by a series of cracks into a large number of elements whose movements have a stochastic character [22]. This environment can be presented by symmetrically arranged elements with the approximately similar dimensions. Such an area does not exist in nature, but this assumption is statistically correct because the pressure change curve in a homogeneous medium is symmetrical and therefore elements in the profile must be symmetrical. Owing to this symmetry, the force got by one element is transmitted and equally divided into two parts on which it relies [25].

If the sides of the excavation panel are $2a$ by the seam strike and $2l$ by the seam dip, the coordinate origin is at the intersection point of the rectangle diagonals, and using the function:

$$\Phi\left(x\right)=\frac{2}{\sqrt{2\pi}}\int_{0}^{x}e^{-\frac{1}{2}t^{2}}dt \tag{1}$$

a definite formula for calculating the *subsidence during horizontal seam excavation* is obtained [2,25].

$$U\left(x,y\right)=U_{0}\cdot X_{0}\left(x\right)\cdot Y_{0}\left(y\right) \tag{2}$$

where:

$$X_0(x)=\frac{1}{2}\cdot\left[\Phi\left(\frac{a+x}{n}\right)+\Phi\left(\frac{a-x}{n}\right)\right]$$

$$Y_0(y)=\frac{1}{2}\cdot\left[\Phi\left(\frac{l+y}{n}\right)+\Phi\left(\frac{l-y}{n}\right)\right]$$

The function Φ from expression represents the standard Gaussian distribution curve.

Equation (2) presents a general case for the subsidence calculation during excavating the horizontal seam of a rectangular area which is illustrated in Figure 1.

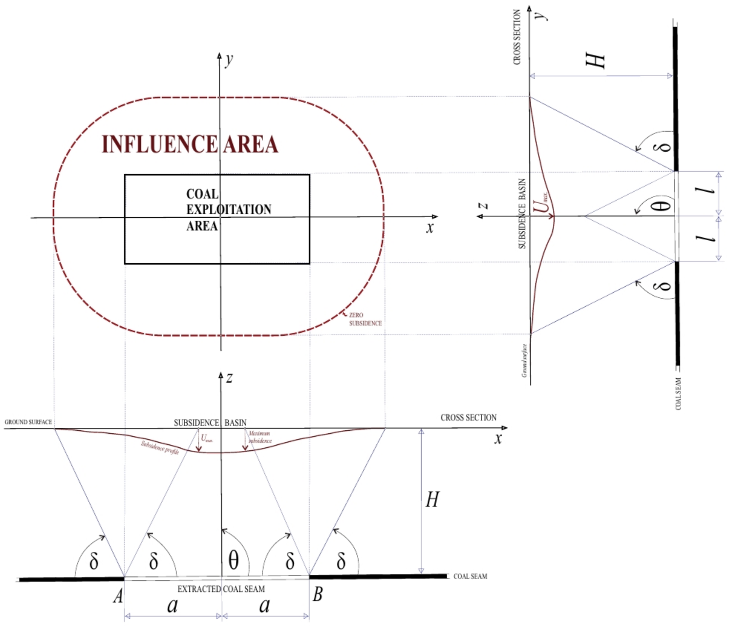

Figure 1 *Subsidence during excavating the horizontal seam of a rectangular area with parameters:* H *- seam depth;* $2a$, $2l$ *- dimension of excavation area;* U_{max} *- maximum subsidence;* δ *-draw angle;* θ *- angle of maximum subsidence.*

Basic formula for calculating the *subsidence during inclined seams excavation* is obtained [2,25]:

$$U(x,y)=U_0\ X(x,y)Y(y), \qquad (3)$$

where:

$$X(x,y)=\frac{1}{2}\left[\Phi\left(p\frac{a+x}{\sqrt{H\cdot ctg\alpha-y}}\right)+\Phi\left(p\frac{a-x}{\sqrt{H\cdot ctg\alpha-y}}\right)\right]$$

$$Y(y)=\frac{1}{2}\left[\Phi\left(q\frac{b+m+y}{\sqrt{H\cdot ctg\alpha-y}}\right)+\Phi\left(q\frac{b-m-y}{\sqrt{H\cdot ctg\alpha-y}}\right)\right]$$

where:

$$p = \frac{p_0}{\sqrt{\sin\alpha}}\,,\ q = (1-\lambda\sin\alpha)Q\,,\ b = \frac{l\cos\alpha}{1-\lambda\sin\alpha}\,,\ m = \frac{H\,\lambda\cos\alpha}{1-\lambda\sin\alpha}$$

The subsidence curve will be the same in any profile by the dip, so it is a plane subsidence:

$$U(y) = U_0\,Y(y) \tag{4}$$

where $Y(y)$ is calculated from the formula (3).

Figure 2 presents subsidence during excavation of the inclined coal seam

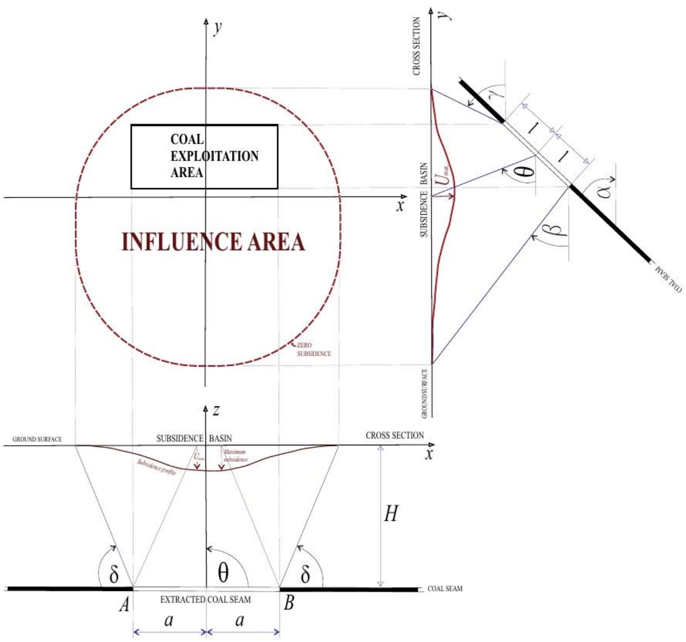

Figure 2 *Subsidence during excavation of the inclined coal seam with parameters δ, β, γ - angles of the draw.*

In the case that $\alpha = 0$, formula (3) is reduced to the basic formula (2) for calculating the subsidence of a horizontal seam [2,25].

3 RESULTS AND DISCUSSION

The problem of subsidence and protecting objects above the mining works has been present for decades in the coal mine "Rembas"-Resavica with an underground exploitation of the "Strmosten" pit. This study presents a predictive calculation of the subsidence based on the stochastic method by Pataric and Stojanovic and GIS model using the input data from this underground coal mine in Serbia [13].

3.1 Characteristic of the research site

The "Rembas" coal mine is engaged in the underground exploration of a high-quality brown coal. It is part of the Public company for the underground coal mining

"Resavica" (JP PEU "Resavica"), the most important center of underground coal mining of the Balkan. Brown coal mine "Rembas" has a tradition of coal mining for more than 150 years (wwwhttp://www.jppeu.rs). Today, the "Rembas" coal mine consists of three production pits: "Jelovac", "Strmosten" and "Senj mine". The "Strmosten" pit as well as its wider environment is formed of rocks with the different lithological composition. The carboniferous Miocene series is inserted between the cretaceous limestones and andesites, which form the paleorelief, and the Permian red sandstones. The Pliocene and Quaternary sediments lie transgressively across the Permian sandstones that represent the coal seam roof. The floor seam consists of clayey sandstones, clays, conglomerates and rarely of marl.

The coal seam thickness (d) is taken from the geological interpretation of the deposit and isolines of the main coal seam; it ranges from 2 to 8 m. The dip of coal seam (α) is determined as the mean value of certain parts of an excavation field, with values in the range of 5-15°. For the predictive calculation of the subsidence parameters, the mean values of the seam dip for each excavation panel (EP) are taken. Seam depths (H) were determined based on the geological interpretation of the deposit with the values ranged from 380-525 m. So far, during the exploitation of the "Strmosten" deposit several excavation methods have been used in order to reach the optimal solutions for very complex and difficult layer conditions. Traditionally, the pillar excavation methods "G" and "V" were used, as well as the longwall mining method with mechanized hydraulic support. Coal deposit reco-very (i) is determined with losses of g = 35%, which corresponds to the projected excavation method and its value is confirmed to i = 65%. Under the given conditions, it can be considered as the highest deposit recovery. The rate of caving (q) is adopted based on the analysis of the previous studying of the displacement process of the undermined rock massif in the "Strmosten" deposit. The value q = 0.70 is accepted [13].

3.2 Software solution for the mine subsidence prediction based on the stochastic method

The prediction of subsidence using the equations of the stochastic Pataric-Stojanovic method is a very complex mathematical calculation considering the accuracy of determining the input parameters, choice of density of the grid of points and interpolation of the subsidence contour lines, which would be a time-consuming in case of manual data processing. Therefore, for internal purposes, the original computer program package with the title MITSOUKO has been created based on the stochastic method proposed by Pataric and Stojanovic.

The MITSOUKO program package enables calculating the process of mine subsidence at any point of the land surface and representating the results owing to possibility of their integration and futher processing in the GIS [25]. It offers the sequential subsidence calculations by simulating the excavation process accor-ding to the adopted dynamics of mining the excavation panels in the excavation field. The MITSOUKO software is designed in the Python v. 3.8 programming language.

The excavation field, with a total area of 29 ha, is composed of 21 excavation panels, which are exploited one by one successively from 2018 to 2038 (Figure 3).

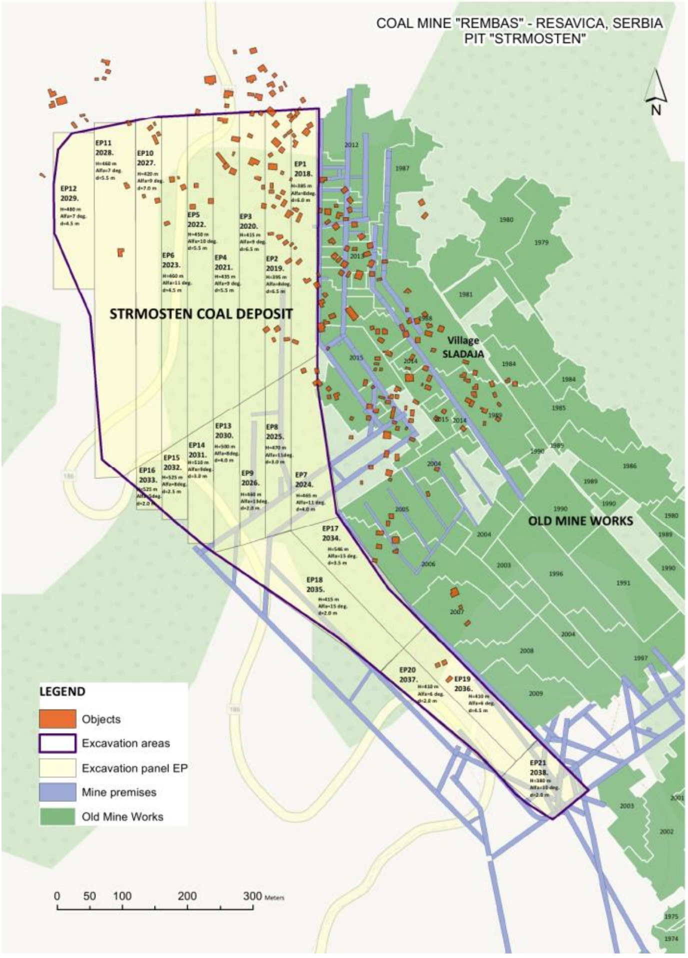

Figure 3 *Excavation panels (EP) mined successively in the excavation field of the "Strmosten" pit [13]*

The MITSOUKO software consists of two modules: PARAMETERS and SUBSIDENCE which represent the individual independent functions and are mutually connected by a hierarchical structure [25]. Names of the modules suggest their functions and purpose in the MITSOUKO program. Each module starts with form according to a textual description explaining its name and function, tags of the input data that are loaded (Read parameters) or computed (Calculate parameters) into a particular module, and data values returned by a module through the control loop.

Firstly, by entering the MITSOUKO program, in the PARAMETERS module, the function (Eq. 1) is initialized, according to the tabular data [26]. Then, through the menu, the data obtained based on geometric characteristics for each excavation panel are entered: ID, dimensions (a, l), seam depth (H), seam thickness (d) and seam dip angle (α). In the next step, in a specified subroutine of the PARAME-

TERS module, the following is calculated for each panel: maximum subsidence (U_0), parameters (m, b, p), rate of caving (q), angles of draw (δ, β, γ), and angle of full subsidence (θ). The local coordinate system is situated symmetrically with respect to the first excavation panel (EP1), with x-axis in a direction of seam strike, y - axis in a direction of seam dip and coordinate origin in the diagonal intersection of this panel. The positions of all excavation panels (x_i, y_i, F_i) are determined with respect to the defined local coordinate system. During the calculation for each excavation panel (EP), it is necessary to rotate its coordinate axes for the value of angle F_i (expressed in degrees) to a direction of axes of the local coordinate system. The calculated parameters, together with the geometric characteristics of each EP and information concerning their positions in the local coordinate system (x_i, y_i, F_i), represent the input data for subsidence calculation in the SUBSIDENCE computational module (Table 1).

Table 1 *Input parameters for subsidence calculation [13]*

[EP]ID	a[m]	l[m]	H[m]	d[m]	Alf[s]	U0[mm]	m[m]	b[m]	p	q	Teta[deg]	xi[m]	yi[m]	Fi[deg]
EP1	20.00	195.00	385.00	6.00	8.00	3151	26.92	197.00	0.73923	0.52316	86.00	0.00	0.00	0.00
EP2	20.00	206.00	395.00	6.50	8.00	3414	27.62	208.00	0.73923	0.52316	86.00	-40.00	-13.50	0.00
EP3	20.00	218.00	415.00	6.50	9.00	3405	29.02	220.70	0.69634	0.49346	86.00	-79.70	-24.80	0.00
EP4	20.00	229.00	435.00	5.50	9.00	2881	30.42	228.69	0.69634	0.49346	86.00	-119.00	-42.00	0.00
EP5	20.00	241.00	450.00	5.50	10.00	2873	39.37	241.00	0.65997	0.46836	86.00	-159.00	-54.00	0.00
EP6	20.00	252.00	460.00	4.50	11.00	2343	40.24	251.58	0.62857	0.44680	86.00	-199.00	-67.00	0.00
EP7	20.00	263.00	465.00	4.00	11.00	3667	29.37	125.83	0.69634	0.49346	86.00	4.50	-284.00	0.00
EP8	32.00	272.00	470.00	3.00	11.00	2895	32.17	118.13	0.79088	0.55907	86.00	-41.00	-339.00	0.00
EP9	31.50	120.00	460.00	2.00	13.00	2369	33.56	112.12	0.79088	0.55907	86.00	-80.00	-359.00	0.00
EP10	28.00	126.00	420.00	7.00	9.00	2083	40.68	262.56	0.62857	0.31888	86.00	-238.50	-81.50	0.00
EP11	23.50	118.00	460.00	5.50	7.00	1562	41.12	271.54	0.62857	0.44680	86.00	-291.00	-92.00	0.00
EP12	23.00	112.00	480.00	4.50	7.00	1034	48.35	119.76	0.57676	0.41150	86.00	-353.00	38.00	0.00
EP13	24.00	105.00	500.00	4.00	8.00	2101	34.96	105.00	0.73923	0.52316	86.00	-120.00	-383.00	0.00
EP14	23.00	87.00	510.00	3.00	9.00	1572	35.66	86.88	0.69634	0.49346	86.00	-161.00	-384.00	0.00
EP15	20.00	57.00	525.00	2.50	8.00	1313	36.71	57.00	0.73923	0.52316	86.00	-200.00	-382.00	0.00
EP16	20.00	36.00	525.00	2.00	5.00	1057	27.51	36.03	0.93692	0.66110	86.00	-242.00	-384.00	0.00
EP17	115.00	30.00	415.00	3.50	15.00	1793	50.96	29.93	0.53537	0.38363	86.00	110.00	-546.00	-46.00
EP18	140.00	40.00	415.00	2.00	15.00	1025	50.96	39.91	0.53537	0.38363	86.00	35.00	-557.00	-46.00
EP19	123.00	23.00	410.00	4.50	6.00	2374	21.49	23.00	0.85481	0.60367	86.00	254.00	-702.00	-46.00
EP20	123.00	21.00	410.00	2.00	6.00	1055	21.49	21.00	0.85481	0.60367	86.00	227.00	-732.00	-46.00
EP21	38.00	53.00	380.00	2.00	10.00	1045	33.25	53.00	0.65997	0.46836	86.00	370.00	-841.00	-136.00

Subsidences are calculated in the SUBSIDENCE module. A certain subroutine allows entering the coordinates of points in a grid of a given density, through the assigned distances between points ($\Delta x, \Delta y$), in the x and y axes directions of the local coordinate system. In this way, it is possible to define the calculation limits for all panels up to a limit subsidence value of 10 mm. Further, the subsidence values after mining each panel are calculated cumulatively, according to the projected mining dynamics of excavation field (Figure 3). The results of predictive subsidence calculation can be exported in tabular form in an Excel file, individually for each excavation panel, which is also the preparation of data for graphical presentation and spatial analysis of these results in GIS.

3.3 Spatial analysis in GIS

Spatial analysis in GIS is based on integration the subsidence prognosis results obtained using the MITSOUKO computer program package and data processing in ArcGIS [13]. The main steps in this integration are: transfer of mining subsidence prediction tabular data from MITSOUKO to GIS, building a geodatabase, spatial data analysis, and combination of maps layers to predict the subsidence [27].

GIS is used for creating a complex geodatabase, converting numerical data, imported from the SUBSIDENCE module, in feature classes and graphical data as well as for performing the spatial analyses of subsidence and deformations [6,7]. Since the "Strmosten" pit consists of multiple EPs with complex geometry, using the stochastic method for spatial analysis of subsidence requires a long time without GIS because for each EP subsidence must be presented cumulatively, assuming all previous and current EP.

Implementing the stochastic method for spatial analyses of subsidence in GIS is performed in two steps [25]:

The first step, **Data module,** involves creating a geodatabase of the "REMBAS" coal mine in ArcCatalog, within the ArcGIS application (ESRI http://www.esri.com/software/arcgis/) with feature classes, tables, and rasters. The feature class is a set of homogeneous spatial attributes in the form of digitized vector data, in the same National Coordinate System (MGI Balkans7). In order to integrate feature classes thematically and spatially into the mine model, within the given excavation panels (EP), feature datasets have been created, in which all types of feature classes are entered. Feature datasets with feature classes related to the spatial geometry: terrain topographies, buildings, mining facilities, old mining works and new exploitation field in "Strmosten" pit, excavation panels with mining dynamics by years, active and old mining premises, and geological interpretation of the coal seam are created in a geodatabase of "Rembas"- Resavica mine. Outside the feature datasets, tables with subsidence, calculations from the SUBSIDENCE module in the MITSOUKO program, rasters for the subject area in the form of orthophoto, geographic maps, situational plans of mine and photographs are imported in the geodatabase. Feature Datasets have been created, in which all types of feature classes are entered. Also, using the ArcMap, an integrated part of the ArcGIS software package, to create layers for displaying feature classes from the ArcCatalog (ESRI) is included. All the tables of the subsidence calculations have been transferred from the geodatabase coal mine to the ArcMap.

The second step, **Subsidence module,** involves using ArcMap, which is an integrated part of the ArcGIS software package, to create layers for displaying feature classes taken from ArcCatalog (ESRI), then editing geometry and attributes of geoobjects, querying spatial data and conducting spatial data analysis (geoprocessing) with a map creation. All tables of the subsidence calculations have been transferred from the geodatabase "REMBAS" coal mine to the ArcMap. Using the Display XY Data command, the selected table of excavation panel, e.g. EP21, which contains the x and y coordinates of the points and calculated subsidence values, is added as a new layer in the Table of Contents. Thereby, a new feature class, EP21_events, was formed, which for this excavation panel EP21 contains 21760 points with values of x and y coordinates and associated subsidences, georeferenced to the adopted coordinate system MGI Balkans7. Following the same procedure, the new feature classes were created for all excavation panels [13].

The created feature classes contain x and y coordinates of all points in the grid 10x10 m with associated subsidence values. All the calculation results can be stored into a GIS point-grid. The Spline interpolation method from the Spatial Analyst Tools palette is then used to create the new layers with contour subsidence lines for each excavation panel (EP1-EP21), by cumulative subsidence transformation from the previous to the new state. This provides a successive following of the subsidence process on the map at all stages of the coal seam excavation in the "Strmosten" pit. The subsidence contour lines are calculated from the maximum values to the adopted limit subsidence value of 10 mm after mining the entire excavation field in the "Strmosten" pit.

The third step involves the transformation of feature clases with subsidence contour lines for each excavation panel determined in the local coordinate system to the global MGI Balkans7 coordinate system in which a mine model of the respective observation field is presented [13].

3.4 Subsidence analysis during mining the excavation panels in the "Strmosten" pit

The stochastic method was used to calculate the mine subsidence values in the MITSOUKO program package. The subsidence contour lines are graphically presented in the ArcGIS software package by interpolation and cumulative transition from the previous to the new state, formed on the data of the seam, and according to the adopted excavation dynamics [7,9]. Based on the predicted subsidence values, the impact of mining works for all EPs was analyzed. With the progress of mining, the subsidence value for each EP is obtained cumulatively, that is, by superimposing the subsidence effects of all previously excavated panels and the actual one.

Figure 4 shows excavations panels (from EP1 to EP20) in the coal mine "Rembas" Resavica - Serbia with the adopted excavation dynamics, subsidence contour lines obtained by simulation the mine subsidence process by the stochastic prediction method and maximum subsi-dence values.

As it can be seen in Figure 4, the predicted maximum subsidence values on the ground surface continuously increase from -1893 mm reached after excavation of EP3 in 2020 to -2927 mm after excavation of EP16 in 2033. Value of -2927 mm remains unchanged with further excavation, ending with EP20 in 2037.

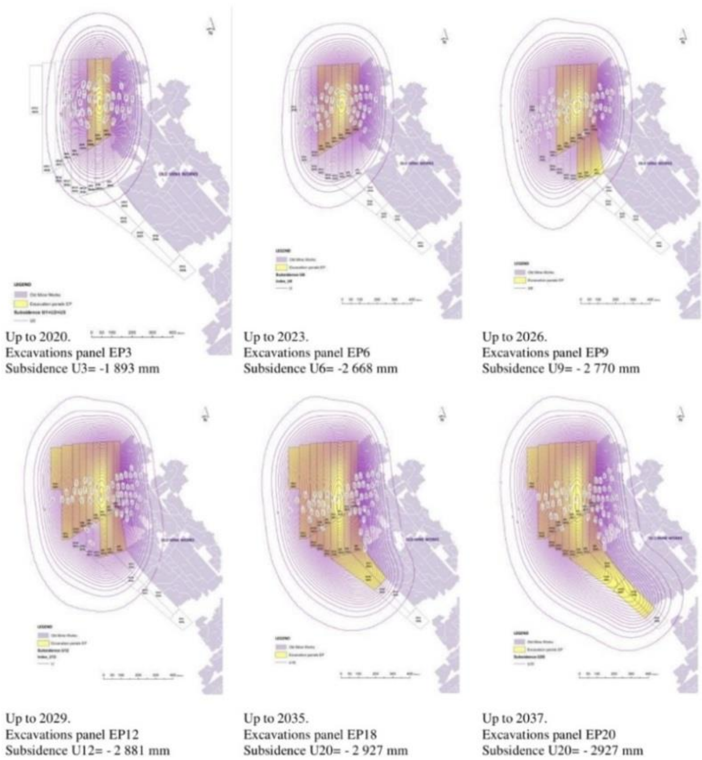

Figure 4 *Simulation of the mine subsidence process in the "Strmosten" pit [*13]

Finally, Figure 5 presents the mining operation plan and predicted subsidence contour lines with the maximum subsidence value (U_{max} = -2927 mm) after mining 21 excavation panels in 2038, that is the entire excavation field in the "Strmosten" pit [13].

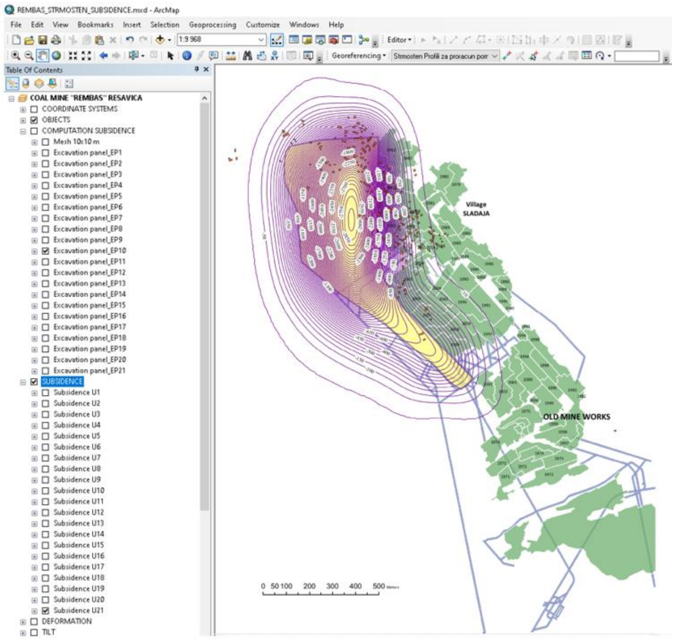

Figure 5 *Subsidence contour lines after mining the entire excavation field in the "Strmosten" pit [13]*

Figure 6 presents a digital elevation model (DEM) of the final mine subsidence, with the maximum subsidence value U_{max} = -2927 mm, in the "Strmosten" pit.

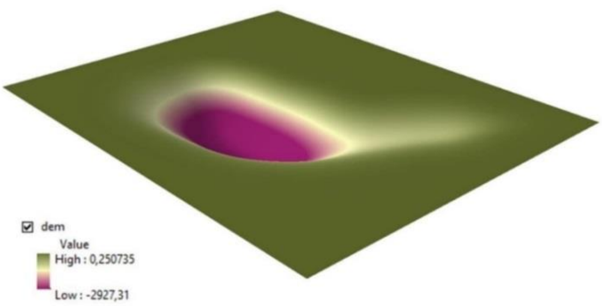

Figure 6 *Digital elevation model (DEM) of the final maximum subsidence in the "Strmosten" pit [13]*

According to the predictive calculations, the maximum relative subsidence was determined as the highest subsidence value (- 2925 mm) after exploitation the excavation panels EP1-EP15. With the progression of mining operations, this value grows towards the value of maximum absolute subsidence. Maximum absolute subsidence, U_{max} =-2927 mm, is the highest subsidence value, achieved after mining EP16, which does not increase with further mining works (EP16-EP21), but a flat-bottomed subsidence trough, collapsed for that value, appears. The shape of subsidence curve on the profile by the seam dip is in a fundibuliform. On the profile by the seam strike, the shape of subsidence curve is infundibuliform, but with a flat bottom in the narrow central part of the curve, formed because several points have the same value of the maximum absolute subsidence, U_{max} = -2927 mm.

3.5 Mine subsidence monitoring

The values of the predicted parameters for the ground surface subsidence should be verified throughout the entire period of coal seam excavation. This requires the systematic geodetic surveying. The main goal of these surveying is to realize the surface subsidence process in space and time during the excavation of the coal seam [28,29].

The basic grid for surveying consists of profile lines arranged in directions of seam dip and seam strike. This grid must satisfy the requirement of long-term subsidence observations, which will last more than twenty years so that the stability of benchmark should not be compromised. Working benchmarks are stabilized in the zone to be affected by the subsidence process and by periodic defining the benchmark position, intensity, and state of the subsidence process for a certain period of time. Figure 7 shows the profile lines I-I and II-II for coal seam strike and coal seam dip with predicted subsidence curves at cross sections [13].

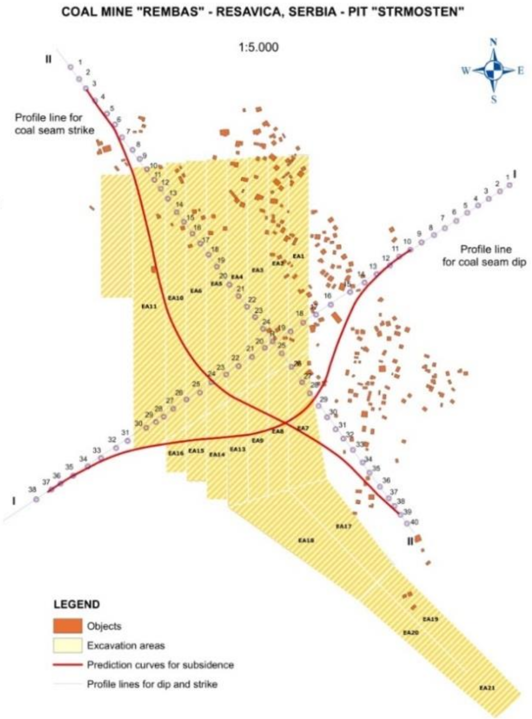

Figure 7 *Profile lines I-I and II-II for dip and strike of the coal seam with the associated predicted subsidence curves in the coal mine "Rembas" Resavica, Serbia* [13]

Geodetic surveying on profile lines gradually follow the general development of subsidence process through the data that define the beginning of displacement, beginning of the intensive displacement phase, intensive displacement phase, completion of this phase and regression phase process.

The extent, type of measurements, field conditions and required accuracy of measurements demand the application of modern geodetic surveying methods and processing of measurement results. Surface movement and deformations in wider areas have been simpler monitored by introducing the airborne, satellite-based remote sensing techniques, GPS and UAV systems (drones). The rapid development of remote sensing techniques such as LiDAR is leading to very high accuracy and cost-effectiveness and therefore more viable option.

The tabular and graphical processing of the measurement results give the values of characteristic displacement parameters: subsidence, horizontal displacement, slope, deformation and radius of curvature. The subsidence trend during time is tracked on charts. There are two types of charts along the profile lines - the first are the subsidence curves while the second are the parameters of displacement process in the form of diagrams of horizontal displacements, diagrams of slope change and diagrams of curvature change which serve to estimate the vulnerability degree of objects [1-3,13,25].

4 CONCLUSION

The stochastic method for the subsidence prediction and analysis of spatial data in GIS enable the calculation and presentation the subsidence on the surface of undermined terrain at any point in the grid with a large number of numerical data which require a long time of processing and interpretation of the obtained results by the standard data processing method. The answer to the set task lies in the MITSOUKO program package, intended for the predictive subsidence calculation according to the stochastic method, which allows user to process a large amount of data, thus excluding the time factor, and the obtained numerical data can be quickly and easily graphically processed and displayed in GIS.

The calculation of subsidence by the stochastic method Pataric- Stojanovic and integration with GIS is a powerful and reliable tool for predicting the subsidence and monitoring the impact of underground mining works on the land surface. This work presents an important research study, actual and significant for the mining profession and practice.

REFERENCES

[1] Djordjevic D., Vusovic N., Prognosis of the Displacement and Deformation of the Underground Terrain, University of Belgrade-Faculty of Mining and Geology, Belgrade, 2014.

[2] Pataric M., Stojanovic A., Moving the Underground Terrain and Protecting Objects from Mining Works. University of Belgrade - Faculty of Mining and Geology, Belgrade, 1994.

[3] Diyab RT., Comparative Analysis of Predicted and Measured Values of Displacement and Deformation of Undermined Terrain at Coal Mines in Serbia. Dissertation, University of Belgrade - Faculty of Mining and Geology, Belgrade, 2011.

[4] Burrough PA., McDonnel RA., Principles of Geographical Information Systems. 2nd ed. Oxford, London, 2006.

[5] McDonald J., Evaluating Mine Subsidence Using a GIS Software Application, Conference: Digital Mapping Techniques'10,-Workshop Proceedings, Sacramento, California, 2010.

[6] Cao J., Ma F., Guo J., Lu R., Liu G., Assessment of Mining-Related Seabed Subsidence Using GIS Spatial Regre-ssion Methods: a Case Study of the Sanshandao Gold Mine (Laizhou, Shandong Province, China). Environ-mental Earth Sciences 78 (2019) 25-35.

[7] Cai Y., Jiang Y., Liu B., Djamaluddin I., Computational Implementation of a GIS Developed Tool for Prediction of Dynamic Ground Movement and Deformation due to Underground Extraction Sequence, International Journal of Coal Science & Technology 3(4) (2016) 379–398.

[8] Trofymchuk O., Anpilova Y., Yakovliev Y., Zinkiv I., Ground Deformation Mapping of Solotvyno Mine Area Using Radar Data and GIS, European Association of Geoscientists & Engineers, Conference Proceedings, Geoinformatics: Theoretical and Applied Aspects (2020), pg.1-5 - https://doi.org/10.3997/2214-4609. 2020geo138

[9] Esaki T., Djamaluddin I., Mitani Y., A GIS-based Prediction Method to Evaluate Subsidence - Induced Damage from Coal Mining Beneath a Reservoir Kyushu, Japan, Q J Eng Geol Hydroge 41(3) (2008) 381-392.

[10] Esaki T., Zhou G., Djamaluddin I., Development of GIS-based Rigorous Subsidence Prediction System for Protecting Surface Environment, Environmental Rock Engineering, Saito & Murata (eds) Swets & Zeitlinger, Lisse, 2003.

[11] Miao F., Mingxing Y., Xiaoying Q., Chengming Y., Baocun W., Rui L., Chen J., Application of DInSAR and GIS for Underground Mine Subsi-dence Monitoring, The International Archives of the Photogrammetry, Remote Sensing and Spatial Information Sciences. Vol. XXXVII. Part B1. Beijing, 2008.

[12] Unlua T., Akcinb H., Yilmaza O., An Integrated Approach for the Prediction of Subsidence for Coal Mining Basins, Engineering Geology 166 (2013)186-203.

[13] Vusovic N., Technical Mining Project for Determining the Parameters of Displacement of Undermined Terrain and Protection of Sladaja Village Objects from the Influence of Underground Mining Works Above the "Strmosten" Pit at RMU "Rembas" Resavica, University of Belgrade-Technical Faculty in Bor, Bor, 2018.

[14] Liu B., Liao G., Basic Regulars of Coal Mine Subsidence, China Industry Press, Beijing, China, 1965.

[15] Kratzsch H., Mining Subsidence Engineering, Springer-Verlag, Berlin, Germany, 1983.

[16] Vulkov M., About the Generalisation Possibilities in a New Stochstical Model of Mining Subsidence, 50 Years University of Mining and Geology “St. Ivan Rilski” Annual, Vol. 46, Part II, Mining and Mineral Processing, Sofia, 2003, pp.153-154

[17] Djamaluddin I., Mitani Y., Esaki T., Evaluation of Ground Movement and Damage to Structures from Chinese Coal Mining Using a New GIS Coupling Model, International Journal of Rock Mechanics and Mining Sciences 48(3) (2011) 380-393.

[18] Blachowski J., Application of GIS Spatial Regression Methods in Assessment of Land Subsidence in Complicated Mining Conditions: Case Study of the Walbrzych Coal Mine (SW Poland). Nat Hazards 84 (2016) 997-1014.

[19] Borela VR., Stochastic Modeling and DEM Simulation of Granular Media Subsidence due to Underground Activity, Master Thesis, Purdue University, West Lafayette, Indiana, 2016.

[20] Malinowska A., Hejmanowski R., Dai H., Ground Movements Modeling Applying Adjusted Influence Function, International Journal of Mining Science and Technology 30(2) (2020) 243–249.

[21] Knothe S., Equation of the Subsidence Profile. Archives of Mining and Metallurgy 1 (1953) 22–38.

[22] Litwiniszyn J., The theories and Model Research of Movement of Ground Masses. In: Proceedings of the European Congress on Ground Movement. University of Leeds, 1957, pp. 202–209.

[23] Liu B., Theory of Stochastic Medium and its Application in Surface Subsidence Due to Excavation, Transactions of Nonferrous Metals Society of China, 2(3) (1992)

[24] Li P., Yan L.,Yao D., Study of Tunnel Damage Caused by Underground Mining Deformation: Calculation, Analysis, and Reinforcement, Advances in Civil Engineering Vol. 2019, pp.1-18.

[25] Vusovic N., Vlahovic M., Ljubojev M., Vlahovic M., Krzanovic D., Software Solution for Mine Subsidence Prediction Based on the Stochastic Method Integrated with GIS, Mining and Metallurgy Institute Bor. No. 1 (2020)

[26] Djordjevic D., Vusovic N., Ganic A., Svrkota I., Angular Parameters of Undermined Ground Movement Process in Unknown Areas, University of Belgrade, Faculty of Mining and Geology, Belgrade Underground Mining Engineering 19 (2011) 125-136.

[27] Banerjee TK., Roy S., Dey S., A GIS Solution for an Integrated Underground Coal Mine Management: A Conceptual Framework, Journal of Management Policies and Practices 2(2) (2014) 129-143.

[28] Cui X., Wang JA., Liu Y., Prediction of Progressive Surface Subsidence Above Longwall Coal Mining Using a Time Function, International Journal of Rock Mechanics and Mining Sciences 38(7) (2001) 1057-1063.

[29] Malinowska A., Hejmanowski R., Evaluation of Reliability of Subsidence Prediction Based on Spatial Statistical Analysis. Int J Rock Mech Min Sci 46 (2009) 432–438.

MINING AND METALLURGY INSTITUTE BOR
UDK: 622

ISSN: 2334-8836 (Štampano izdanje)
ISSN: 2406-1395 (Online)

UDK: 622.33:621.879(045)=111

DOI: 10.5937/mmeb2004025B

Uglješa Bugarić[*], Miloš Tanasijević[**], Miljan Gomilanović[***], Andrija Petrović[*], Miloš Ilić[***]

ANALYTICAL DETERMINATION OF THE AVAILABILITY OF A ROTARY EXCAVATOR AS A PART OF COAL MINING SYSTEM - CASE STUDY: ROTARY EXCAVATOR SchRs 800.15/1.5 OF THE DRMNO OPEN PIT[****]

Abstract

Rotary excavators as the basic machines at the open pits of lignite operate in very difficult working conditions, where they are constantly expected to be highly productive, reliable, available and safe as the production carriers. Determining the availability as well as the duration and number of failures using the analytical methods allows to analyze the key influencing factors on their occurrence and values of these parameters and to determine the essential elements of system maintenance and management in order to optimize them.

Keywords: *rotary excavator, reliability, convenience of maintenance, availability*

1 INTRODUCTION

Coal is the basic energy fuel in electricity production. Rotary excavators are used to excavate coal at the open pits of the Electric Power Industry of Serbia. Coal exploitation in the Kostolac basin began in 1870. The open pit "Drmno" is the only active mine in the Kostolac basin. The open pit "Drmno" produces 25% of coal (lignite) in Serbia.

A growth of capacity on coal from the current $9x10^6$ to $12x10^6$ t/year and overburden from $40x10^6$ to the maximum $55x10^6$ m^3/year is designed at the open pit "Drmno". Coal mining takes place with two BTD systems with one export conveyor, with occasional engagement of dragline excavator as necessary auxiliary equipment. The mined coal from both systems is transported by a groupage conveyor to the distribution bunker and further to the crushing plant, landfill and thermal power plant. The BTD systems are systems that consist of the following elements: a rotary excavator, series of conveyors and crushing plant. These systems are connected in a series connection as it can be seen in Figure 1. If one element of the BTD system fails, the entire system stops working.

[*] *University of Belgrade, Faculty of Mechanical Engineering, Belgrade*
[**] *University of Belgrade, Faculty of Mining and Geology, Belgrade*
[***] *Mining and Metallurgy Institute Bor*
[****] *This work is financially supported by the Ministry of Education, Science and Technological Development of the Republic of Serbia, Agreement on the realization and financing of scientific research work in 2020 for the Mining and Metallurgy Institute Bor, no. 451-03-68 / 2020-14 / 200052.*

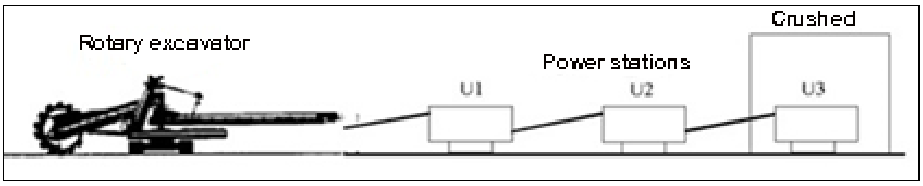

Figure 1 *Overview of the BTD system (rotary excavator-conveyor-crusher)*

Equipment on the BTD systems:
I BTD system:
- excavator SchRs 800.15/1,5;
- excavator SRs 400.14/1;
- 2 self-propelled conveyors BRs 2400;
- 2 level conveyors, width 1800 mm.

II BTD system:
- excavator ERs 710.17,5/13-16;
- excavator SRs 400.14/1;
- self-propelled conveyor BRs 2400;
- self-propelled conveyor BRs 1400;
- conveyor, width 1400 mm;
- conveyor, width 1800 mm. [5]

Figure 2 *View of the I BTD system at the open pit "Drmno"*

This paper presents an analytical determination of the reliability and availability of the SchRs 800.15/1.5 rotary excavator based on the collected data related to delays (mechanical, electrical and other delays) on the I BTD system of the open pit "Drmno".

1.1 Characteristics of an excavator

The SchRs 800.15/1.5 rotary excavator works within the I BTD system. The manufacturer of this rotary excavator is the German company O&K. The excavator was purchased in 1995.

A rotary excavator is in itself a very complex machine system. Like any system, it is composed of a number of subsystems:

1. Excavation subsystem
2. Subsystem for excavator movement
3. Receiving conveyor subsystem
4. Storage conveyor subsystem
5. Subsystem for rotating the upper structure [4]

According to the German classification, the rotary excavators are divided into classes A (compact excavator), B (C frame excavator) and C (giant excavator) according to the basic construction characteristics. [3]

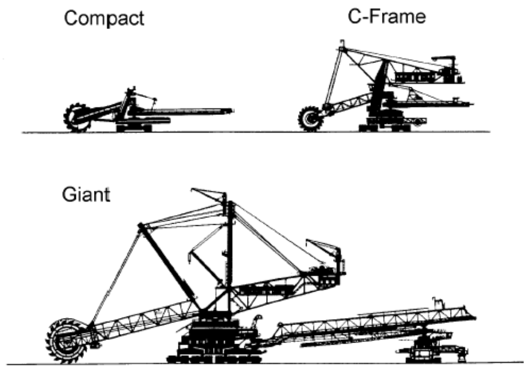

Figure 3 *Types of rotary excavators* [3]

This excavator belongs to a group of compact rotary excavators. Compact excavators have a relatively short boom in relation to a diameter of the working wheel. [3] The advantages of compact rotary excavators are primarily in their low weight; therefore, they have a lower purchase price and are characterized by the outstanding maneuverability. The disadvantages are reflected in the lower coefficient of utilization, high load of a ball and frequent damage to the supporting structure. The basic technical characteristics of the SchRs 800.15/1.5 rotary excavator are given in Table 1. In general, the operation technology of rotary excavators, including this specific one, depends on three basic factors: technological characteristics, geomechanical properties of the excavated material and deposit conditions. The basic technology of SchRs 800.15/1.5 excavator operation is work in a height block (height work in a block with vertical cuts, excavation the entire block height in several cuts). The maximum floor height is up to 15 m.

Figure 4 *Rotary excavator SchRs 800.15/.5 in operation*

Table 1 *Basic technical characteristics of the rotary excavator SchRs 800.15/15 [5]*

Theoretical capacity (m^3/h)	3024
Guaranteed capacity (m^3/h)	1350
Impeller diameter (m)	9.1
Installed drive power RT (kW)	800
Specific excavation force (N/cm)	1200
Nominal bucket volume (m^3)	0.8
Number of buckets	14
Number of bucket shakes (1/min)	79
Excavation height (m)	15
Excavation depth (m)	1.2
Boom length RT (m)	14.5
Unloading belt length (m)	25.5
Height of the boom suspension point RT (m)	8.3
Suspension point distance from the vertical rotary axis of the excavator (m)	1.2
Boom angle RT (°)	19.5/15.5
Excavator weight in operation (t)	560

The rotary excavator works in very difficult conditions, where a high productivity, reliability, availability and safety at work are constantly expected from it as a carrier of production. The effects of operation the mining machines depend on the reliability, their functioning, technical and technological performance, handling, maintenance, logistical support, adaptability-compliance of the relationship between the performance of machines and characteristics of the working environment. [2]

Reliability of systems with series connected elements. Basic terms. Availability

Reliability is the probability with a certain level of confidence that the system, machine will successfully perform the function for which it is intended, without failure and within defined performance limits, taking into account the previous time of the system use, during the given time of task duration. [1]

The reliability of a system of n series-connected elements is equal to the product of reliability of all these elements. [1].

$$R = R_1 \cdot R_2 \cdot R_3 \cdot \dots R_n$$

where: R_1, R_2,... R_n - reliability of system elements. [1]

Structure of a system with a series connection of elements is the simplest model of the system.

When there is a large amount of data on failures of system elements, as is the case in this paper, there is a possibility to determine the theoretical distribution of failure probability and repair of system elements.

If the system has N series-connected elements with different constant failure intensities $\lambda_1, \lambda_2, \dots, \lambda_n$, with exponential distribution of element operating time to failure, then the distribution of system operating time to system failure is also exponential, with intensity $\lambda = \lambda_1 + \lambda_2 + \dots + \lambda_n$. [1]

One of the most important indicators of reliability is the intensity of failure. In a large number of technical systems, the change in failure rate over time appears as in Figure 5. [7]

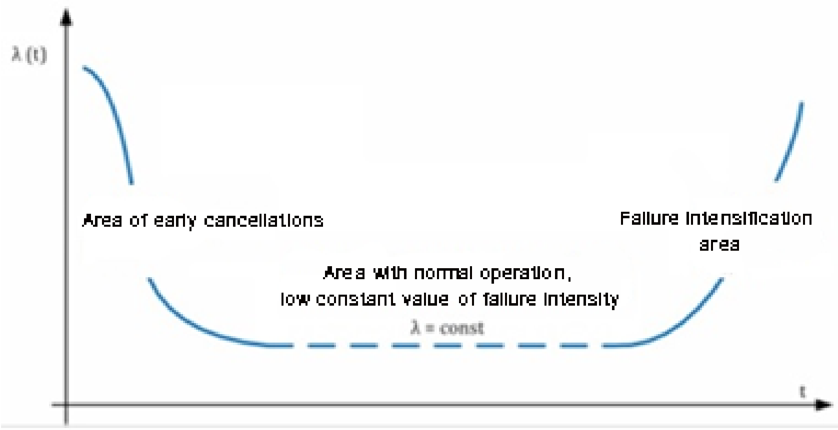

Figure 5 *Function of failure interval density [7]*

The curve in Figure 5, the so-called Bathtube curve, shows 3 areas in the lifetime of the technical system:

1. Area of early failures
2. Area with normal operation (period of exploitation) - constant failure rate,
3. Area of failure intensification of failures - end of lifetime, [7]

Maintenance convenience function

In order for the machine (rotary excavator) to meet the high requirements when it comes to reliability, availability and safety in operation, it is necessary to perform a maintenance process. Convenience of maintenance is a very important feature of the machine. It is a feature of an element or system that the maintenance measures can easily prevent, detect or eliminate faults and malfunctions. [1].

The more complex the machine, the harder it is to detect failures. A large percentage of maintenance time is taken up by a fault finding and thus increases maintenance costs and production losses.

The maintenance function is defined as the distribution of time that the machine (technical system) spends "in failure".

Determining the availability makes it possible to optimize the maintenance function, identify the important parameters that affect the maintenance function and represent the basic indicators of the production system efficiency.

The availability of technical systems

The availability is calculated based on a time state picture, in which the times when the system in a good condition, the "up-time" state, is changed with the times when the system is out of order, the "down-time" state). The time picture of the state can be shown in Figure 6. The time when the system is in a good condition can be divided into an inactive time, i.e. the time while the system is waiting for work (stand-by) (t_{11}) and the time when the system is working (t_{12}). The time when the system is in failure is divided into: organizational time (t_{21}), logistic time (t_{22}) and active repair time (t_{23}) which can be the time for corrective repairs (t_{231}) and time for preventive repairs (t_{232}). [6]

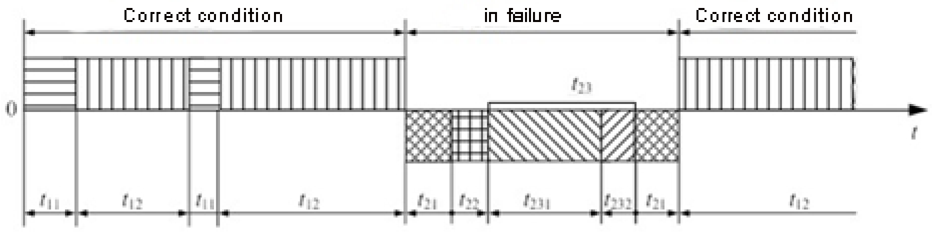

Figure 6 *Time image condition* [6]

The availability is determined as the quotient of the total time during which the system is in a good condition and the total time that makes the time in a good condition and time in failure (Operational availability). [6]

$$A(t) = \frac{\sum t_{11}, t_{12}}{\sum t_{11}, t_{12}, t_{21}, t_{22} t_{231}, t_{232}} \quad [6]$$

2 DATA STRUCTURE OF FAILURE. STATISTICAL PROCESSING OF FAILURE DATA

There is no machine (rotary excavator) that works without failure. Failures on rotary excavators have negative production and economic effects, and the goal of maintenance and operation function is to minimize these negative consequences.

A failure or malfunction is the cessation of an element ability to perform its function. There is a complete (stoppage of the machine operation) and partial failure (the machine operates but with worsened characterristics). [1]

Based on the data obtained from Elektroprivreda Srbije, which also includes the open pit "Drmno", databases related to the mechanical (damage to the superstructure bearings, cracking of caterpillars, tooth replacement, etc.), electrical (cable breakdown, TT connection interruption, interruption of blockage, etc.) were formed as well as the other failures (overhaul, service, conditional stop due to the bad weather conditions, etc.) of the SchRs 800.15/1.5 rotary excavator for a period of 3 years (2016, 2017 and 2018).

Figure 7 shows the layout of one of database. In each cancellation database there is a column in which the date, the object on which the failure occurred (delay), the beginning of delay, the end of delay and the total time in delay.

Determining the affiliation of sample to the theoretical distribution can be done by applying the χ^2 - test, i.e. the agreement of empirical function $F^*(x)$ with the assumed theoretical distribution function $F(x)$ is checked. [8]

The Hi-square test was used to determine whether there was a significant difference between the expected frequency distributions and observed frequency distributions in one or more data categories.

Table 2 shows the results of applying the χ^2 - test.

	A	B	C	D	E	F	G	H	I	J
1										
2	Datum	Mesec	Godina	Sistem	Objekat	Zastoj	Početak zastoja	Kraj zastoja	Vreme zastoja	Ukupno vreme zastoja u minutima
944	5/8/2016	MAJ	2016	BTD SchRs-800	BAGER SchRs-800	ELEKTRO	7:00:00 AM	9:40:00 AM	2:40	160
965	5/11/2016	MAJ	2016	BTD SchRs-800	BAGER SchRs-800	ELEKTRO	3:00:00 PM	6:30:00 PM	3:30	210
966	5/11/2016	MAJ	2016	BTD SchRs-800	BAGER SchRs-800	ELEKTRO	11:00:00 PM	11:35:00 PM	0:35	35

Figure 7 *Database form - electrical downtime*

Table 2 *Results of application the $\chi 2$ test*

Ord. No.	Object	Delay type	Sample size	Distribution of repair time		Distribution between failure times	
				Type	**Parameter μ**	**Type**	**Parameter λ**
1.	EXCAVATOR SchRs-800.15/1,5	Electro	262	E1	0.016292425	E1	0.004015940
2.	EXCAVATOR SchRs-800.15/1,5	Mechanical	359	E1	0.028463641	E1	0.002598397
3.	EXCAVATOR SchRs-800.15/1,5	Others	161	E1	0.004390628	E1	0.004407482
4.	EXCAVATOR SchRs-800.15/1,5	E+M+O	782	E1	0.019389661	E1	

E1 – Exponential distribution,

λ – *exponential distribution parameter - failure intensity,*

μ – *exponential distribution parameter - maintenance intensity.*

Figure 8 shows the exponential distributions of electrical, mechanical and other failures with the values of parameter λ (exponential distribution parameter - failure intensity) and parameters μ (exponential distribution parameter - maintenance intensity).

Failure type	Repair time (in failure)	Operating time to failure (in operation)
Electro	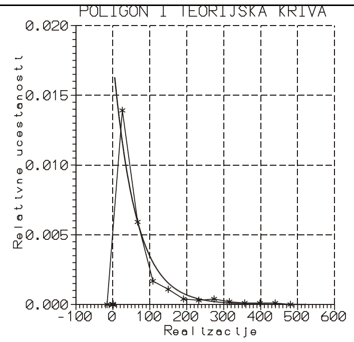 $\mu_{beo} = 0.016292425$	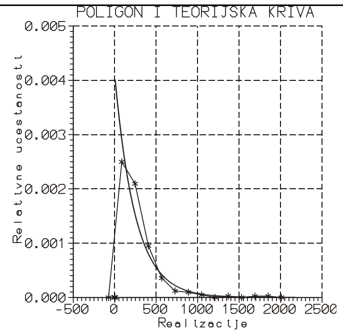 $\lambda_{bed} = 0.004015940$
Mechanical	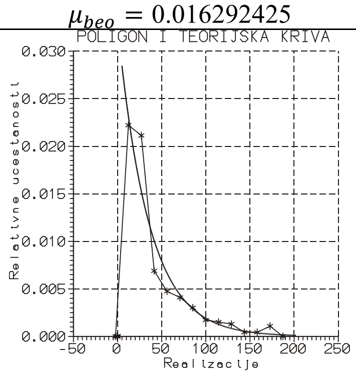 $\mu_{bmo} = 0.028463641$	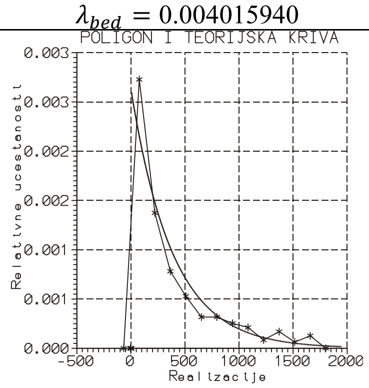 $\lambda_{bmd} = 0.002598397$

Others	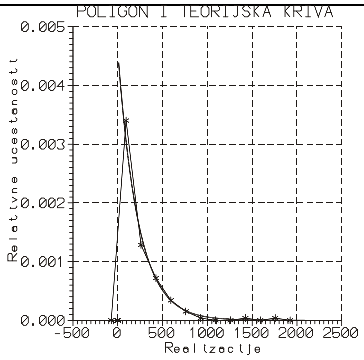 $\mu_{boo} = 0.004390628$	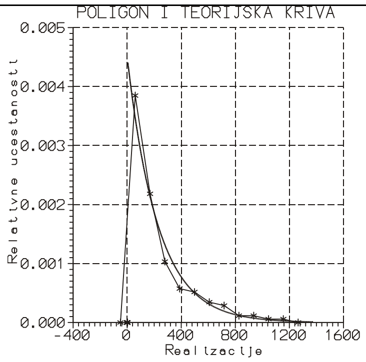 $\lambda_{bod} = 0.004407482$
Mechanical+Electro+Others	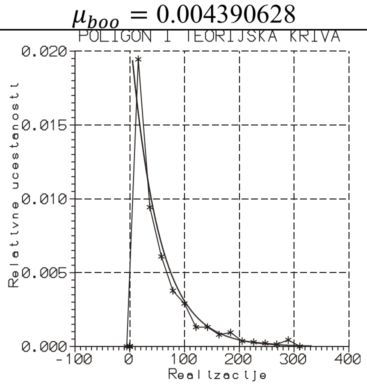 $\mu_{bo} = 0.019389661$	

Figure 8 *Exponential distributions of electro, mechanical and other failures*

μ_{beo} – maintenance intensity of the electrical elements of excavator
μ_{bmo} – maintenance intensity of the excavator machine elements
μ_{boo} – maintenance intensity of the other failures
μ_{bo} – maintenance intensity of the SchRs 800.15/1.5 excavator
λ_{bed} – failure rate of the excavator electrical elements
λ_{bmd} – failure rate of the excavator machine elements
λ_{bod} – intensity of the other failures

3 ANALYTICAL EXPRESSION FOR THE SCHRS-800.15/1.5 EXCAVATOR AVAILABILITY

3.1 Reliability of the SchRs-800.15/1.5 excavator

Reliability of the electrical elements of excavator, based on the testing of sample of the operating time to failure, can be shown by the exponential distribution forms:

$$R_E(t) = e^{-\lambda_{bed} \cdot t} = e^{-0.004015940 \cdot t},$$

where: λ_{bed} $[1/h]$ - failure rate of the excavator electrical elements.

The average operating time between the failures, excavator electrical elements, $MTBF_{be}$ is equal to:

$$MTBF_{be} = \frac{1}{\lambda_{bed}} = \frac{1}{0.004015940} = = 249.01\ h.$$

The function of restoring the electrical elements of excavator $H_{be}(t)$ is of the form:

$$H_{be}(t) = \lambda_{bed} \cdot t.$$

For a period of one year (8760 h), the value of restoring function of the electrical elements of excavator has the value:

$$H_{be}(8760) = 0.004015940 \cdot 8760 = 35.18,$$

which means that the expected number of failures of the electrical elements of excavator SchRs-800.15/1.5 for one year is equal to ~ 36.

Reliability of the machine elements of excavator, based on the testing of sample of operating time to failure, can be shown by the exponential distribution form:

$$R_M(t) = e^{-\lambda_{bmd} \cdot t} = e^{-0.002598397 \cdot t},$$

where: λ_{bmd} [1/h] - failure rate of the excavator machine elements

The mean operating time between failures, excavator machine elements, $MTBF_{bm}$ is equal to:

$$MTBF_{bm} = \frac{1}{\lambda_{bmd}} = \frac{1}{0.002598397} = = 384.85\ h.$$

The function of restoring the mechanical elements of excavator $H_{bm}(t)$ is of the form:

$$H_{bm}(t) = \lambda_{bmd} \cdot t.$$

For a period of one year (8760 h), the value of restoring function of the mechanical elements of excavator has the value:

$$H_{bm}(8760) = 0.002598397 \cdot 8760 = = 22.76,$$

which means that the expected number of failures of the mechanical elements of excavator SchRs-800.15/1.5 for one year is equal to ~ 23.

Reliability of the excavator connected to the other failures, based on the testing of sample of operating time to failure, can be shown by the exponential distribution form:

$$R_O(t) = e^{-\lambda_{bod} \cdot t} = e^{-0.004407482 \cdot t},$$

where: λ_{bod} [1/h] – intensity of the other failures.

The mean operating time between other failures of excavator, $MTBF_{bo}$ is equal to:

$$MTBF_{bo} = \frac{1}{\lambda_{bod}} = \frac{1}{0.004407482} = = 226.90\ h.$$

The function of restoring the other failures of excavator $H_{bo}(t)$ is of the form:

$$H_{bo}(t) = \lambda_{bod} \cdot t.$$

For a period of one year (8760 h), the value of restoring function of the other failures of excavator has the value:

$$H_{bo}(8760) = 0.004407482 \cdot 8760 = = 38.61,$$

which means that the expected number of other failures of the SchRs-800.15/1.5 excavator for one year is equal to ~ 39.

The adopted principle at the open pits of lignite of EPS, when it comes to consider the failure of rotary excavators, is that the electrical, mechanical and other failures are independent of each other. If any type of failure occurs, the excavator stops working. Based on this, the reliability of the SchRs-800.15/1.5 excavator can be shown by a serial connection. (Figure 9)

Figure 9 *Reliability of the SchRs-800.15/1.5 excavator - serial connection (electrical - mechanical - other)*

Reliability of the SchRs-800.15/1.5 excavator $R_b(t)$ is equal to:

$$R_b(t) = R_E(t) \cdot R_M(t) \cdot R_O(t),$$

$$R_b(t) = e^{-(\lambda_{bed}+\lambda_{bmd}+\lambda_{bod})\cdot t} =$$

$$= e^{-\lambda_{bd}\cdot t} = e^{-0.011021819\cdot t},$$

where: λ_{bd} [1/*h*] – failure rate of the SchRs-800.15/1.5 excavator

The unreliability function of the SchRs-800.15/1.5 $F_b(t)$ excavator is equal to:

$$F_b(t) = 1 - R_b(t) = 1 - e^{-\lambda_{bd}\cdot t} =$$

$$= 1 - e^{-0.011021819\cdot t}.$$

The mean operating time of excavator between the failures, $MTBF_b$ is equal to:

$$MTBF_b = \frac{1}{\lambda_{bd}} = \frac{1}{0.011021819} = 90.73\ h.$$

The function of restoring the excavator $H_b(t)$ is of the form:

$$H_b(t) = \lambda_{bd} \cdot t.$$

For a period of one year (8760 *h*), the value of restoring function of excavator has the value:

$$H_b(8760) = 0.011021819 \cdot 8760 =$$

$$= 96.55,$$

which means that the expected number of failures of the SchRs-800.15/1.5 excavator for one year is equal to ~ 97

3.2 Maintenance convenience function of the SchRs-800.15/1.5 excavator

The maintenance convenience function of the SchRs-800.15/1.5 $M_b(t)$ excavator was determined by testing a sample consisting of the time required for repair due to electrical, mechanical and other failures. The maintenance convenience function is of the exponential shape:

$$M_b(t) = 1 - e^{-\mu_{bo}\cdot t} =$$

$$= 1 - e^{-0.019389661\cdot t},$$

where: μ_{bo} [1/*h*] – maintenance intensity of the SchRs-800.15/1.5 excavator

The average repair time of the excavator, the failure time, MDT_b is equal to:

$$MDT_b = \frac{1}{\mu_{bo}} = \frac{1}{0.019389661} = 51.57\ h.$$

The mean repair times due to the failures of electrical and mechanical elements and other failures are:

Electrical:

$$MDT_{be} = \frac{1}{\mu_{beo}} = \frac{1}{0.016292425} =$$

$$= 61.38\ h.$$

Mechanical:

$$MDT_{bm} = \frac{1}{\mu_{bmo}} = \frac{1}{0.028463641} =$$

$$= 35.13\ h.$$

Others:

$$MDT_{bo} = \frac{1}{\mu_{boo}} = \frac{1}{0.004390628} =$$

$$= 227.76\ h.$$

3.3 Availability of the SchRs-800.15/1.5 excavator

Statistical processing of data on operating time to failure and repair time of the SchRs-800.15/1.5 excavator showed that the unreliability function of excavator can be described by the exponential distribution form $F_b(t) = 1 - e^{-\lambda_{bd} \cdot t}$, while the function of benefits the excavator maintenance can also be described by the exponential distribution form $M_b(t) = 1 - e^{-\mu_{bo} \cdot t}$.

Finally, based on the results of statistical data processing on operating time to failure and repair time, the analytical expression for availability of the SchRs-800.15/1.5 excavator is of the following form:

$$A(t) = \frac{\mu_{bo}}{\lambda_{bd}+\mu_{bo}} + \frac{\lambda_{bd}}{\lambda_{bd}+\mu_{bo}} \cdot e^{-(\lambda_{bd}+\mu_{bo}) \cdot t},$$

$$A(t) = \frac{0.019389661}{0.011021819+0.019389661} + \frac{0.011021819}{0.011021819+0.019389661} \cdot e^{-(0.011021819+0.019389661) \cdot t},$$

$$A(t) = 0.637577027 + 0.362422973 \cdot e^{-0.0304114800 \cdot t},$$

where: $k_A = \frac{\mu_{bo}}{\lambda_{bd}+\mu_{bo}} = 0.637577027$ – availability coefficient, i.e. stationary availability value A.

The approximate time t_{stac} , when the excavator availability reaches a stationary value of A, can be determined based on the expression:

$$\frac{|A(t)-A|}{A} \times 100 \leq 1\% \quad \rightarrow \quad t_{stac} = t.$$

Solving the above inequality gives that: $t_{stac} = 133\ h$.

The change in availability of the SchRs-800.15/1.5 rotary excavator over time is shown in Figure 10.

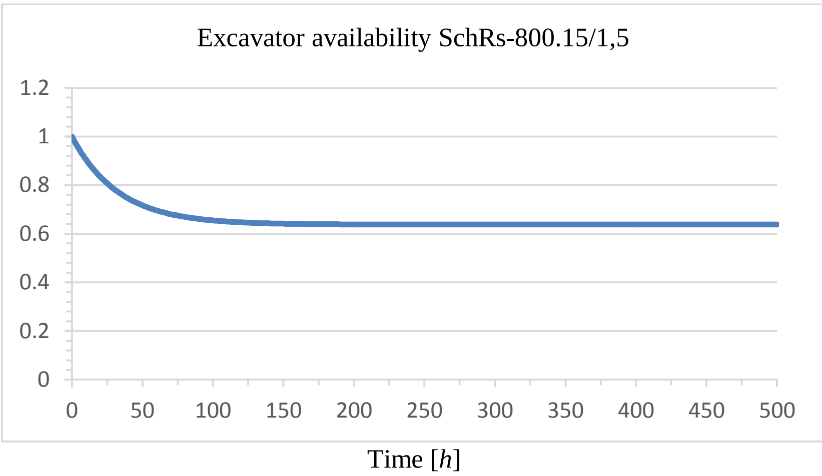

Figure 10 *The change in availability of the SchRs-800.15/1.5 excavator*

4 CONCLUSION

The application of analytical method for determining the availability and other parameters of the operation reliability of rotary excavators allows efficient determination the key factors of system operation as a function of time. By modeling the work process as a function of time, applying the appropriate statistical methods, the functional dependence of parameters such as availability, failure time, work time, etc. is defined. as a function of time.

In order to determine the relevant indicators, it is necessary to have data on the operation and failures of system for a longer period of time, and then to select the characteristic cases. Within the selected characteristic cases, it is necessary to determine a representative sample and perform the presented analysis on it.

Statistical analysis according to the presented methodology and performed on a representative sample, for the SchRs 800.15/1.5 rotary excavator, shows that the intensity of all failures (λ_{bd}) is 0.011021819 and the maintenance intensity (μ_{bo}) is 0.019389661.

The values of these parameters indicate at what stage of life time the rotary excavator is located. In the specific case, the rotary excavator SchRs 800.15/1.5, according to the curve of tub, is in the operation phase, which corresponds to the real situation. The calculated parameters serve to determine the availability of a specific rotary excavator and system as a whole, which is the basic input data for production planning at the lignite open pits of EPS, but also the other activities in the field of planning, monitoring of production or maintenance of equipment.

REFERENCES

[1] Ivković S.: Failures of Mining Machine Elements, University of Belgrade, Faculty of Mining and Geology, Belgrade, 1997.

[2] Vujić S., Stanojević R., Tanasković T., Zajić B., Živojinović R., Maksimović S.: Methods for Optimization the Exploitation Life Time of Mining Machines, Faculty of Mining and Geology, Belgrade, Electric Power Industry of Serbia, Engineering Academy of Serbia and Montenegro, 2004 (in Serbian)

[3] Polovina D.: Methodology for Determining The Remaining Possibilities of Rotary Excavators in Exploitation and Revitalization - Doctoral Dissertation, University of Belgrade, Faculty of Mining and Geology, Belgrade, 2010 (in Serbian)

[4] Vukotić V., Čabrilo D.: Increasing the Reliability of Excavation Subsystem of a Rotary Excavator by Adjusting the Tribological Characteristics of Cutting Elements, 13th International Conference on Tribology Serbiatrib 13, 2013 (in Serbian)

[5] Milovanović I., Dimitrijević Ž., Vučković B., Radovanović B., Bogdanović V., Stojanović S., Vučković M., Šubaranović T., Polomčić D., Božić M., Miletić D., Raščanin Z., Spasić A., Milovanović S., Kulić Z., Lukić V.: Additional Mining Project of The Open Pit "Drmno" for a Capacity of 12x10^6 tons of Coal Per Year, PE EPS Belgrade, Branch RB Kolubara, Organizational Unit "PROJECT" Lazarevac, May 2019 (in Serbian)

[6] Djenadić S., Ignjatović D., Tanasijević M., Bugarić U., Janković I., Šubaranović T.: Development of the Availability Concept Using The Fuzzy Theory with AHP Correction, a Case Study: Bulldozers at the Open-Pit Lignite Mine, Energies, October 2019.

[7] Đurić R.: Concept of Availability in Defining The Efficient Maintenance of Auxiliary Machinery at the Open Pits, Doctoral Dissertation, University of Belgrade, Faculty of Mining and Geology, Belgrade, 2016 (in Serbian)

[8] Bugarić U., Petrović D.: Service System Modeling, University of Belgrade, Faculty of Mechanical Engineering, Belgrade, 2011 (in Serbian)

MINING AND METALLURGY INSTITUTE BOR
UDK: 622

ISSN: 2334-8836 (Štampano izdanje)
ISSN: 2406-1395 (Online)

UDK: 622.33/.272:6814.325(045)=111

DOI: 10.5937/mmeb2004037V

Nenad Vušović, Milica Vlahović***

PREDICTION OF SURFACE SUBSIDENCE AND DEFORMATIONS DUE TO THE UNDERGROUND COAL MINING***

Abstract

Throughout its historical development, mining has faced the problem of moral and material responsibility due to various types of endangerment and damage to the environment. As a result of the underground coal exploitation, a movement of the rock massif above the coal seam, and changes on the terrain surface due to the process of massif stabilizing take place. The process occurs in space and time, from the moment of balance disturbance in the massif, i.e., the beginning of excavation, during excavation, and after the final excavation of deposit, when the equilibrium state is reestablished in the massif. The character and intensity of these movements and principles according to which they are performed, depend on numerous natural and mining-technological conditions, and are specific to each individual coal deposit. Deformations on the terrain surface in the sinkhole occur in the horizontal and vertical directions. Their values serve to determine the vulnerability level of individual objects on the terrain surface. On the basis of the Patarić-Stojanović stochastic method for the predictive subsidence and deformations calculation, an original MITSOUKO program package, supported by the spatial analyses in the Geographic Information System (GIS), was designed. A case study in Sladaja village influenced by the underground exploitation in the coal mine "Rembas"- Resavica, one of the biggest Serbian coal mines, has been chosen. The data processed in the GIS provided determining the module, sense, and direction of the displacements, sinking velocity, and possible effects of subsidence on facilities.

***Keywords**: underground coal mining, ground surface movements, stochastic theory, GIS, spatial analysis*

INTRODUCTION

The surface subsidence and its harmful effects on infrastructures above mining operations is a serious problem resulting from the underground coal mining in mining basins. The inevitability of consequences for objects on the terrain surface can be related to the conditionality of the mine location. Deposits of mineral raw materials, which are often near and below populated areas or natural and technical facilities, dictate the position of underground pits and surface mines. It is truly claimed that the fight against these phenomena is the main feature of the entire mining history. The environment and surface objects can be seriously affected by the subsidence [1].

* *University of Belgrade, Technical Faculty in Bor, Vojske Jugoslavije 12 Bor, Serbia, e-mail: nvusovic@tfbor.bg.ac.rs*

** *University of Belgrade, Institute of Chemistry, Technology and Metallurgy, Njegoševa 12, Belgrade, Serbia, e-mail: m.vlahovic@ihtm.bg.ac.rs, mvlahovic@tmf.bg.ac.rs*

*** *This work was financially supported by the Ministry of Education, Science and Technological Development of the Republic of Serbia (Grant Nos. 451-03-68/2020-14/200131 and 451-03-68/2020-14/200026).*

In the zone of mining works, an impact sinkhole occurs on the terrain surface. The shape and position of the sinkhole in relation to the excavated space depend on the mining and geological conditions of excavation. When the deposit lies horizontally, the sinkhole is symmetrical with regard to the excavated space, while with steep seams it acquires an asymmetrical shape.

Damages due to the surface subsidence can be provoked by the surface slope changes, differential vertical displacements, and horizontal strains and based on their values, the vulnerability level for individual objects on the terrain surface can be estimated. Structural damages on facilities depend on the construction method and used materials; also, the chosen mining method has a great influence [2].

Case study presents a predictive calculation of the subsidence and deformations based on the stochastic method by the Pataric and Stojanovic in the MITSOUKO program package, and the GIS model using the input data from the underground coal mine "Rembas"- Resavica in Serbia.

The calculated subsidence and deformations in the analysed period have been presented graphically and described in the spatial analysis in GIS. Hence, the system created can be a useful tool to manage the subsidence data, determine its evolution, predict deformations and future environmental and social impacts, and control corrective measures. The application of the presented method supported by GIS on the chosen area enables a more automated assessment of building damage caused by the mining activity. The procedure outlined in this paper may also be satisfactorily applied in the other counties which cope with the problem of building damage risk assessment optimization [3].

STOCHASTIC MODEL OF THE GROUND SURFACE MOVEMENTS DUE TO THE UNDERGROUND COAL MINING

Surface subsidence can be caused by the underground mining during operations or later owing to deformations in the rock mass whereby the geologic factors such as the quantity and quality of the subsoil, rock components and superficial conditions are of significant importance [4].

The developed subsidence prediction methods with different starting assumptions for deriving equations that describe the subsidence curve are: profile function methods, inluence function methods, empirical methods and numerical models. Theoretical methods try to explain a mechanism that can predict the magnitude of subsidence: profile function methods are based on the application of inluence function of the elementary excavated volume on the ground surface subsidence; influence function methods are based on the effect of extraction the infinitesimal elements of an area; empirical methods based on the results of systematic measurements in the local conditions of a coal basin; numerical models use the finite elements methods, boundary elements method, distinct elements method and finite difference methods to calculate the displacements and subsidence of ground surface [3].

Mining prophylaxy was greatly disturbed and disabled because of the modest calculation capacity and lack of automation. Computer technology and GIS enabled benefits in this field [2,3].

Stochastic medium theory for subsidence and deformations prediction

Ground surface movements, caused by the underground coal mining, are very complex and therefore difficult for modeling due to the complicated behavior of the overlying rock mass and land profiles. Since the behavior of overlying strata is complicated due to numerous known and unknown factors that affect and conduct moving of the rock mass, the stochastic theory of ground moving was used in these models for the mine subsidence prediction.

Generally, it is easier to predict the definite subsidence than the movements caused by sequential and complicated mining processes. Therefore, the stochastic theory can be a universal method for the mine-subsidence and deformations.

Litwiniszyn (1950) proposed a stochastic subsidence model presuming the ground mass as a discontinuous medium where an element movement towards a collapsing cavity is considered as the Markovian process [5,6]. According to the stochastic theory, moving of the rock mass above the excavated element might happen randomly with a certain likeliness. It assumes that the rock mass can be moved from one location to another and its shape can vary under unit element mining, however its total volume remains the same. The procedure is based on the concept of stohastic process. Since its beginning, this theory has undergone numerous and constant improvements.

Liu and Liao (1965) established a stochastic method named the Stochastic Medium Theory Model (SMTM), a profile function based on the statistic medium algorithm method, for the prognosis of underground mining-induced surface movement, which is the most commonly used method in China [7,8].

The Pataric-Stojanovic (1994) stochastic method applies the mathematical statistics and starts from the assumption that the massif is multi-layered, divided by a series of cracks into a large number of elements whose movements have stochastic character. Since the subsidence is plane, two coordinates are sufficient: an abscissa parallel to the layers (horizontally) and an elevation vertically with the upward direction-to determine the position of elements in the massif [9,10]. For the boundary transition from a discrete division to a continuous massif, the starting point is the position of elements that are defined by the coordinates, i.e.:

$$F\left(x, z+h\right) = \frac{1}{2}\cdot\left[F\left(x-a, z\right)+F\left(x+a, z\right)\right], \quad (1)$$

where $F(x,z)$ is the ***function of subsidence probability.***

Basic formula for calculating subsidence during the inclined seams excavation is obtained:

$$U\left(x, y\right) = U_0\ X\left(x, y\right) Y\left(y\right), \quad (2)$$

where:

$$X\left(x,y\right) = \frac{1}{2}\left[\Phi\left(p\frac{a+x}{\sqrt{H\cdot ctg\alpha - y}}\right)+\Phi\left(p\frac{a-x}{\sqrt{H\cdot ctg\alpha - y}}\right)\right]$$

$$Y\left(y\right) = \frac{1}{2}\left[\Phi\left(q\frac{b+m+y}{\sqrt{H\cdot ctg\alpha - y}}\right)+\Phi\left(q\frac{b-m-y}{\sqrt{H\cdot ctg\alpha - y}}\right)\right]$$

where:

H - seam depth; α - angle of seam dip;
a - dimension of excavation area;

parameters:

$$p = \frac{p_0}{\sqrt{\sin\alpha}};\quad q = \left(1-\lambda\sin\alpha\right)Q;$$

$$b = \frac{l\cos\alpha}{1-\lambda\sin\alpha};\; m = \frac{H\,\lambda\cos\alpha}{1-\lambda\sin\alpha};$$

$$\lambda = \frac{\cos\theta}{\sin(\alpha+\theta)};\; q = \frac{q_0}{\sqrt{\sin\alpha}};$$

θ - angle of full subsidence.

The stochastic subsidence prediction enables the calculation and presentation of surface subsidence at any point in a grid with a large number of numerical data. The subsidence curve will be the same in any profile by the dip, so it is a plane subsidence:

$$U(y) = U_0\,Y(y), \tag{3}$$

where $Y(y)$ is calculated from the Eq. (1).

Deformations during subsidence

Deformations are relative changes that occur as a result of uneven subsidence or horizontal displacements on the undermined terrain. They are calculated from the difference of absolute subsidence values, or horizontal displacements of adjacent points, reduced to a length unit.

Based on their values, the vulnerability level of individual objects on the ground surface is determined. Vertical deformations are expressed through the slope changes and curvature of the terrain. Horizontal deformations-dilatations, are expressed through elongation or shortening of individual intervals between adjacent points [11].

Slope

Subsidence values can only be measured at a limited number of discretely arranged points and the slope can be calculated from this data. The slope (N) represents the ratio of difference in the subsidence of adjacent points according to their distance. It is expressed in (mm/m). In fact, it is the mean slope between the tendon AB of the subsidence curve and the horizontal (Figure 1):

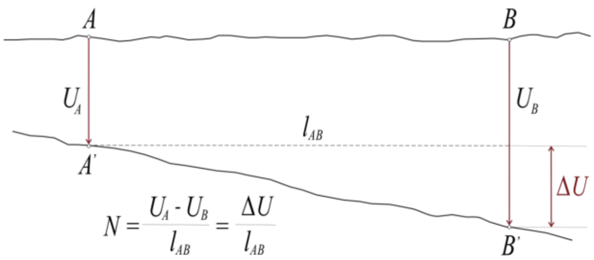

Figure 1 *Slope [9]*

With the coordinate origin above the middle of excavated space, the x-axis in a direction of coal seam dip and the y-axis in a direction of coal seam strike, the slopes will be positive (+) by the strike and negative (-) by the dip.

If the equation $U(\xi)$ in a given profile is known, its first derivative determines the slope of tangent at some arbitrarily chosen point M, determined by the coordinate ξ:

$$N_M = N(\xi) = \frac{\partial U}{\partial \xi}. \tag{4}$$

In the general case, when the equation of the subsidence curve $U(x, y)$ is known, the point M and slope direction at that point must be given, because an unlimited number of vertical planes can be placed through each point on the surface of subsidence curve, whereby to each plane corresponds a different subsidence curve and thus the other slope value (Figure 2).

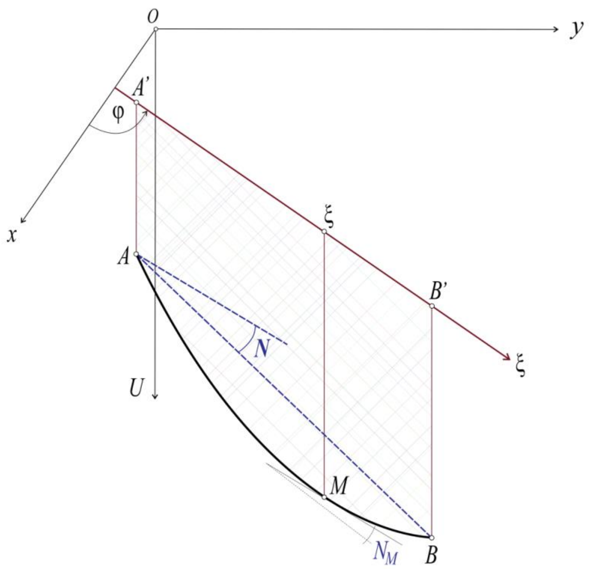

Figure 2 *Slope value determination at a point M on the surface of the subsidence curve [9]*

To solve practical problems, it is necessary to know the main slope in the plane, in which it has the maximum value. If π is a vertical plane through a point M, which makes an angle φ with the axis O_x (Figure 2), the coordinates of the point M are:

$$x_M = x_A + \xi_M \cdot \cos\varphi$$

$$y_M = y_A + \xi_M \cdot \sin\varphi,$$

then, according to Eq. 4, the slope equation will be:

$$N_M(\varphi) = \frac{\partial U}{\partial x}\frac{\partial x}{\partial \xi} + \frac{\partial U}{\partial y}\frac{\partial y}{\partial \varphi},$$

that is:

$$N_M(\varphi) = \frac{\partial U}{\partial x}\cos\varphi + \frac{\partial U}{\partial y}\sin\varphi. \quad (5)$$

If $\frac{\partial U}{\partial x} = N_x(x, y)$ and $\frac{\partial U}{\partial y} = N_y(x, y)$, for a certain point $M(x_M, y_M)$ it follows that:

$$N_x(x_M, y_M) = N_x(M)$$

and

$$N_y(x_M, y_M) = N_y(M).$$

Main slope. It can be seen from Eq. (5) that there is such a value of the angle $\varphi = \varphi_0$ for which the slope at an arbitrarily chosen point M will be $N_M(\varphi_0) = 0$, so using:

$$N_x(M)\cos\varphi_0 + N_y(M)\sin\varphi_0 = 0$$

it follows that:

$$tg\varphi_0 = -\frac{N_x(M)}{N_y(M)}. \quad (6)$$

The angle φ_0 obviously determines a direction of subsidence contour line at the point M.

Also, a position of the plane π such that the slope has an extreme value $N_M(\varphi)$ can be found; if $\varphi = \varphi_I$ is the angle determining that position, from the condition $\frac{N_M(\varphi)}{\partial_\psi} = 0$, it follows that:

$$-N_x(M) - \sin\varphi_I + N_y(M)\cos\varphi_I = 0$$

so it is:

$$tg\varphi_I = \frac{N_y(M)}{N_x(M)} \tag{7}$$

The angle φ_I determines the ***main direction***, and the extreme value of the slope $N_M(\varphi_1) = N_1(M)$ is called the ***main slope at the point*** M [9].

Based on Eq. (7) for known projections $N_x(M)$ and $N_y(M)$, using familiar trigonometric identities, the following can be calculated:

$$\sin\varphi_1 = \frac{tg\varphi_I}{\sqrt{1+tg^2\varphi_I}} = \frac{N_y(M)}{\sqrt{N_x^2(M)+N_y^2(M)}}$$

$$\cos\varphi_1 = \frac{1}{\sqrt{1+tg^2\varphi_I}} = \frac{N_x(M)}{\sqrt{N_x^2(M)+N_y^2(M)}}.$$

If these results are entered in Eq. (4), the value of the main slope is obtained:

$$N_M(\varphi_1) = N_I(M)$$

$$N_I(M) = \sqrt{N_x^2(M)+N_y^2(M)}. \tag{8}$$

Since the second derivative is:

$$\frac{\partial^2 N_M(\varphi)}{\partial\varphi^2} = -\left[\left(N_x(M)\cos\varphi + N_y(M)\sin\varphi\right) = -N_I(M)\right] \le 0,$$

then this extreme value is also the maximum.

From Eqs. (6) and (7), it follows that: $tg\varphi_0 \cdot tg\varphi_I + 1 = 0$, so the main direction φ_I is perpendicular to the subsidence contour line at the point M is: $U(\mathrm{x},\mathrm{y}) = U(x_M, y_M) = const.$

Since the main plane π_I is determined by the vertical and main direction φ_I, it also contains the normal at the point M of sinkhole, and the main slope $N_I(M)$ also represents the angle between the vertical and this normal. For example, it is the angle that the axis of a pillar after the massif sinking will form with its original direction (vertical).

In practice, depressions and deformations are most often determined in the main profiles, in which their extreme values also occur. However, if the excavated surface is not full, i.e., the subsidence did not reach its maximum possible value on the terrain surface, general conclusions about these values cannot be made, neither the places where the greatest deformations occur, because the result depends on the excavated field [9,10].

Curvature

Curvature represents the ratio of difference in the slope of adjacent intervals and the mean value of their lengths. It is denoted by K, ant its unit is (1/km). With slope signs, the convex curves are positive with a (+) sign, and concave curves are negative with a (-) sign, as shown in Figure 3.

Radius of curvature is the reciprocal of curvature. It is denoted by R and its unit is (km).

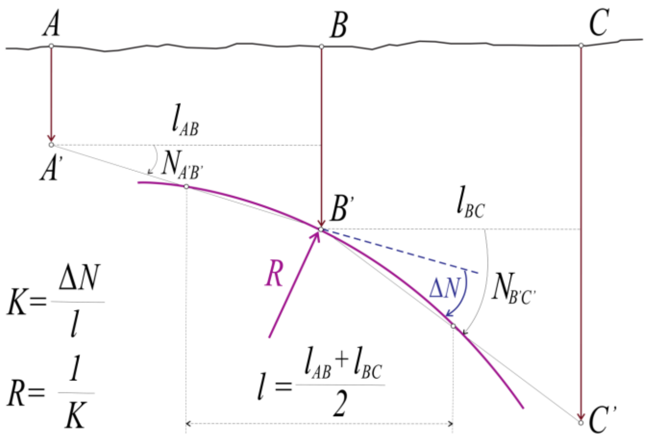

Figure 3 *Curvature [9]*

If the equation $U(\xi)$ of the subsidence curve in the observed profile is known, its first derivative defines the slope $N = U'(x)$ and the second derivative determines the curvature. The curvature at any point M determined by the coordinate ξ can be calculated, using a known formula from differential geometry:

$$K(\xi) = \frac{U''}{\left(1+U'^2\right)^{3/2}} .$$

As the value of the slope is small, the member $U'^2(\xi) = N^2(\xi)$ can be neglected in relation to the unity, so a sim pler formula is used to calculate the curvature at a point:

$$K(\xi) = \frac{\partial^2 U(\xi)}{\partial \xi^2} \qquad (9)$$

Finally, if the equation of the subsidence sinkhole $U(x, y)$ is known, a curvature can be calculated at any point $M(x, y)$ of the profile that angle φ forms with the axis Ox. From Figure 3, it is obvious that:

$$x_M = x_A + \xi_M \cdot \cos\varphi$$

$$y_M = y_A + \xi_M \cdot \sin\varphi ,$$

so, based on Eq. (12):

$$K_M(\varphi) = \frac{\partial^2 U}{\partial x^2}\left(\frac{\partial x}{\partial \xi}\right)^2 + 2\frac{\partial^2 U}{\partial x \partial y}\frac{\partial x}{\partial \xi}\frac{\partial y}{\partial \xi} + \frac{\partial^2 U}{\partial y^2}\left(\frac{\partial U}{\partial \xi}\right)^2 ,$$

or, if shorter forms are introduced:

$$K_x = \frac{\partial^2 U}{\partial x^2}\,,\; K_{xy} = \frac{\partial^2 U}{\partial x \partial y}\,,\; K_y = \frac{\partial^2 U}{\partial y^2}\,,$$

it follows that:

$$K_M(\varphi) = K_x \cos^2\varphi + 2K_{xy} \sin\varphi \cos\varphi + K_y \sin^2\varphi\,. \tag{10}$$

Instead of squares, i.e., products of sines and cosines, a double angle can be introduced, based on the known trigonometric identities:

$$\cos^2\varphi = \frac{1}{2}(1+\cos\ 2\varphi);$$

$$\sin^2\varphi = \frac{1}{2}(1-\cos\ 2\varphi)$$

and $2\sin\varphi\cdot\cos\varphi = \sin 2\varphi$.

So, a simpler form of the equation is obtained:

$$K_M(\varphi) = \frac{1}{2}(K_x + K_y) + \frac{1}{2}(K_x - K_y)\cos\ 2\varphi + K_{xy}\sin 2\varphi\,. \tag{11}$$

The members K_x and K_y in this formula according to Eq. (9) represent the ***curvatures*** at the point $M(x,y)$ for profiles parallel to the coordinate axes. The third member, $K_{xy} = \frac{\partial^2 U}{\partial x \partial y}$ represents the ***twist*** in a direction of coordinate axes at the point $M(x,y)$.

Main curvatures. To solve practical problems, it is necessary to determine the extreme values of curvatures K_I and K_{II} at the point $M(x,y)$, which are called the ***main curvatures at a point***, and the angles φ_1 and φ_2 of the corresponding profiles determine the ***main directions***. According to Eqs. (10) and (11), the value of curvature at a point depends on the angle φ, so determiniation of extreme values of the function $K_M(\varphi)$ is mathematically reduced to the trigonometric equation:

$$\frac{\partial K_M(\varphi)}{\partial\varphi} = -(K_x - K_y)\sin 2\varphi + 2K_{xy}\cos 2\varphi = 0\,, \tag{12}$$

whose solution:

$$\tan 2\varphi = \frac{2K_{xy}}{K_x - K_y} \tag{13}$$

determines the main directions. If the main direction is known, the other is $\varphi_2 = 90^o + \varphi_1$, because: $\tan 2\varphi_2 = \tan(180^o + 2\varphi_1) = \tan 2\varphi_1$ and therefore φ_2 is the solution of Eq. 13. The main directions are orthogonal.

If trigonometric identities:

$$\sin 2\varphi = \frac{\tan 2\varphi}{\sqrt{1+\tan^2 2\varphi}} = \frac{2\mathrm{K}_{xy}}{\sqrt{(\mathrm{K}_x - \mathrm{K}_y)^2 + 4K_{xy}^2}}$$

$$\cos 2\varphi = \frac{1}{\sqrt{1+\tan^2\varphi}} = \frac{\mathrm{K}_x - K_y}{\sqrt{(\mathrm{K}_x - \mathrm{K}_y)^2 + 4K_{xy}^2}}$$

are entered in Eq. (11), values of the main curvatures are:

$$K_I = \frac{1}{2}\left(K_x + K_y\right) + \frac{1}{2}\sqrt{\left(K_x - K_y\right)^2 + 4K_{xy}^2} \quad (14)$$

$$K_{II} = \frac{1}{2}\left(K_x + K_y\right) - \frac{1}{2}\sqrt{\left(K_x - K_y\right)^2 + 4K_{xy}^2}$$

whereby K_I is the highest and K_{II} the lowest value of the main curvatures [9, 10].

Members K_x, K_y and K_{xy} are calculated by the formulas:

$$K_x = \frac{U_0}{n^2} \cdot X_{02}(x) \cdot Y_0(y);$$

$$K_y = \frac{U_0}{n^2} \cdot X_0(x) \cdot Y_{02}(y);$$

$$K_{xy} = \frac{U_0}{n^2} \cdot X_{01}(x) \cdot Y_{01}(y)$$

where:

$$X_{02}(x) = -\left[\frac{a+x}{n}\varphi\left(\frac{a+x}{n}\right) + \frac{a-x}{n}\varphi\left(\frac{a-x}{n}\right)\right]$$

$$Y_{02}(x) = -\left[\frac{l+y}{n}\varphi\left(\frac{l+y}{n}\right) + \frac{l-y}{n}\varphi\left(\frac{l-y}{n}\right)\right].$$

Horizontal deformations - dilatations

Horizontal deformations- dilatations, D, with the unit (mm/m), are determined from the displacement of neighbouring points on the terrain surface in the horizontal plane (Figure 4) and expressed through elongation (+), or shortening (-) of the interval between adjacent points (Eq. 15):

$$\pm D = \frac{\Delta P}{l_{AB}} \quad (15)$$

where: $\Delta P = P_B - P_A$

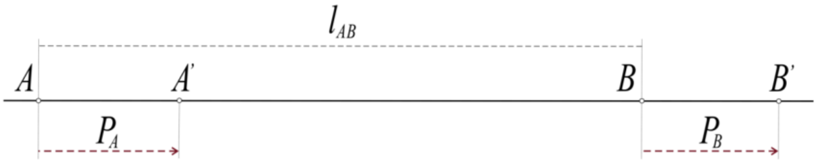

Figure 4 *Horizontal deformations- dilatations [9]*

Elongation occurs if, after moving the undermined terrain, the horizontal distances between adjacent points are increased, and shortenings in the opposite case. When the points on the undermined massif surface move horizontally, deformations similar to those during subsidence, also occur. Two arbitrarily chosen points, A_0 and B_0, of undisturbed massif, at a distance $A_0\,B_0 = l_0$ after consolidation, move into position A, that is B, and angle ν between the line segments $A_0\,B_0$ and AB (Figure 4) can be found analogously to the slope (Eq. 16):

$$\nu = \frac{P_{\eta A} - P_{\eta B}}{l_0}, \quad (16)$$

where $P_{\eta A}$ and $P_{\eta B}$ are the distances of the points A and B from the original direction; the angle ν is called the ***shear strain.***

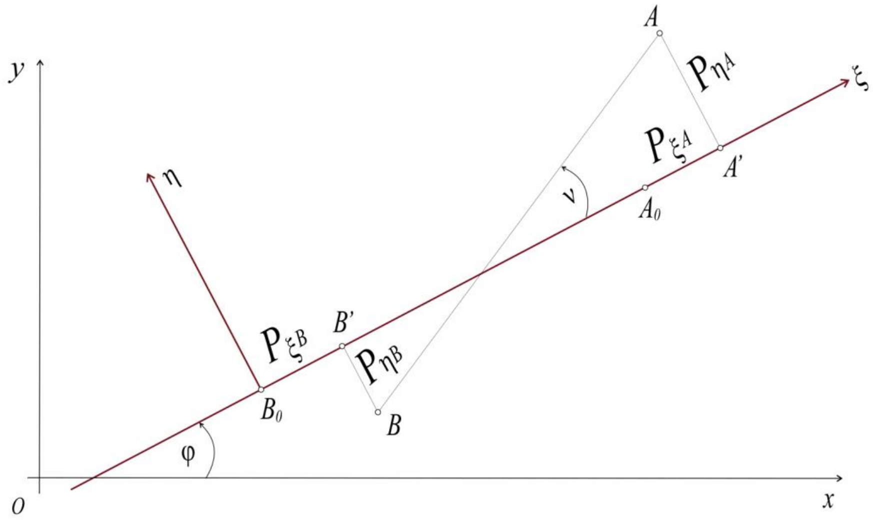

Figure 5 *Shear strain [9]*

The shear strain at a point $M(x, y)$ is calculated according to Eq. (17):

$$\nu_M = \varphi_{xy} + \gamma_{xy} \cos^2 2\varphi - \frac{1}{2}\left(D_x - D_y\right)\sin 2\varphi \tag{17}$$

whereby:

$$\varphi_{xy} = \frac{1}{2}\left(\frac{\partial P_y}{\partial x} - \frac{\partial P_x}{\partial y}\right),$$

$$\gamma_{xy} = \frac{1}{2}\left(\frac{\partial P_y}{\partial x} + \frac{\partial P_x}{\partial y}\right);$$

$$D_x = \frac{\partial P_x}{\partial x}, \quad D_y = \frac{\partial P_y}{\partial y}.$$

where γ_{xy} denotes slide that will be explained in the following text.

The points A, B and C of the undisturbed massif surface are at distances $AB = l_1$ and $AC = l_2$, and at a right angle ($ABC = 90^o$). Due to the rock massif undermining, there is a horizontal movement and these points move to positions A_1, B_1 and C_1, whereby, in general case, the angle $A_1B_1C_1$ is no longer a right angle. Shear strain of the line segment (AB), $\nu_{AB} = \frac{\Delta\eta}{l_1}$ will be positive if $\Delta\eta > 0$; the deflection ν_{AC} is positive if $\Delta_\xi > 0$, so the change of right angle is $\nu_{AB} + \nu_{AC}$. Half of this change is ***slide***:

$$\gamma_{\xi\mu} = \frac{1}{2}\left(\frac{\Delta\eta}{l_1} + \frac{\Delta\xi}{l_2}\right) \tag{18}$$

As $P_\xi = P_x \cos\varphi + P_y \sin\varphi$, it follows that:

$$P_\xi = P_x \cos\varphi + P_y \sin\varphi$$

$$P_\eta = P_x \sin\varphi + P_y \cos\varphi$$

and:

$$\gamma_{\xi\mu} = \gamma_{xy} \cos 2\varphi - \frac{1}{2}\left(D_x - D_y\right)\sin 2\varphi$$

Half the difference $\varphi_{\xi\mu} = \frac{1}{2}\left(\frac{\Delta\eta}{l_1} + \frac{\Delta\xi}{l_2}\right)$ is ***rotation***. This quantity is not a deformation, because it does not change the shape of triangle ABC, but only its rotation. For the point rotation, the following can be applied:

$$\varphi_{\xi\eta} = \varphi_{xy} = \frac{1}{2}\left(\frac{\partial P_y}{\partial x} - \frac{\partial P_x}{\partial y}\right),$$

so the ***shear strain*** at the point is the sum of rotation and slide:

$$v_M\left(\varphi\right) = \varphi_{\xi\eta} + \gamma_{\xi\eta} . \qquad (19)$$

Main dilatations. If $l = A'B'$ is the distance between the projection of points A and B on their original direction $A_0\ B_0$, according to Figure 5, it is obvious that:

$$l = \xi_{A'} - \xi_{B'} = l_0 + P_{\xi A} - P_{\xi B}$$

$$\Delta l = l - l_0 = P_{\xi A} - P_{\xi B} .$$

In the general case $P_{\xi A} - P_{\xi B} \neq 0$, so Δl is an ***elongation*** when $P_{\xi A} > P_{\xi B}$, or a ***shortening*** when $P_{\xi A} - P_{\xi B} < 0$.

According to Eq. (15), the relation $D_\xi = \frac{\Delta l}{l_0}$ is dilatation of line segment AB; it is the average elongation or the shortening of this line segment.

When the equations $P_x\left(x, y\right)$ and $P_y\left(x, y\right)$ for horizontal displacements are known, the dilatation at a point is defined analogously to the slope:

$$D_\xi = \frac{\partial P_\xi}{\partial \xi} = \frac{\partial P_x}{\partial x}\cos^2\varphi + \left(\frac{\partial P_y}{\partial x} + \frac{\partial P_x}{\partial y}\right)\sin\varphi\cos\varphi + \frac{\partial P_y}{\partial y}\sin^2\varphi \qquad (20)$$

If denotations and a double angle are introduced, the following is obtained:

$$D_\xi = \frac{1}{2}\left(D_x + D_y\right) + \frac{1}{2}\left(D_x - D_y\right)\cos 2\varphi + \gamma_{xy}\sin 2\varphi . \qquad (21)$$

This formula has the same form as Eq. (11), so the ***main dilatations directions*** are determined similarly as for curves [9,10]:

$$\tan 2\varphi = \frac{2\gamma_{xy}}{D_x - D_y} , \qquad (22)$$

as well as their values:

$$D_I = \frac{1}{2}\left(D_x + D_y\right) + \frac{1}{2}\sqrt{\left(D_x - D_y\right)^2 + 4\gamma_{xy}^2}$$

(23)

$$D_{II} = \frac{1}{2}\left(D_x + D_y\right) - \frac{1}{2}\sqrt{\left(D_x - D_y\right)^2 + 4\gamma_{xy}^2} .$$

Since the formulas have the same form as those for the curvature, it follows that the sliding in the main directions is $\gamma_{12} = 0$, and the greatest sliding:

$$\gamma_{xy} = \frac{1}{2}\left(D_1 - D_2\right) \qquad (24)$$

is for the axes Ox and Oy, which form the angle of 45^o with the principal axes.

PROTECTION OF FACILITIES AND PROTECTION CRITERIA

A protective pillar is a part of deposit under a facility that is not excavated or is excavated in such a way that no harmful deformations appear on the object. The endangerment of objects on the terrain surface outside the boundary of the non-excavated protective pillar, or within its boundaries if it is excavated, depends on the type and value of deformations that may occur on the object [9].

The type of deformation according to a certain criterion depends on the object type, and the level of these deformations depends on the construction of object. There are objects, in terms of damage, sensitive only to a certain-primary type of deformation, while the other types of deformation are of secondary importance. Buildings and similar masonry buildings are most vulnerable to the horizontal deformations, which lead to the appearance of cracks. Tall buildings, chimneys, and towers are sensitive to changes in a slope. The main structures (railways, roads, pipelines) are sensitive to changes in curvature. There are objects of complex constructions that are simultaneously vulnerable to the appearance of several types of deformations, and in that case, they must be expressed through some common criterion [2,9,12].

A long-term observation of behavior and damage of various facilities in different excavation conditions, empirical and statistical laws of occurrence of certain deformation types were obtained thus enabling to distinguish the limits between different intensities of damage, and to define the protection criteria. Such observations were performed in many mining developed countries with different levels of population, in different mining conditions, on facilities of different construction methods and characteristics, so that various protection criteria were created. The main difference between them is in terms of their generality, or their detail, which arises from the scope and level of study in the individual countries around the world [12,13]. In Serbian mining practice, there are still no adopted criteria for the protection of facilities from the impact of underground mining works [9].

According to the Polish instructions for assessing the dangerous impact of mining on buildings at the planned mining sites, which are most often used in solving these problems in the Serbian coal mines [9], the basic criteria for protection of objects are the allowed values of slope (N), radius of terrain curvature (R) and horizontal deformations - dilatations (D). To determine the degree of dangerous impact of continuous deformations on the existing and planned facilities in the analyzed area, the mining terrain is divided into categories [2,12,14], whereby the limits are determined on the basis of the highest maximum values of deformations for a given category. Then the area of a given category is determined by selection the maximum ranges, which are the result of the least favorable distributions of specific deformation indices. Accordingly, the facilities are divided into four protection categories (I-IV), whereby for each category, the allowed values of deformations are prescribed, as shown in Table 1.

Table 1 *Criteria for classification the surface movements and deformations* [12]

Terrain category	Magnitude of expected deformations			Possible degree of damaging; types of surface structures	Usability for spatial development
	N_{max} (mm/m)	R_{min} (km)	D_{max} (mm/m)		
0	N <0.5	R ≥40	D ≤ 0.3		
I	<0.5 N ≤2.5	40> R ≥20	0.3< D ≤1.5	Small, easily fixable damage may occur. Mo-numental objects, industrial systems, especially important for safety of life rea-sons, or regarded as especially important, e.g., gas pipelines, the damaging of which may cause gas outbursts; water reservoirs.	Safe areas, no protection of ob-jects is needed
II	<2.5 N ≤5.0	20> R ≥12	1.5< D ≤3.0	Small damage of objects may occur; rela-tively easy to remove. The most important objects, industrial objects, large-furnaces, coke furna-ces, hoisting shafts and ma-chines, Industrial objects-monolith or with overhead cranes, public utility objects, e.g., hospitals, theatres, vaulted churches), river valleys, water reservoirs, main railways and stations, tunnels, vaulted bridges, main water-works unprotected against mining damage, huge houses of residence (longer than 20 m). Big cities.	Areas, where partial protection of all objects is not profitable
III	5.0< N ≤10.0	12> R ≥6	3.0< D ≤6.0	Bigger damage of objects may occur, with-out destroying them. The main roads, routes and small railway stations, industrial objects which are less susceptible to the movement of the subsoil (no overhead cranes), uncoated freezer-rooms, high chimneys, smaller houses of residence (10–20 m in horizontal prospection), city sewage treatment plants, main collectors, sewage pipelines, gas pipe-lines, steel gas pipelines.	Areas requiring partial protection of objects (type of protection de-pends on the type of object, its sensitivity, subsoil properties, and magnitude of deformations)
IV	10.0< N ≤15.0	6> R ≥4	6.0< D ≤9.0	Serious damage, objects are nearly de-stroyed. Stadiums, small houses, other less important objects.	Areas requiring serious protection of objects
V	N >15.0	R <4	D >9.0	Very serious damage, objects are destroyed.	Areas which are not fit for spatial development

A CASE STUDY

The entire raw material potential of coal in Serbia, which is predisposed to the underground exploitation systems, belongs to the JP PEU coal mines. In active coal deposits, the dominant geological forms are layered sloped structures with the pronounced tectonic deformations, whose consequences are irregular shapes of limited exploitation areas as well as possible short lengths of excavation fields and panels with frequent changes in the strike and angles of seam dip. These phenomena are the result of complex post-tectonics in the deposits. The seams from several to 40 m thick are from horizontal to steep. It should be added that the basic physico-mechanical properties of the working environment are relatively unfavorable because predominant are the deposits where the values of compressive strength of the mine roof and floor are lower or significantly lower than coal, which greatly narrows the possibility for application of large mechanized systems and concentration of production in them. In terms of the depth of coal seams, most deposits belong to the group of mines with a medium depth of exploitation, up to 500 m. The natural-geological conditions in the deposits have a decisive role in choosing certain technological solutions of exploitation, excavation systems (methods and technologies) and security measures in the underground mining facilities [15].

Characteristics of the research site

The "Strmosten" coal deposit has a syncline shape whose wings spread to the southwest. The axis of syncline extends from the east and sinks to the west at an angle of 10-20°. Limestones form the rim and, for the most part, the basis of productive series, thus presenting the paleorelief of basin together with the andensites. A developed coal seam with complex structure in the "Strmosten" deposit is stratified in three parts in the northeastern area, and in two parts in the central, eastern and western areas. The thickness of coal is from 2 to 8 m, on average 5.87 m at a depth of 380 to 525 m. The barren sediments in the layer are composed of marly and coal clays, marls, clayey sandstones and sandstones. Roof deposits, with the exception of the roof immediately above the coal seam which are of the Miocene age (red sandstones, marls, sandstones, limestones and conglomerates) are most often homogeneous and undamaged. Most of the roof sandstones are red sandstones, and the conditions of collapse during excavation and level of the manifestations of pit pressures depend on their structural and physico-mechanical characteristics [15,16,17,18].

Mine subsidence prediction based on the stochastic method and spatial analysis in GIS

The problem of surface subsidence and protecting infrastructure above the mining operations has been actual for decades in the “Strmosten“ deposit. In the Technical Mining Project, the parameters of displacement the undermined terrain and protection of the facilities of the Sladaja village from the impact of underground mining works above the "Strmosten" pit were determined [17]. According to the stochastic Patarić-Stojanović method, subsidence at any point was calculated in the coordinate system placed in the centre of a certain excavation panel (EP). This enabled to calculate the parameters of displacement process for each EP and obtain complete information on the consequences of undermining on the terrain surface in the form of subsidence (U) and slope (N), cumulatively after successive mining of 21 EP in the excavation field OP2 of the "Strmosten" deposit (Figure 6).

Calculating and graphical presenting the subsidence of undermined terrain is based on the originally developed software application MITSOUKO and the possibilities of spatial analysis in GIS, which are the result of modern scientific research [3,19,20,21,22]. Subsidence and deformations using the MITSOUKO are calculated by the simulation of excavation according to the polygonal EP and adopted mining dynamics, whereby the results were integrated and processed in GIS [3].

The basic formulas in the Patarić-Stojanović stochastic method, contain parameters dependent on the excavated space (a, l, H, d, b) and included in the mining project, as well as parameters (U_0, p, m, q), which are not determined in physical meaning, but define the behavior of the undermined terrain during consolidation and have to be brought into connection with the geometric characterristics of displacement process in the rock massif. Angles of draw ($\delta_1, \beta_1, \gamma_1$),

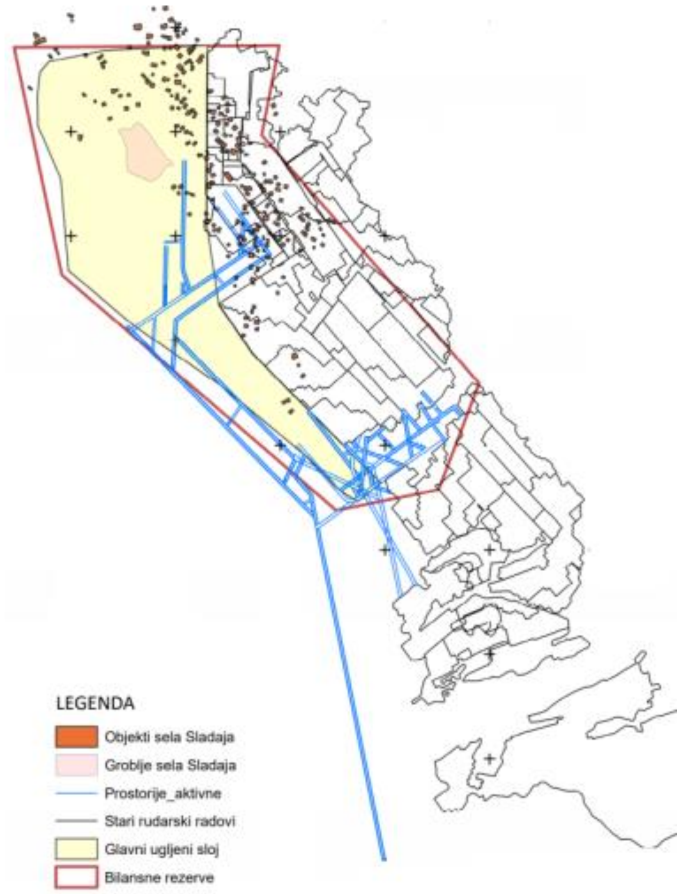

Figure 6 *Excavation field OP2 of the "Strmosten" deposit [17]*

which limit the zone affected by the movements on the ground surface, and angle of full subsidence (θ), as the basic angular parameters of displacement process, are among them [17]. When deriving the empirical formulas for the predictive subsidence calculation by the Patarić-Stojanović method, all points of the massif were observed, although the application of formulas is li-mited only to its surface-undermined terain, since a long-term systematic subsidence monitoring in mines over the world were performed mainly on the surface of undermined terrain. Finally, Figure 7 presents the mining operation plan and predicted the subsidence contour lines with the maximum subsidence value (U_{max} = − 2927 mm) after mining 21 excavation panels in 2038, that is the entire excavation field in the "Rembas" Resavica - Serbia coal mine [17].

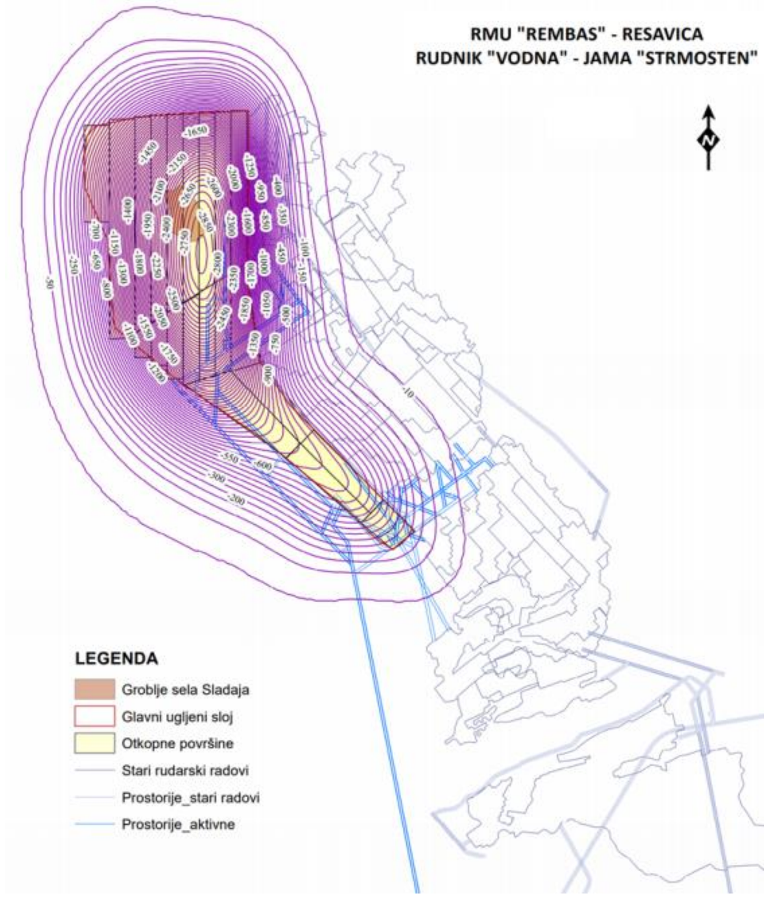

Figure 7 *Subsidence contour lines after mining the entire excavation field in the coal mine "Rembas" Resavica- Serbia [17]*

The MITSOUKO software, in the TILT module, calculates and tabulates the slope components at the specified points of defined EP. First, the slopes in a direction of the absolute coordinate system, formed by excavating one EP, are calculated, and then the procedure is repeated for all EPs. The components of the total slope in a direction of axes of the absolute coordinate system at a given point are obtained by summing the components of slopes of individual EPs [3,17].

Vulnerability Assessment of the Cemetery in the Sladaja Village

The cemetery in the Sladaja village covers an area of 10100 m^2 and a perimeter of 426 m. Specific objects, such as monuments in the area of the cemetery in the village, are most sensitive to changes in slope (N). On the other hand, this type of objects is not affected by the horizontal deformations (D) and radius of curvature of the terrain (R) because the dimensions of monuments are relatively small.

To protect the terrain surface from subsidence, and thus the rural cemetery in the village, the management of the Rembas - Resavica mine decided to leave a protective pillar in a part of coal seam below the subject area [18]. Based on the prediction [17], after excavation of all EPs without leaving a protective pillar, the calculated subsidence values in this area were from U =- 2,200 mm to U = - 2,920 mm (Figure 8).

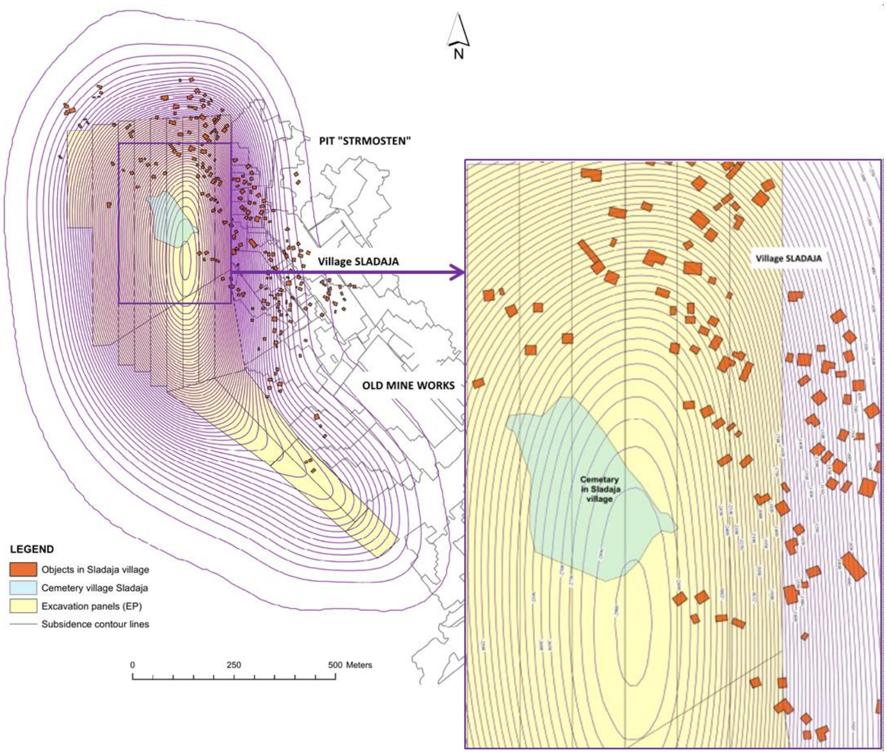

Figure 8 *Subsidence contour lines after mining the entire excavation field in the surrounding of the Sladaja village and cemetery [17]*

Based on these subsidence data, the slope values were calculated for the purpose of determining the deformations in the area of rural cemetery. The maximum slope was calculated at a value of N_{max} = 11.0 mm/m in the eastern part at a very border of the cemetery; slope values N in the central part of the cemetery ranged from 2 to 7 mm/m and increased in the eastern part to a value of 14 mm/m (Figure 9). Higher slope values in this part can be explained by the greater layer thickness (d = 6.5 m), smaller excavation depth (H ranged from 385 m to 415 m) and proximity of the old mining operations [17,18].

By comparison the calculated slope values with the allowable values, it can be concluded that the maximum slope value of 11 mm/m is below the allowable for objects of protection category IV (Table 1) [12,17,18].

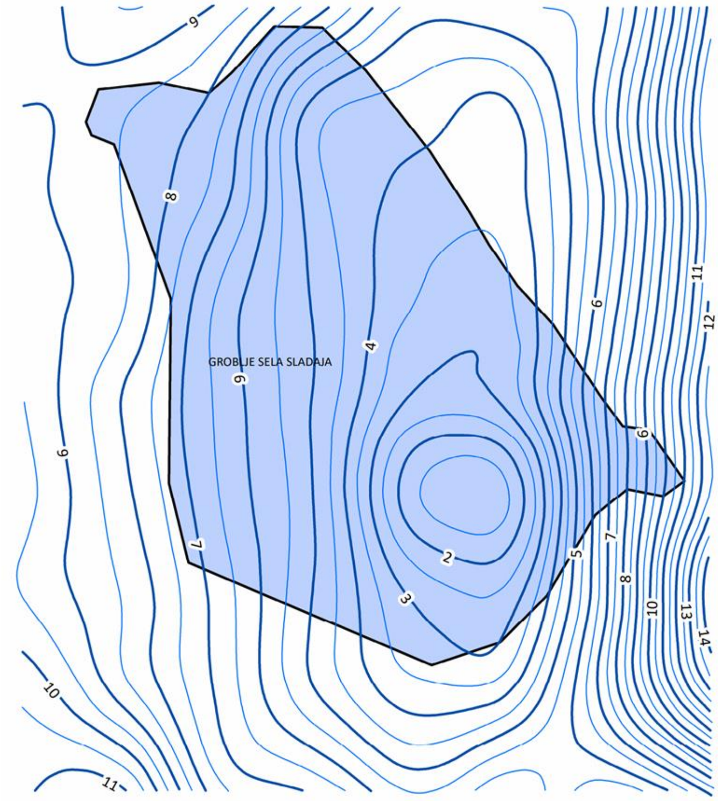

Figure 9 *Slope values in the region of Sladaja village [17]*

In the subsidence calculation, the deposit recovery is taken with a value of 65%, which can be considered as the highest in the given conditions of mining works of the "Strmosten" pit. According to the real estimation, the excavation losses will be significantly higher, i.e., the recovery will be lower, so there is a certain uncertainty in estimation the maximum slope value on the terrain surface. It is realistic to expect that the maximum slope value will be significantly below the calculated values in the area of cemetery in the village [17].

Based on the above facts concerning the predicted values of subsidence and slope, it can be concluded that under the area of cemetery in the Sladaja village when excavating the remaining coal reserves in the OP2 excavation field of the "Strmosten" pit in RMU "Rembas" – Resavica ***a protective pillar should not be left*** [17,18].

CONCLUSION

Deformations are relative changes that occur due to an uneven subsidence or horizontal displacements on the undermined terrain. Damages owing to the surface subsidence can be the result of surface slope changes, differential vertical displacements, and horizontal strains. Based on their values, the vulnerability level for individual objects on the terrain surface is determined. Case study presents a predictive calculation of subsidence and deformations using the input data from the underground coal mine "Rembas"- Resavica in Serbia by the MITSOUKO program package, designed based on the stochastic Pataric-Stojanovic method, and supported by spatial analyses in the GIS.

REFERENCES

[1] Bell F., Stacey T., Genske D., Mining Subsidence And Its Effect on the Environment: Some Differing Examples. Environmental Geology 40 (2000) 135–152.

[2] Malinowska A., Hejmanowski R., Building Damage Risk Assessment on Mining Terrains in Poland With GIS Application, International Journal of Rock Mechanics and Mining Sciences 47 (2010) 238–245.

[3] Vušović N., Vlahović M., Ljubojev M., Kržanović D., Software Solution for The Mine Subsidence Prediction Based on the Stochastic Method Integrated With The GIS. Mining and metallurgy Engineering Bor No. 1-2 (2020) 1-16.

[4] Sanmiquel L., Bascompta M., Vintró C., Yubero T., Subsidence Management System for Underground Mining. Minerals 8(6) (2018) 243.

[5] Litwiniszyn J., The Theories and Model Research of Movements of Ground Mass, Proceedings of the European Congress in Ground Movement, Leeds, 1957.

[6] Borela V. R., Stochastic Modeling And DEM Simulation of Granular Media Subsidence Due To Underground Activity, Master Thesis, Purdue University, West Lafayette, Indiana, 2016.

[7] Liu B., Liao G., Basic Regulars of Coal Mine Subsidence, China Industry Press, 1965.

[8] Li P., Yan L., Yao D., Study of Tunnel Damage Caused by Underground Mining Deformation: Calculation, Analysis, and Reinforcement. Advances in Civil Engineering, Article ID 4865161 (2019) 18.

[9] Patarić M., Stojanović A., Moving the Underground Terrain and Protecting Objects from Mining Works, University of Belgrade - Faculty of Mining and Geology, Belgrade, 1994.

[10] Djorđević D., Vušović N., Prognosis of the Displacement and Deformation of the Underground Terrain, University of Belgrade, Faculty of Mining and Geology, Belgrade 2014, pg. 311.

[11] Meng F., Li-Chun W., Jia-Sheng Z., Guo-Dong D., Zhi-hui N., Ground Movement Analysis Based on Stochastic Medium Theory. Hindawi Publishing Corporation e Scientific World Journal, Article ID 702561 (2014) 1-6.

[12] Malinowska A., Hejmanowski R., Dai H., Ground Movements Modeling Applying Adjusted Influence Function. International Journal of Mining Science and Technology, 30(2) (2020) 243–249.

[13] Djamaluddin I., Mitani Y., Esaki T., Evaluation of Ground Movement and Damage to Structures from Chinese Coal Mining Using A New GIS Coupling Model. International Journal of Rock Mechanics and Mining Sciences 48(3) (2011) 380-393.

[14] Blachowski J., Application of GIS Spatial Regression Methods In Assessment of Land Subsidence In Complicated Mining Conditions: Case Study of The Walbrzych Coal Mine (SW Poland). Nat Hazards (84) (2016) 997-1014.

[15] Ivković M., Systematization of Natural-Geological Conditions of Coal Exploitation in the Underground Mines in Serbia, Monograph, Committee for Underground Exploitation of Mineral Resources - Resavica. Family Press, Kragujevac, 2012 (in Serbian)

[16] Patarić M., Supplementary Mining Project For The Exploitation Of The Main Seam at The "Strmosten" Pit, Technical Mining Project for The Excavation Impact on The Damage of Objects on The Surface. Ugaljprojekat, Belgrade 1983.

[17] Vušović N., Technical Mining Project for Determining The Parameters of Displacement of Undermined Terrain and Protection of Sladaja Village Objects From The Infuence of Underground Mining Works Above The “Strmosten” Pit at RMU “Rembas” Resavica. University of Belgrade - Technical Faculty in Bor, Bor 2018.

[18] Djukić B., Vušović N., et al., Supplementary Mining Project for Development and Excavation the Remaining Reserves in the Excavation Field 2 of the Pit "Strmosten", The Mine "Vodna", RMU "Rembas" - Resavica, Ugaljprojekat, 2019 (in Serbian)

[19] Esaki T., Djamaluddin I., Mitani Y., A GIS-based Prediction Method To Evaluate Subsidence-Induced Damage From Coal Mining Beneath A Reservoir Kyushu, Japan. Q J Eng Geol Hydroge, 41(3) (2008) 381-392.

[20] Djamaluddin I., Mitani Y., Ikemi H., GIS-Based Computational Method for Simulating the Components of 3D Dynamic Ground Subsidence during the Process of Undermining, International Journal of Geomechanics, 12(1) (2012) 43-53.

[21] Banerjee T. K., Roy S., Dey S., A GIS Solution for an Integrated Underground Coal Mine Management: A Conceptual Framework. Journal of Management Policies and Practices 2(2) (2014)129-143.

[22] Cai Y., Jiang Y., Liu B., Djamaluddin I., Computational Implementation of A GIS Developed Tool for Prediction of Dynamic Ground Movement and Deformation Due to Underground Extraction Sequence. International Journal of Coal Science & Technology 3(4) (2016) 379-398.

MINING AND METALLURGY INSTITUTE BOR
UDK: 622

ISSN: 2334-8836 (Štampano izdanje)
ISSN: 2406-1395 (Online)

UDK: 622.271.3/.46(045)=111

DOI: 10.5937/mmeb2004057I

Miloš Ilić, Sandra Milutinović*, Branislav Rajković*, Daniela Urošević**

SELECTION OF A DEDUSTING SYSTEM FOR THE LIME STONE PREPARATION PLANT IN THE DEPOSIT "ZAGRADJE - 5"**

Abstract

This paper presents an example of a dedusting system in the deposit "Zagradje - 5" with the use of two different dedusting systems in order to more efficiently removal of harmful dust from the plant. The analysis is done by calculation and is a universal method of calculating the dedusting system, the results of which are necessary to verify the reliable operation of selected equipment. The technical characteristics of the filter and deduster as well as the technological scheme of dedusting are also given.

Keywords: *central dedusting, single deduster, bag filter*

1 INTRODUCTION

The problem of clean, unpolluted air in the industrial environments has become very acute today, and it must be solved very quickly. The air we breathe at workplaces in the factory halls is increasingly expressed in the number of concentrated dust particles. In fact, a large number of air pollutants in cities come from industry.

This paper is aimed at sizing and selection of technological and mechanical equipment that will ensure that the concentration of dust in the plant that occurs during operation is within the acceptable limits [7]. According to the standard SRPS Z.B0.001-1991 [8] entitled the "maximum permissible concentrations of harmful gases, vapors and aerosols in the atmosphere of working premises and construction sites" ("Official Gazette of SFRY", No. 54/91), the maximum permissible concentration of the total dust in the working medium for mineral dust with less than 1% SiO_2 is 15 mg/m^3.

The allowed concentration of dust in the air in the working environment is ensured by removal of dusty air from the source of dust by forced air circulation by means of a fan and its one-stage purification in the appropriate dedusting devices - bag filters so that the concentration of dust emitted into the atmosphere after purification is within the allowed limits.

According to the Decree on Limit Values for Emissions of Pollutants into the Air from the Stationary Pollution Sources, Except for the Combustion Plants (Official Gazette of RS, No. 111/2015) [9], the emission limit values for the total particulate matter in waste gas are 20 mg/m^3 for the mass flow greater than or equal to 200 g/h or 150 mg/m^3 for the mass flow of less than 200 g/h.

* *Mining and Metallurgy Institute Bor, Zeleni bulevar 35*

** *This work is financially supported by the Ministry of Education, Science and Technological Development of the Republic of Serbia, Agreement on the realization and financing of scientific research work in 2020 for the Mining and Metallurgy Institute Bor, no. 451-03-68 / 2020-14 / 200052.*

2 DESCRIPTION OF A TECHNOLOGICAL SCHEME OF DEDUCTING

Figure 1 shows the Technological scheme of dedusting installation, which shows the positions that will be processed in this text.

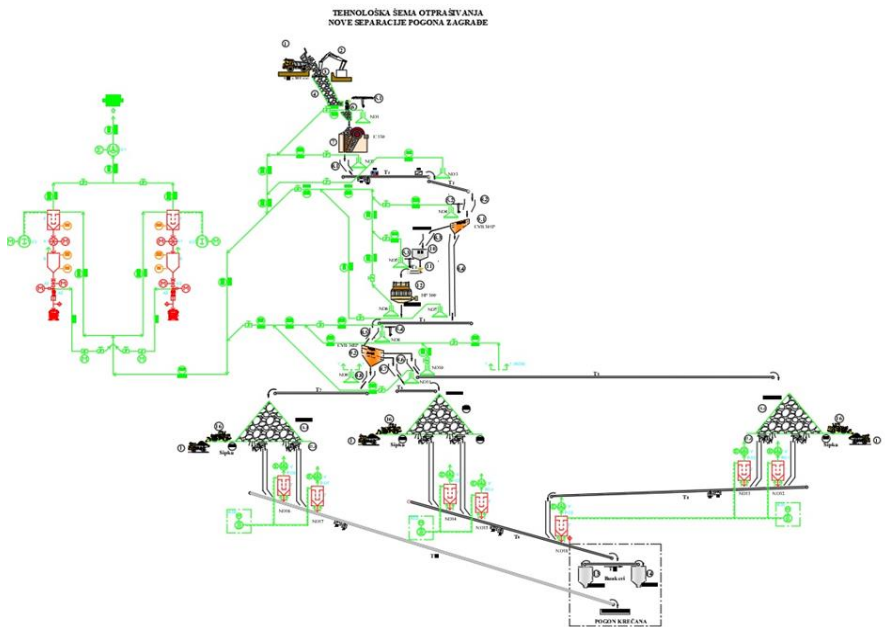

Figure 1 *Technological scheme of dedusting installation*

The central dedusting system will be installed next to the open warehouses at positions 15.1,15.2,15.3, and after that, the individual dedusters will be used.

The central dedusting system will use two HVP bag filters with involute input 8HVP504, filter area: 453,274 m². Dimensions of the HVP filter are: Ø4267.2 × 12911 mm.

From the open pit "Zagradje -5", the excavated limestone is transported by trucks to the shaft pit, where there is a robust steel grid with square openings. Limestone passes through the grid and then falls into the shaft pit. It descends directly to a jaw crusher. A feeder with chains (Pos.6) is provided in front of the jaw crusher. Through this feeder and one slider (Pos.8.1), limestone is dosed in a controlled manner into the hatch of the C130 jaw crusher. The "Jaw crusher C 130" performs the primary reduction of limestone size.

At the loading point above the primary crusher, a suction hood will be installed, pos. N01 on a section D01 which extracts the dusty air in an amount of 5000 m³/h, wherein the concentration of dust of 11.5 g/m³. Via the slide (Pos.8.1), the primarily crushed limestone is directed to a belt conveyor Pos. T-1 which transports the material to the conveyor at position T-2, which transports the limestone to the primary screen (Pos. 9.1).

A suction hood, pos. N02, is installed at the unloading point of the crusher, which sucks out dusty air in the amount of 14000 m^3/h, where the dust concentration is 11.87 g/m^3 on section D08.

A suction hood was installed at the pressure point pos. N03 between the belt conveyors T1 and T2, which sucks out dusty air in the amount of 3350 m^3/h, where the dust concentration is 6.5 g/m^3. The sieve has a sieving surface of 11.4 m^2 and circular openings of the sieving surface of the sieve of 88 mm (separation 80 mm). A suction hood, pos. N04, is installed above the sieve, which sucks out dusty air in the amount of 9800 m^3/h.

The screening of the sieve at Pos.9.1 through one slide (Pos.8.3) is directed to the receiving hopper of small capacity (Pos.10) below when there is a belt feeder T3 (Pos.11). The mentioned feeder doses limestone into the hatch of the secondary Cone crusher HP300 in which the secondary reduction of the size of limestone is performed (Pos. 12). A suction hood, Pos. N05, will be installed in the recessed place above the crusher, as well as at the exit from the crusher Pos. N06. An exhaust hood N07 will be installed at the loading point of the T4 belt conveyor from the sieving of the CVB301P sieve.

The crushed material of the secondary crusher HP 300 is combined with the sieve of the primary screen CVB 301P where another hood Pos. N07 will be installed, where the air capacities are 4000 m^3/h, 8500 m^3/h and 5400 m^3/h, respectively. The material is then transported with a T-4 conveyor to the sieving via a slide (Pos. 8.5), on a secondary sieve CVB 302P (Pos.9.2) manufactured by Metso minerals. The sieve has two sieving areas of 11.4 m^2. Above the sieve is placed the hood Pos.N08. The openings of sieving surfaces of wire panels are: 48 × 48 mm (separation 40 mm) and 23 × 23 mm (separation 20 mm). Screening of sieve I, sieving area on (Pos.9.2) size class - 80 + 40mm over one slide (Pos.8.7) is directed to the conveyor Pos. T-5, which deposits this size class, which is the first finished product of the limestone preparation plant, to the first open warehouse (Pos.15.1). From there, this size class - 80 + 40 mm through concrete openings and 4 bars (Pos.8.19-4) and 4 vibrating feeders (Pos.17.1) is dosed to the conveyor with a rubber conveyor belt Pos.T-8, which this size class, i.e. the finished product of crushing and screening is transported to the conveyor on Pos.T9, more precisely it is connected to this conveyor. Via the conveyor T9, which will work in alternating mode with the conveyor T8, i.e. the alternating functioning and dosing of the material will be provided, via the reversible conveyor T11, to the receiving bunkers of the lime plant (Pos. 13 and 14).The sieving of the secondary sieve CVB 302P of the I sieving surface, size class - 40 + 0.0 mm, immediately falls on the II sieving surface of the sieve CVB 302P (Pos.9.2) on the third sieving. The screening of this sieve CVB302P (Pos.9.2) II sowing surface, size class - 40 + 20 mm, is the second finished product of the limestone preparation plant. This size class -40 + 20 mm, i.e. the screening of the sieve II of the sieving surface is directed via one slide (Pos.8.7) to the conveyor Pos.T-6, which deposits this class of size to another open stack (Pos.15.2). From there, this size class - 40 + 20 mm is dosed to the transporter with a rubber conveyor belt via concrete openings and 4 bars (Pos.8.10-4) and 4 vibrating feeders (Pos.17.2). T-9 which this class of size i.e. the finished product of crushing and sifting is transported to the receiving bunker of the lime plant (Pos 13). Therefore, the two main products, fractions -80 + 40 mm and -40 + 20 mm, will be transported to the receiving bunkers, Pos.13 and 14, via the reversible conveyor T-11. This further means that the T-8 conveyor, as already mentioned in the text, "connects" to the T-9 conveyor, which disposes of the mentioned fractions in the receiving bunkers via the T-11 reversing conveyor, each intended for a specific fraction. While the conveyor T-8 is in operation mode, and delivers the size class - 80 + 40 mm, from the warehouse Pos.15.1, to the conveyor T-9, it is clear that the dosing of product -40 + 20 mm, through the warehouse 15.2, will be suspended and vice versa, when dosing, i.e. feeding the bunker pos.13, with the product - 40 + 20 mm, via the conveyor T-9 and T-11, feeding the bunker Pos.14 with the product - 80 + 40 mm, via the conveyor T-8, T-9 and T-11 will be suspended. The introduction of the T-11 reversible conveyor enables uninterrupted feeding of the provided bunkers for the appropriate required products, while the alternating operation of the T-8 and T-9 conveyors, more precisely the alternating dosing of materials from open warehouses to the mentioned conveyors, enables uninterrupted transport of defined products without mixing them.

Above the CVB302P vibrating screen, a NO8 extraction hood is provided for an air volume of 10200 m³/h at a dust concentration of 11 g/m³.

A closed hood will be installed at the loading point of screening sieves on the belt conveyor Pos. NO9, for the air capacity of 2650 m³/h, and at the unloading places Pos. NO10 and NO11 on belt conveyors T5 and T6 hoods for the air capacity 2300 m³/h and 1700 m³/h, respectively, where the dust concentration for all three suction points is 6.5 g/m³.

Furthermore, sieve of the screen CVB302P class size - 20 + 0.0 mm is a product that is transported by conveyor Pos.T-7 to the third open warehouse (Pos.15.3) and which will be through 4 concrete openings and 4 bars (Pos.8.11- 4) and 4 vibration feeders (Pos.17.3) for further treatment should be sent to a new conveyor with a rubber conveyor belt Pos. T-10, on micronization in the lime plant.

Individual dust collectors PO1-PO7 with compressor stations for production the compressed air for impulse blowing of individual dust collectors, manufactured by KDK-EKO or similar, will be installed at the filling points pos. NO12-NO17.

All dust will be unloaded from the central dedusting system from these two HPV filters into two pyramidal steel dust collection bunkers, and from there via telescopic devices for unloading material into trucks.

2.1 Calculation of the Suction Air Quantities

The quantities of exhaust air for all exhaust points are given in Table 1.

The quantities of exhaust air for loading places NO1, NO2, NO5 and NO6 were adopted from the literature No11k [1]. For loading places NO7, NO9, NO10, NO11, NO12, NO13, NO14, NO15, NO16, NO17, NO18, the Molčanov [2] calculation method was used. And for loading places NO4 and NO8, the Volkov method was used.

The **Molčanov** calculation method is the following:

The quantity of suction air is calculated according to the following formula:

$$L_{NO} = L_E + L_N [m^3/h]$$

where:

L_E - quantity of air introduced by material

L_N - quantity of air entered through the openings

Quantity of air introduced by material is calculated by the following formula:

$$L_E = 0.12 * k_y * V_m * v_k^2 [m^3/h]$$

where:

k_y - coefficient (depending on construction and type of material) - in this case we adopt 1.4 for ordinary loading troughs

V_m – volume flow of material

v_k – final speed of material

The final speed of material is calculated by the following formula:

$$v_k = 4.43 * \sqrt{H * (1 - f_t * ctg \propto)}$$

where:

H – height of material drops

f_t - coefficient of material friction against the walls (according to the document SN 155-61[3] it can be seen for lime 0.56)

$\propto$ - inclination angle of a section

Volume flow of material is calculated:

$$V_m = \frac{Q}{\rho}[m^3/_h]$$

where:

Q – mass flow of material

ρ - bulk density of material (according to OHTII-10-85[4] for lime is 1.5 $\left[t/_{m^3}\right]$)

The quantity introduced through the openings is calculated by the formula:

$$L_N = A * C * B^2 * v_k * M_y$$

where:

A - coefficient for material loading from a belt conveyor

C – coefficient for a belt width 800 mm

M_y - coefficient for impassable loading place

B – width

By **Volkov**[5] the quantity of suction air for sieve is calculated by the formula:

$$L_{NO} = L_E + L_N[m^3/_h]$$

where:

L_E – quantity of air introduced by material

L_N – quantity of air that enters through the openings

The amount of air introduced with the material is calculated according to the following formula:

$$L_E = 0.2 * V_m * v_k^2[m^3/_h]$$

where:

V_m – volumetric flow of material

v_k – final speed of material

Final speed of material is calculated by the following formula:

$$v_k = 4.43 * \sqrt{H * (1 - f_t * ctg \propto)}$$

where:

H – height of material falls

f_t - coefficient of material friction against the walls (according to the document SN 155-61[3] it can be seen for lime 0.56)

$\propto$ - inclination angle of a section

Volume flow of material is calculated:

$$V_m = \frac{Q}{\rho}[m^3/_h]$$

where:

Q - mass flow of material

ρ- bulk density of material (according to OHTII -10-85[4] for lime is 1.5 $\left[t/_{m^3}\right]$)

The quantity introduced through the openings is calculated by the formula:

$$L_N = 3600 * F * v$$

where:

F– surface of tightness

v - air speed through tightness (by Volkov [5] it can be adopted for sieves of 2)

$$F = 0.1 * P$$

where:

0.1 - coefficient of tightness (by Volkov it can be adopted for sieves of 0.1)

P – surface

Table 1 is formed on the basis of given calculations.

Table 1 *Amount of suction air in the limestone preparation plant*

Suction mark	Amount of air in m^3/h	Dust concentration in g/m^3
NO1	5000	11,50
NO2	14000	12,00
NO3	3350	6,50
NO4	9800	11,00
NO5	4000	20,00
NO6	8500	20,00
NO7	5400	6,50
NO8	10200	11,00
NO9	2650	6,50
NO10	2300	6,50
NO11	1700	6,50
NO12	1260	6,50
NO13	1700	6,50
NO14	1260	6,50
NO15	1700	6,50
NO16	1260	6,50
NO17	1700	6,50
NO18	2520	6,50

2.2 Dust Concentration at Suction Points

For dust concentration at suction points, the recommendations for certain devices, given in the literature SN 155-61[3], were used.

Following the example of calculation the dust concentration on the following sections, Table 2 is given.

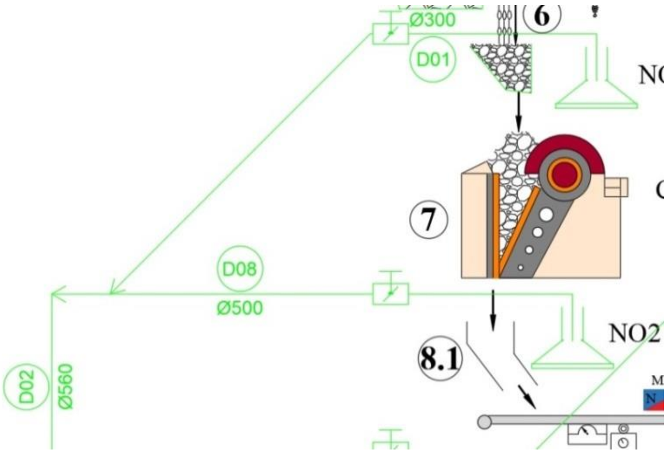

Figure 2 *Section view*

$$Q_{DO2} = Q_{DO1} + Q_{DO8} = 5000 + 14000 = 19000\ [m^3/h]$$

where:

Q_{DO2}– air quantity in given section

$$C_{DO2} = \frac{C_{DO1} * Q_{DO1} + C_{DO8} * Q_{DO8}}{Q_{DO2}} = \frac{5000 * 11.5 + 14000 * 12}{19000} = 11.87\ [g/m^3]$$

where:

C_{DO2}– dust concentration in given section

Table 2 *Air quantities and dust concentrations in given sections*

Section mark	Amount of air in m^3/h	Dust concentration in g/m^3
D01	5000	11,50
D02	19000	11,87
D03	22350	11,06
D04	50500	12,80
D05	66900	11,90
D05a	33450	11,90
D05b	33450	11,90
D06a	33450	0,0119
D06b	33450	0,0119
D06	66900	0,0119
D07	66900	0,0119
D08	14000	12,00
D09	3350	6,50
D010	8500	20,00
D011	12500	20,00
D012	22300	16,04
D013	27700	14,18
D014	4000	20,00
D015	9800	11,00
D016	5400	6,50
D017	2650	6,50
D018	4950	6,50
D019	15150	9,53
D020	16850	9,22
D021	2300	6,50
D022	1700	6,50
D023	10200	11,00

Based on the given parameters, the machine design and selection of dedusting system equipment in the limestone preparation plant is done.

3 TECHNICAL DESCRIPTION OF A DEDUSTING SYSTEM

The dedusting system of the limestone preparation plant comprises two units or phases. **Phase 1** includes a transport system from the primary crushing to the two-level sieve facility, and since it is a dependent system that is in operation at the same time, a central dedusting system is adopted where dust is suctioned from all dust sources that are in operation at the same time.

The central filter plant is located on a filter facility located on the existing road near the two-level sieve facility. It consists of two symmetrical lines that work in parallel. Each line consists of a bag filter with air blowing under which there is a pyramidal steel bunker for dust collecting with the associated equipment. Technical characteristics of the filter are as follows:

Type: HVP bag filter with involute inlet
Producer: CAMCORP
Designation: 8HVP504
Filter area: 453,274 m^2
Filter capacity: 33450m^3/h
Dimensions: Ø4267,2x12911mm
Total mass: 9915 kg

From the fan, the purified air is ejected into the atmosphere through the exhaust element with a protective net. On this section, a connection for measuring and sampling dimensions is provided, and in its vicinity, the same connection is also provided on the incoming pipeline of dusty air on the section. The choice of a fan with a frequency regulator enables a relaxed start when starting the fan, easier regulation of the plant as well as the possibility for more flexible operation of the plant. Dust separated in the filters is first collected in the conical lower part of the filter. A level measuring device for signaling the maximum level as protection against overfilling will be mounted on the wall of the conical part of the filter. From the conical part of the filter, dust is discharged into bunkers via a star feeder on electric drive.

Phase 2 includes dedusting of the loading parts of conveyor, and since the transport system is independent, i.e. the conveyors work independently of each other, an individual dedusting system was adopted. The mentioned system is based on purification the dusty air in a deduster itself (which is installed at the suction point), and then returns it to the belt conveyor as purified. Depending on the required amount of air for suction, 3 dedusters, manufactured by KDK-EKO, with the following characteristics were selected:

- Designation: KFE-12-TV/2-R
- Filter area15 m^2
- Capacity: 1260 m^3/h
- Power: 4 kW

- Designation: KFE-16-TV/2-R
- Filter area: 20 m^2
- Capacity: 1700 m^3/h
- Power: 4 kW

- Designation: KFE-24-TV/2-R
- Filter area: 30 m^2
- Capacity: 2520 m^3/h
- Power: 5 kW

3.1 Calculation

The following calculation formulas were used in the aerodynamic [6] calculation of the pressure drop:

$d = \sqrt{\frac{4 \cdot Q}{3600 \cdot \pi \cdot v}} [m]$ - diameter of a pipeline section (equivalent diameter)

$\lambda = 0.013 + \frac{0.001}{d}$ – friction coefficient

$v_{kr} = 0.3 \cdot \sqrt{c \cdot g \cdot d \cdot \frac{\rho_č}{\rho_v}} \left[\frac{m}{s}\right]$ - critical air speed

$\Delta p_v = \left(l \cdot \frac{\lambda}{d} + \Sigma\varsigma\right) \cdot \frac{\rho_v \cdot v^2}{2} [Pa]$ - presure drop in clean air flow

$\Omega = 0.02 \cdot \frac{v^2}{g \cdot \frac{d}{2} \cdot cos\beta}$ - pressure increase factor

$\Delta p_č = \Delta p_v \cdot (1 + k \cdot c)[Pa]$ – pressure drop during dusty air flow

Individual labels in formulas have the following meanings:

$v \left[\frac{m}{s}\right]$ - air speed

$Q \left[\frac{m^3}{h}\right]$ - volume air flow

$c \left[\frac{kg_č}{kg_v}\right]$ - concentration of solid particles in the air

$\rho_č = 2660 \left[\frac{kg}{m^3}\right]$ - density of solid particles

$\rho_v = 1.2 \left[\frac{kg}{m^3}\right]$ - air density

$g = 9.81 \left[\frac{m}{s^2}\right]$ - gravitational constant

$l[m]$ - length of a pipeline section

$\Sigma\varsigma[-]$ - sum of the coefficients of local resistance of a pipeline section

$\beta[°]$ - inclination angle of a pipeline section

$k = 1.4[-]$ za $\Omega > 1$ - coefficient of pressure increase

$k = 0.4 \div 0.6[-]$ za $\Omega < 1$- coefficient of pressure increase

The total pressure drop includes the additional pressure drops in the appropriate sections, as follows:

1. $\Delta p_p = 50[Pa]$ - underpressure in suction hoods
2. $\Delta p_f = 2000[Pa]$ - pressure drop in a bag filter with pulse shaking

Calculation of the pressure drop in a pipeline for the most unfavorable circuit is given in the table.

AERODYNAMIC CALCULATION OF AIR PIPELINE FOR DEDUSTING OF THE LIMESTONE PREPARATION PLANT IN ZAGRADJE

Calculation of pressure drop for the circuit with sections D01, D02, D03, D04, D05, D05a, D06a, D06 and D07 for dedusting from the loading place above the primary crusher - suction point NO1

1	2	3	4	5	6	7	8	9	10	11	12	13	14	15	16	17	18	19
NO. OF SECTION	SECTION LENGTH	VOLUME FLOW	VOLUME FLOW	SPEED	CALCULATION DIAMETER	ADOPTED OUTER DIAMETER	ADOPTED INNER DIAMETER	ACTUAL SPEED	CONCENTRATION OF PARTICLES IN AIR	CRITICAL SPEED	FRICTION COEFFICIENT	SUM OF LOCAL RESISTANCE COEFFICIENTS	PRESSURE DROP IN AIR FLOW	PRESSURE INCREASE FACTOR	PRESSURE INCREASE COEFFICIENT	PRESSURE DROP IN FLOW DUSTY AIR	PRESSURE DROP DUE TO THE ADDITIONAL RESISTANCES	TOTAL PRESSURE DROP
	L	Q*	Q	v*	d*	d	d	v	c	vkr	λ	Σς	Δpv	Ω	k	Δpč	Δpd	Δp
	m	m^3/h	m^3/s	m/s	m	mm	mm	m/s	kgč/kgv	m/s	-	-	Pa	-	-	Pa	Pa	Pa
01	11.1	5000	1.389	20	0.297	300	294	20.46	0.00958	2.35	0.016	1.62	562.6	5.81	1.4	570.1	50	620.1
02	145.1	19000	5.278	20	0.580	560	554	21.90	0.00989	3.27	0.015	0.72	1322.9	3.53	1.4	1341.2	0	1341.2
03	15.5	22350	6.208	20	0.629	630	624	20.30	0.00922	3.35	0.015	0.30	163.9	2.69	1.4	166.1	0	166.1
04	65.0	50050	13.903	20	0.941	900	894	22.15	0.01067	4.32	0.014	0.51	452.4	2.24	1.4	459.2	0	459.2
05	35.1	66900	18.583	20	1.088	1120	1114	19.07	0.00992	4.65	0.014	0.39	180.6	1.33	1.4	183.1	0	183.1
5a	15.0	33450	9.292	20	0.769	800	794	18.77	0.00992	3.93	0.014	1.69	414.2	1.81	1.4	419.9	0	419.9
6a	34.9	33450	9.292	15	0.888	900	894	14.81	0.00001	0.13	0.014	1.92	325.0	1.00	1.4	325.0	2000	2325.0
06	16.1	66900	18.583	15	1.256	1250	1244	15.29	0.00001	0.16	0.014	0.53	99.4	0.77	0.5	99.4	0	99.4
07	17.0	66900	18.583	15	1.256	1250	1244	15.29	0.00001	0.16	0.014	1.43	227.1	0.77	0.5	227.1	0	227.1
																Total pressure drop		5614.1

4 CONCLUSION

If the problem of spreading the air pollutants would be solved where it is regenerated, then it would be a significant contribution to the preservation of the human environment. The importance of clean, unpolluted air in the industrial zones is well known. Well-designed and executed ventilation offers a solution that will bring the air pollutants at least below the maximum allowable concentrations, and thus provide the necessary protection for workers in such conditions. This paper gives a practical solution to the problem related to the appearance of increased dust concentration at the suction points in the plant for limestone preparation Zagradje-5.

Figure 1 defines an optimal layout of air purification equipment. Air purification equipment can be installed in other ways depending on the specific conditions.

REFERENCES

[1] Приложение N°11к Приказу Министра охраны окружающей среды Республики Казахстан от 18 04 2008 года N°100-п: «Методика расчёта выбросов загрязняющих веществ в атмосферу от предприятий по производству строительных материалов»

[2] Борис Семенович Молчанов: «Проектирование промышленной вентиляции», Стройиздат, Ленинград, 1970

[3] Государственный Комитет Совета Министров СССР по делам строительства: «Указания по проектированию санитарно-технических устройств основных цехов и отделений заводов огнеупоров СН 155-61», Москва, 1961

[4] ОНТП-10-85 Минстройматериалов СССР: «Общесоюзные нормы технологического проектирования предприятий по производству извести»

[5] Волков Олег Димитриевич: «Проектирование вентиляции промышленного здания», Харьков, 1989

[6] M. Bogner, D. Vuković: Problems from Mechanical and Hydro-mechanical Operations, Faculty of Mechanical Engineering, Belgrade, 1991 (in Serbian)

[7] Supplementary Mining Project for Excavation and Preparation of Limestone in the Deposit "Zagradje-5", Mining and Metallurgy Institute, Bor, 2020 (in Serbian)

[8] Standard SRPS Z.B0.001-1991 entitled "Maximum Permissible Concentrations of Harmful Gases, Vapors and Aerosols in the Atmosphere of Work Premises and Construction Sites" ("Official Gazette of SFRY", No. 54/91)

[9] Decree on Limit Values for Emissions of Pollutants into the Air from the Stationary Pollution Sources, Except for Combustion Plants ("Official Gazette of RS", No. 111/2015)

MINING AND METALLURGY INSTITUTE BOR
UDK: 622

ISSN: 2334-8836 (Štampano izdanje)
ISSN: 2406-1395 (Online)

UDK: 681.325:622.271.2(045)=111

DOI: 10.5937/mmeb2004067B

Dejan Bugarin, Ivan Jelić*, Miljan Gomilanović*, Aleksandar Doderović**

APPLICATION OF THE COMFAR III SOFTWARE PACKAGE IN DEVELOPMENT A FEASIBILITY STUDY OF INVESTMENT ON AN EXAMPLE OF TECHNICAL-CONSTRUCTION STONE OF THE OPEN PIT GELJA LJUT**

Abstract

This work presents the application of the COMFAR III software package in development a feasibility study of investment. The application of this program enables an efficient analysis of investment justification and numerous variations of both input and graphic and alphanumeric output data. The methodological basis of economic analysis, used in this software package, is based on decades of experience of economists, engineers, managers, ecologists and experts from the other fields, as well as on the experience of numerous investment projects within the United Nations Industrial Development Organization. The applied methodology is the current standard in the field of economic evaluation and analysis of the industrial development projects. The software package was used on a specific example of the open pit of technical stone Gelja Ljut-Gacko, in a function of providing the concession right of this deposit for the needs of the Gacko Mine and Thermal Power Plant.

Keywords: *Investment Feasibility Study, COMFAR III, investments, costs, techno-economic assessment*

1 INTRODUCTION

The Mine and Thermal Power Plant Gacko a.d. Gacko is a subsidiary that operates within the Mixed Holding "Elektroprivreda Republike Srpske", Trebinje. The main activity is the production of thermoelectric energy, and the other special activities are lignite mining at the open pit, quality improvement, transport and storage, quarrying, crushing and breaking of construction stone, chalk and limestone, machine repair, electrical equipment repair and sale of electricity to the customers.

In order to realize its basic goal, to ensure the production of planned amount of electricity, the Mine and Thermal Power Plant Gacko performs a number of activities in the function of stable, reliable and economically efficient production. The complexity of production process, the number and variety of activities and influential factors that are one of the basic characteristics of production within the Mine and Thermal Power Plant Gacko [1]. In the set of activities related to the surface exploitation of lignite and technological processes of excavation and exploitation of coal, there are significant needs for the technical-construction stone of appropriate quality within the preparatory and auxiliary works.

* *Mining and Metallurgy Institute Bor*

** *This work is financially supported by the Ministry of Education, Science and Technological Development of the Republic of Serbia, Agreement on the realization and financing of scientific research work in 2020 for the Mining and Metallurgy Institute Bor, no. 451-03-68 / 2020-14 / 200052.*

In the process of exploitation, technical stone is regularly used for the needs of maintenance the transport and access roads [2], various embankments, construction of plateaus, drainage filling, construction of protective barriers and embankments for the purpose of improving the bearing capacity and stabilization of soil and slopes as well as the other purposes. In addition to this, in the coming period, there is a significant additional need for technical stone in order to regulate the flow of the river Musnica (Phase II) and construction the infrastructure facilities that accompany mining at the open pit.

The need for this type of material is variable and is mainly in the function of dynamics the development of coal mining works. Based on previous experiences, the annual need for limestone as a technical-construction stone of about 30,000 čm^3 has been estimated. For the construction of infrastructure facilities in 2020 and 2021, it is necessary to provide significantly larger quantities of limestone and they are estimated at an additional about 70,000 čm^3. In the previous period, the needs for technical stone the Mine were mainly provided from the open pit Ponikve, which also belongs to the Mine and TPP Gacko.

Considering the dislocation of the surface mine Ponikve in relation to the open pit of lignite, there was a need for analysis the provision of technical stone from the other sources as well. The Gelja Ljut limestone deposit has been identified as one of the possible sources of supply with technical-construction stone.

The area of concession right for exploitation the technical construction stone - limestone at the location of Gelja Ljut borders the concession area of the open pit Gacko - Centralno polje in its southwestern part. The subject concession area is in the immediate vicinity of the regulated course of the river Mušnica and the zone of influence the designed works on the external disposal of overburden and waste from the open pit Gacko - Centralno polje. In addition to this, a road and pipeline are located in the immediate vicinity, the infrastructure facilities that are maintained and exploited by the Mine and Thermal Power Plant Gacko.

As a basis for the future business decision, the management of the Mine and Thermal Power Plant Gacko required a development of a Feasibility Study for investment in providing the concession right at the Gelja Ljut deposit with a comparative economic analysis of providing the technical stone from the Ponikve location. The main goal of this study was to determine the economic parameters of investment in providing, purchase, a concession right for exploitation of limestone for the needs of the Mine and Thermal Power Plant Gacko at the Gelja Ljut deposit in order to make an investment decision.

In order to make this assessment of the Project success as objective as possible, in addition to the economic assessment of providing the concession in question, the other important factors were also considered, such as the possibility of using this space to form an external landfill of the Gacko - Centralno open pit and other forms of this area usage, and also an assessment was given for possible legal, technical and environmental risks both in the case of providing a concession and in the case of maintaining the existing situation [3]. The techno-economic assessment also includes the results of a comparative analysis of limestone providing from the existing open pit Ponikve and the open pit Gelja Ljut.

When providing the technical stone, it was necessary to keep in mind some special requirements, which differ from the usual system of providing technical stone for the market. In the first place, there is a high variability in the need for technical stone at the open pit. Requirements can often be urgent and high capacities are needed only for a limited time. In the periods of construction the important infrastructure facilities, it is necessary to provide the quantities that exceed the capacity of the open pit many times, and these requirements are expressed in the periods related to the construction of the facilities themselves, i.e. they do not have a permanent character.

Also, the special purpose of purchasing a concession at the Gelja Ljut site is to prevent the occurrence of conflicts of interest in two neighboring concession areas. As both spaces are in the zone of influence of the other, it is possible for them to appear, and in the recent past there have been such cases when the interests of the owners of both exploitation fields are inconsistent. So far, this has not affected the works on coal exploitation at the open pit Gacko - Centralno polje in a way that would prevent the realization of planned works, but such a scenario is known in the future considering the formation of an external landfill next to the concession area of Gelja Ljut.

Based on the above given, three main purposes of financing have been identified as follows:

- providing a raw material base for the production of technical stone,
- providing adequate quantities of technical stone dynamically, capacitively and qualitatively in accordance with the needs of the Mine and the Thermal Power Plant,
- unification of concession areas in order to prevent conflicts of interest and use of the concession area of the Gelja Ljut deposit for formation an external landfill of the Gacko - Centralno polje open pit.

2 THE OPEN PIT GELJA LJUT

On the territory of the municipality of Gacko, as a distinctly limestone area, two concessions are currently issued for the exploitation of technical-construction stone - limestone. There are two limestone quarries - Ponikve and Gelja Ljut. The position of the concession boundaries is shown in Figure 1.

Figure 1 *Position of the concession area of the limestone deposit as a construction-technical stone Ponikve (1) and Gelja Ljut (2)*

The Gelja Ljut deposit is located on the southern edge of the Gatačko field. Since the development of the open pit Gacko - Centralno polje is planned along the entire Gatacko field, the deposit is located on the south side of the future con tour [4]. The altitude of the deposit area generally ranges between 930 and 970 m above sea level. The deposit is defined within the exploitation field bounded by the coordinates of the breakpoints shown in Table 1 and Figure 2.

Table 1 *Coordinates of the breaking points of the boundaries of exploitation field of the deposit of construction stone - limestone "Gelja Ljut" near Gacko*

Point	Coordinates of points	
	X	Y
A	4,777,264	6,541,716
B	4,777,415	6,541,716
C	4,777,520	6,541,815
D	4,777,510	6,542,245
E	4,777,105	6,542,245
F	4,777,105	6,542,143
G	4,777,190	6,542,850
A	4,777,264	6,541,716

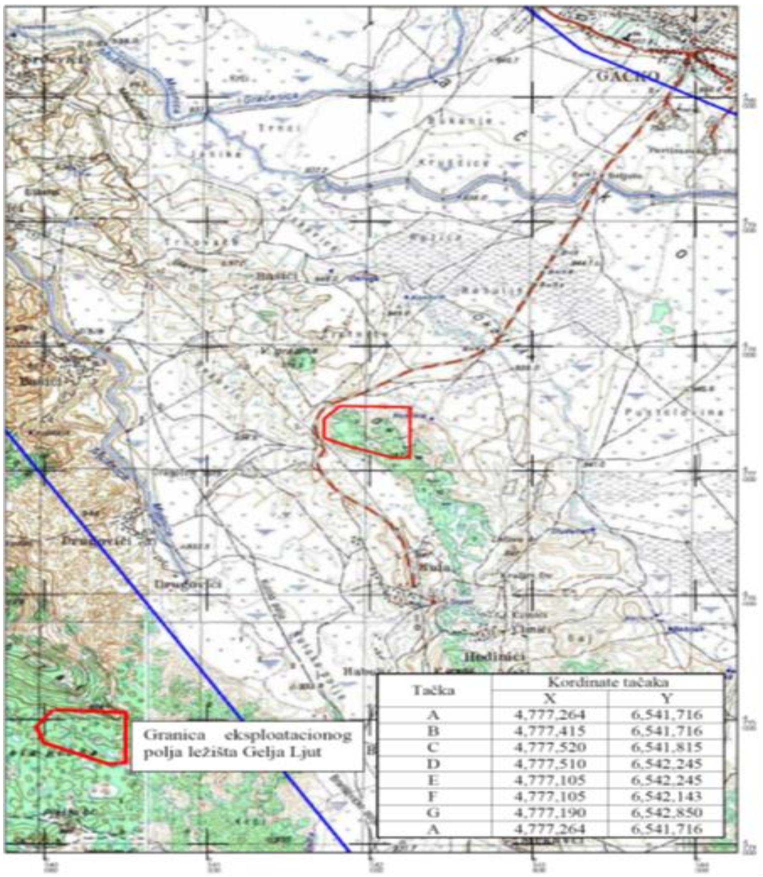

Figure 2 *Position of the exploitation field Gelja Ljut*

The open pit Gelja Ljut was opened in the 80s of the 20^{th} century. During its existence, the open pit changed several owners, while the production was carried out on a larger or smaller scale, with longer or shorter interruptions. The mine is about 15 km away from the settlement of Gacko, while it is 3.6 km away from the open pit Gacko-Centralno polje. Until the moment when the works on coal exploitation in the roof coal series cut the road to the village of Kula, the distance from Gacko was 4 km.

3 COMFAR III

For the calculation of economic parameters, the COMFAR software package, formed by the United Nations Industrial Development Organization (UNDO), and in cooperation with the governments, business associations and individual companies engaged in solving the industrial problems, was used. COMFAR, in essence, is a tool for forming a computer model for feasibility analysis and reporting. The main module of program accepts the financial and economic data, prepares the financial and economic reports and graphical representations and calculates the performance measures. The additional modules help in the analytical process.

The methods of economic analysis developed by the UNIDO and costs and benefits of added value are included in the program, taking into account the methods used by the major international development institutions. The program is applicable for an analysis of investments into the new projects and expansion or rehabilitation of the existing companies, e.g. in the case of privatization projects. For joint ventures, the financial perspective of each partner or class of shareholders can be developed. The analysis can be performed using various assumptions regarding the inflation, currency revaluation and price escalation.

COMFAR III Expert is available for MS Windows 98 / ME and MS Windows 2000 / KSP / 2003 / Vista.

After determining the type of project in the program (industrial, agro-industrial, infrastructural, tourism, mining or environmental) and the level of analysis (feasibility or feasibility study), the user is guided through the data entry, data structuring, calculations, display and printing of results and charts.

COMFAR III Expert allows users a flexibility in determining the detailed analysis. The main features are: [5]

- new option or expansion / rehabilitation project
- joint venture option
- CDM / JI project option (Kyoto Protocol)
- variable planning horizon - up to 60 years
- variable time structure: construction and start-up
- up to 20 products can be listed
- data can be entered in up to 20 currencies
- direct cost option
- escalation / inflation option
- economic analysis option

The standard structure of investment costs, operating and marketing costs is extended to the entry of subchapters. Sources of financing include the capital, long-term loans, short-term finance and defining the terms of profit distribution (Figure 3).

With these facilities, the COMFAR III Expert can be applied to all types of investment projects, investments with the medium-sized companies, to the analysis of large projects or complex production units.

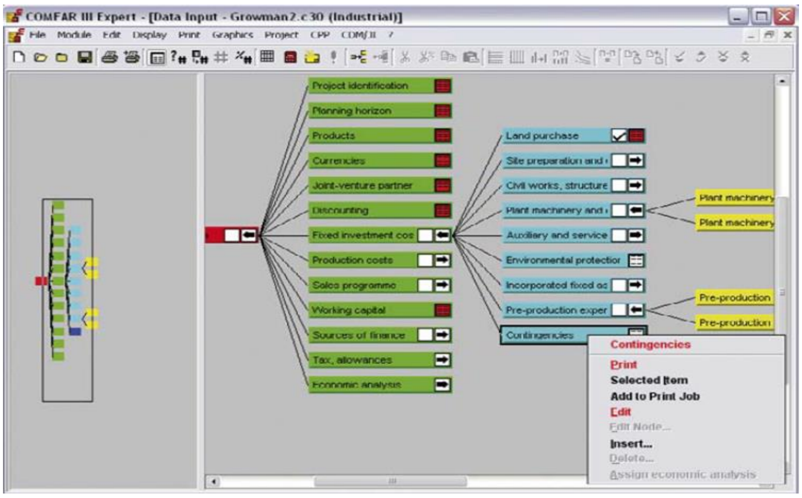

Figure 3 *Data structure within the software*

COMFAR III Expert - Cash flow model:

The COMFAR system distinguishes the cash flows in domestic and foreign currency, and at the same time requires changes in the exchange rates. A number of standard functions are available for calculating the net working capital, debt, annual depreciation of fixed assets and income tax. From different areas of finance and efficiency, the beneficiary can select those data needed to evaluate the project. Direct prices, allocation of indirect costs to profit centers and analysis in constant or current prices are also available.

Financial analysis:

The COMFAR III Expert, based on the entered data, provides the following information in Table with data, investment costs. production costs, production and sales program. Sources of financing and repayment, business results (financial cash flow, discounted cash flow, income statement, balance sheet, data on direct costs and product profitability - Figure 4).

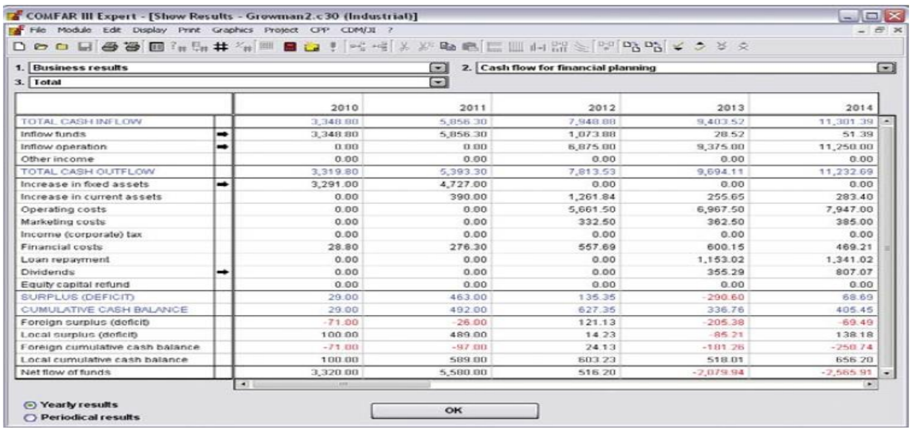
COMFAR III Expert - [Show Results - Growman2.c30 (Industrial)]

1. Business results 2. Cash flow for financial planning
3. Total

	2010	2011	2012	2013	2014
TOTAL CASH INFLOW	3,348.80	5,856.30	7,948.88	9,403.52	11,301.39
Inflow funds	3,348.80	5,856.30	1,073.88	28.52	51.39
Inflow operation	0.00	0.00	6,875.00	9,375.00	11,250.00
Other income	0.00	0.00	0.00	0.00	0.00
TOTAL CASH OUTFLOW	3,319.80	5,393.30	7,813.53	9,694.11	11,232.69
Increase in fixed assets	3,291.00	4,727.00	0.00	0.00	0.00
Increase in current assets	0.00	390.00	1,261.84	255.65	283.40
Operating costs	0.00	0.00	5,661.50	6,967.50	7,947.00
Marketing costs	0.00	0.00	332.50	362.50	385.00
Income (corporate) tax	0.00	0.00	0.00	0.00	0.00
Financial costs	28.80	276.30	557.69	600.15	469.21
Loan repayment	0.00	0.00	0.00	1,153.02	1,341.02
Dividends	0.00	0.00	0.00	355.29	807.07
Equity capital refund	0.00	0.00	0.00	0.00	0.00
SURPLUS (DEFICIT)	29.00	463.00	135.35	-290.60	68.69
CUMULATIVE CASH BALANCE	29.00	492.00	627.35	336.76	405.45
Foreign surplus (deficit)	-71.00	-26.00	121.13	-205.38	-69.49
Local surplus (deficit)	100.00	489.00	14.23	-85.21	138.18
Foreign cumulative cash balance	-71.00	-97.00	24.13	-181.26	-250.74
Local cumulative cash balance	100.00	589.00	603.23	518.01	656.20
Net flow of funds	3,320.00	5,580.00	516.20	-2,079.94	-2,565.91

Yearly results
Periodical results
OK

Figure 4 *Example of cash flow*

Economic analysis (macro level):

The economic analysis option allows the user to enter the approximate (expected, assumed) prices (to express inputs and project results in terms of economic prices) and to calculate the economic rates of return (Figure 5), value added, foreign exchange effects and effects on employment. All results can be calculated, including and excluding the external economic effects.

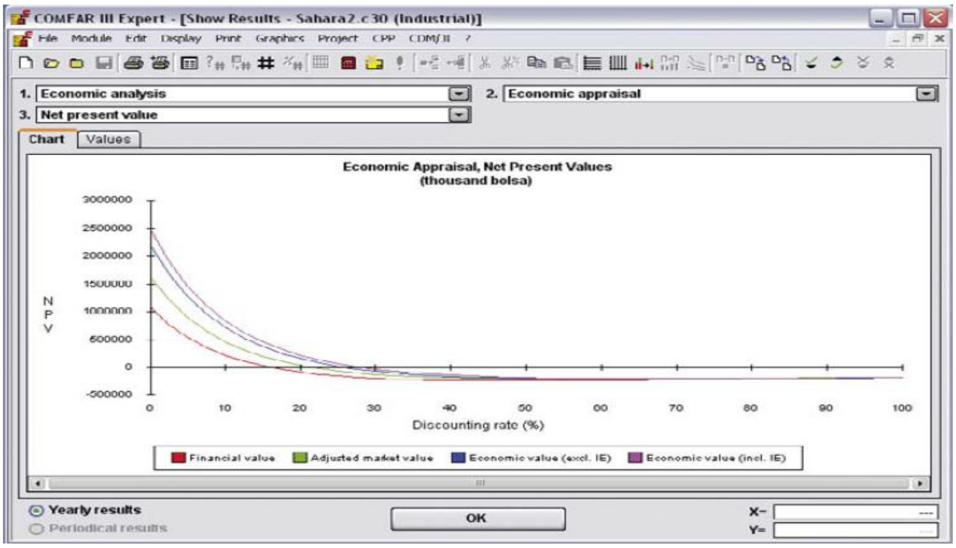

Figure 5 *Form of the program with presentation the results of economic analysis*

The COMFAR III Expert provides the user with an overview of possibilities of the average graphic presentation, as well as the structure of cash flows, costs and revenues (Figure 6).

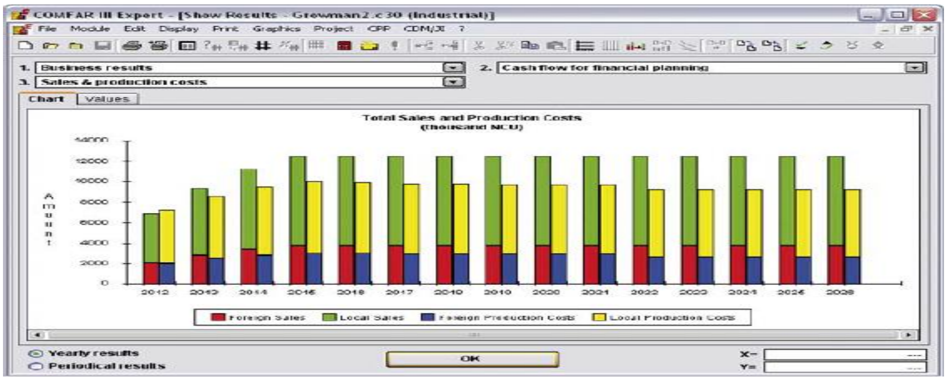

Figure 6 *An example of output graph*

Sensitivity analysis:

Using the sensitivity analysis, it is possible to show how net cash returns or investment profitability change with different values assigned to the variables needed for calculation (sales prices, unit costs, sales volume, etc.). The COMFAR III expert facilitates the assessment of alternative project scenarios and identification of critical variables. Different graphs are available to analyze the structure of input and output projects, e.g. the structure of annual production and sales program, or variable and operating margins as well as the unequal sales volumes. The COMFAR III offers an additional analysis to facilitate the calculation of impact the project extensions or remediation.

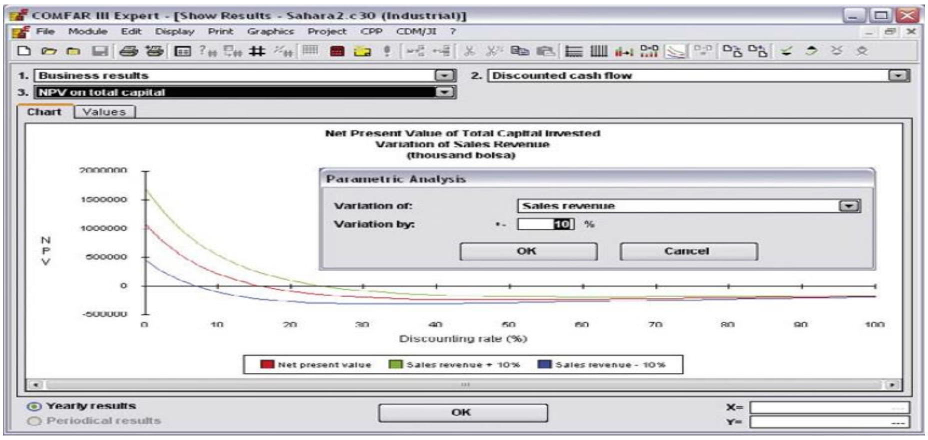

Figure 7 *An example of sensitivity analysis*

4 CALCULATION RESULTS USING THE COMFAR III SOFTWARE PACKAGE

4.1. Calculation and dynamics of income and expenses

Input data for the needs of economic analysis were obtained within the technical part of consideration the exploitation of technical stone from this deposit. They included both capital and operating costs of exploitation. In this part of the activity, the participation of experts from the field of mining is necessary in order to define the appropriate technical solutions, but the experts from other fields such as mechanical engineering, electrical engineering and construction, in order to give a realistic assessment of the value of existing facilities and equipment.

The total revenues from the open pit Gelja Ljut refer to the sale, i.e. placement of technical stone aggregates for the needs of the Gacko Mine and Thermal Power Plant, and infrastructure facilities that are being constructed for the needs of the mine. The annual product placement as well as its dynamics, revenue dynamics and calculation are presented in the form of an output form of the COMFAR III software package (Figure 8).

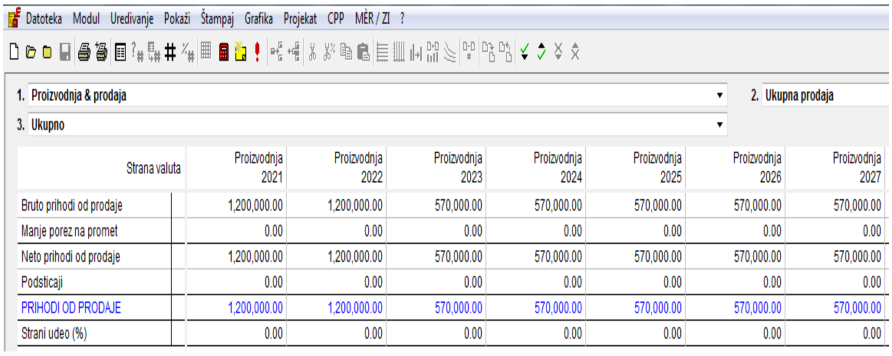

Datoteka Modul Uređivanje Pokaži Štampaj Grafika Projekat CPP MĖR / ZI ?

1. Proizvodnja & prodaja
2. Ukupna prodaja
3. Ukupno

Strana valuta	Proizvodnja 2021	Proizvodnja 2022	Proizvodnja 2023	Proizvodnja 2024	Proizvodnja 2025	Proizvodnja 2026	Proizvodnja 2027
Bruto prihodi od prodaje	1,200,000.00	1,200,000.00	570,000.00	570,000.00	570,000.00	570,000.00	570,000.00
Manje porez na promet	0.00	0.00	0.00	0.00	0.00	0.00	0.00
Neto prihodi od prodaje	1,200,000.00	1,200,000.00	570,000.00	570,000.00	570,000.00	570,000.00	570,000.00
Podsticaji	0.00	0.00	0.00	0.00	0.00	0.00	0.00
PRIHODI OD PRODAJE	1,200,000.00	1,200,000.00	570,000.00	570,000.00	570,000.00	570,000.00	570,000.00
Strani udeo (%)	0.00	0.00	0.00	0.00	0.00	0.00	0.00

Figure 8 *Detail of an output form of the COMFAR 3 software package with dynamics and revenue calculation*

The total costs of production of limestone and aggregates at the open pit Gelja Ljut included:

- costs of standardized material,
- processing costs,
- labor costs,
- maintenance costs,
- investment costs, and
- other expenses.

The annual cost amounts as well as its dynamics are presented in the form of an output form of the COMFAR III software package (Figure 9).

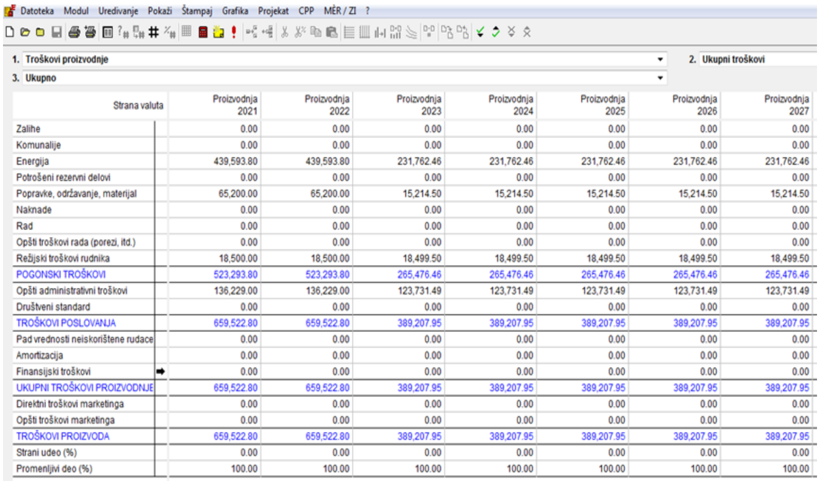

Datoteka Modul Uređivanje Pokaži Štampaj Grafika Projekat CPP MĖR / ZI ?

1. Troškovi proizvodnje
2. Ukupni troškovi
3. Ukupno

Strana valuta	Proizvodnja 2021	Proizvodnja 2022	Proizvodnja 2023	Proizvodnja 2024	Proizvodnja 2025	Proizvodnja 2026	Proizvodnja 2027
Zalihe	0.00	0.00	0.00	0.00	0.00	0.00	0.00
Komunalije	0.00	0.00	0.00	0.00	0.00	0.00	0.00
Energija	439,593.80	439,593.80	231,762.46	231,762.46	231,762.46	231,762.46	231,762.46
Potrošeni rezervni delovi	0.00	0.00	0.00	0.00	0.00	0.00	0.00
Popravke, održavanje, materijal	65,200.00	65,200.00	15,214.50	15,214.50	15,214.50	15,214.50	15,214.50
Naknade	0.00	0.00	0.00	0.00	0.00	0.00	0.00
Rad	0.00	0.00	0.00	0.00	0.00	0.00	0.00
Opšti troškovi rada (porezi, itd.)	0.00	0.00	0.00	0.00	0.00	0.00	0.00
Režijski troškovi rudnika	18,500.00	18,500.00	18,499.50	18,499.50	18,499.50	18,499.50	18,499.50
POGONSKI TROŠKOVI	523,293.80	523,293.80	265,476.46	265,476.46	265,476.46	265,476.46	265,476.46
Opšti administrativni troškovi	136,229.00	136,229.00	123,731.49	123,731.49	123,731.49	123,731.49	123,731.49
Društveni standard	0.00	0.00	0.00	0.00	0.00	0.00	0.00
TROŠKOVI POSLOVANJA	659,522.80	659,522.80	389,207.95	389,207.95	389,207.95	389,207.95	389,207.95
Pad vrednosti neiskorištene rudace	0.00	0.00	0.00	0.00	0.00	0.00	0.00
Amortizacija	0.00	0.00	0.00	0.00	0.00	0.00	0.00
Finansijski troškovi	0.00	0.00	0.00	0.00	0.00	0.00	0.00
UKUPNI TROŠKOVI PROIZVODNJE	659,522.80	659,522.80	389,207.95	389,207.95	389,207.95	389,207.95	389,207.95
Direktni troškovi marketinga	0.00	0.00	0.00	0.00	0.00	0.00	0.00
Opšti troškovi marketinga	0.00	0.00	0.00	0.00	0.00	0.00	0.00
TROŠKOVI PROIZVODA	659,522.80	659,522.80	389,207.95	389,207.95	389,207.95	389,207.95	389,207.95
Strani udeo (%)	0.00	0.00	0.00	0.00	0.00	0.00	0.00
Promenljivi deo (%)	100.00	100.00	100.00	100.00	100.00	100.00	100.00

Figure 9 *Detail of an output form of the COMFAR III software package with operating and investment costs*

4.2 Financial flow

In order to analyze in more detail the possibilities of evaluating the efficiency, i.e. the justification of realization of investments, it is necessary to enter into the analysis and measurement of the effects obtained from one investment project. [6] The measurement of effects brought by an investment project is done by calculating the certain indicators or criteria that express the effects of respective investment project. The financial evaluation includes consideration the effects of the investment project that the Investor has. The financial evaluation includes an assessment the profitability and liquidity of the project. The financial flow of the project is given in the form of an output form of the program package (Figure 10). All values are given in euros.

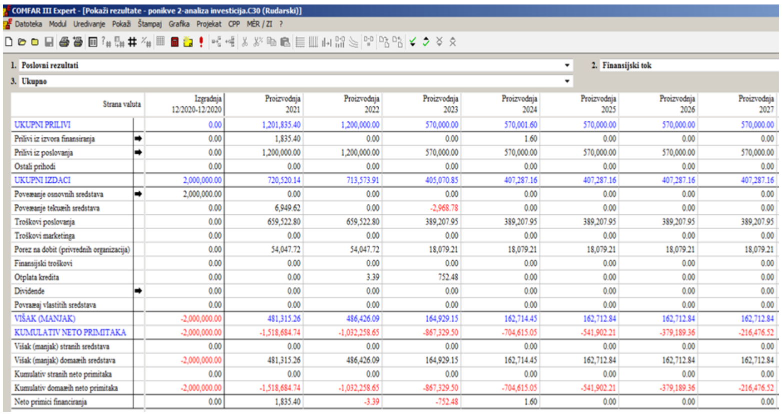
COMFAR III Expert - [Pokaži rezultate - ponikve 2-analiza investicija.C30 (Rudarski)]

Datoteka Modul Uređivanje Pokaži Štampaj Grafika Projekat CPP MĖR / ZI ?

1. Poslovni rezultati — 2. Finansijski tok

3. Ukupno

Strana valuta	Izgradnja 12/2020-12/2020	Proizvodnja 2021	Proizvodnja 2022	Proizvodnja 2023	Proizvodnja 2024	Proizvodnja 2025	Proizvodnja 2026	Proizvodnja 2027
UKUPNI PRILIVI	0.00	1,201,835.40	1,200,000.00	570,000.00	570,001.60	570,000.00	570,000.00	570,000.00
Prilivi iz izvora finansiranja	0.00	1,835.40	0.00	0.00	1.60	0.00	0.00	0.00
Prilivi iz poslovanja	0.00	1,200,000.00	1,200,000.00	570,000.00	570,000.00	570,000.00	570,000.00	570,000.00
Ostali prihodi	0.00	0.00	0.00	0.00	0.00	0.00	0.00	0.00
UKUPNI IZDACI	2,000,000.00	720,520.14	713,573.91	405,070.85	407,287.16	407,287.16	407,287.16	407,287.16
Poveæanje osnovnih sredstava	2,000,000.00	0.00	0.00	0.00	0.00	0.00	0.00	0.00
Poveæanje tekuæih sredstava	0.00	6,949.62	0.00	-2,968.78	0.00	0.00	0.00	0.00
Troškovi poslovanja	0.00	659,522.80	659,522.80	389,207.95	389,207.95	389,207.95	389,207.95	389,207.95
Troškovi marketinga	0.00	0.00	0.00	0.00	0.00	0.00	0.00	0.00
Porez na dobit (privrednih organizacija)	0.00	54,047.72	54,047.72	18,079.21	18,079.21	18,079.21	18,079.21	18,079.21
Finansijski troškovi	0.00	0.00	0.00	0.00	0.00	0.00	0.00	0.00
Otplata kredita	0.00	0.00	3.39	752.48	0.00	0.00	0.00	0.00
Dividende	0.00	0.00	0.00	0.00	0.00	0.00	0.00	0.00
Povraæaj vlastitih sredstava	0.00	0.00	0.00	0.00	0.00	0.00	0.00	0.00
VIŠAK (MANJAK)	-2,000,000.00	481,315.26	486,426.09	164,929.15	162,714.45	162,712.84	162,712.84	162,712.84
KUMULATIV NETO PRIMITAKA	-2,000,000.00	-1,518,684.74	-1,032,258.65	-867,329.50	-704,615.05	-541,902.21	-379,189.36	-216,476.52
Višak (manjak) stranih sredstava	0.00	0.00	0.00	0.00	0.00	0.00	0.00	0.00
Višak (manjak) domaæih sredstava	-2,000,000.00	481,315.26	486,426.09	164,929.15	162,714.45	162,712.84	162,712.84	162,712.84
Kumulativ stranih neto primitaka	0.00	0.00	0.00	0.00	0.00	0.00	0.00	0.00
Kumulativ domaæih neto primitaka	-2,000,000.00	-1,518,684.74	-1,032,258.65	-867,329.50	-704,615.05	-541,902.21	-379,189.36	-216,476.52
Neto primici financiranja	0.00	1,835.40	-3.39	-752.48	1.60	0.00	0.00	0.00

Figure 10 *Detail of an output form of the COMFAR III software package with financial flow*

4.3 Economic flow

For a successful evaluation of investment projects, it is necessary to take into account the preferences of time, i.e. to apply a discount account that reduces the series of future amounts to the present value. The basis of a discount account is a discount rate. In general, the discount rate is the interest rate at which the central bank gives liquidity loans to the commercial banks, but it is more often linked to the process of discounting and measuring the time value of money. In this particular case, the adopted discount rate represents the return expected from investment in the project. In this Study, a discount rate of 12% was adopted and it is significantly higher than the currently valid interest rate on loans with a currency clause of the Central Bank of Bosnia and Herzegovina, which amount to 3.139% for 2020.

A significantly higher discount rate is a measure of expectations of the Project success from community. The economic flow of the project was calculated for a discount rate of 12% and is presented in the form of an output form of the COMFAR III software package (Figure 11).

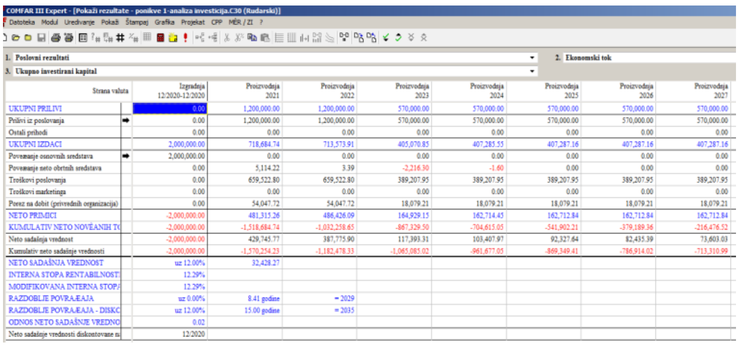
COMFAR III Expert - [Pokaži rezultate - ponikve 1-analiza investicija.C30 (Rudarski)]

Datoteka Modul Uređivanje Pokaži Štampaj Grafika Projekat CPP MĖR / ZI ?

1. Poslovni rezultati — 2. Ekonomski tok

3. Ukupno investirani kapital

Strana valuta	Izgradnja 12/2020-12/2020	Proizvodnja 2021	Proizvodnja 2022	Proizvodnja 2023	Proizvodnja 2024	Proizvodnja 2025	Proizvodnja 2026	Proizvodnja 2027
UKUPNI PRILIVI	0.00	1,200,000.00	1,200,000.00	570,000.00	570,000.00	570,000.00	570,000.00	570,000.00
Prilivi iz poslovanja	0.00	1,200,000.00	1,200,000.00	570,000.00	570,000.00	570,000.00	570,000.00	570,000.00
Ostali prihodi	0.00	0.00	0.00	0.00	0.00	0.00	0.00	0.00
UKUPNI IZDACI	2,000,000.00	718,684.74	713,573.91	405,070.85	407,285.55	407,287.16	407,287.16	407,287.16
Poveæanje osnovnih sredstava	2,000,000.00	0.00	0.00	0.00	0.00	0.00	0.00	0.00
Poveæanje neto obrtnih sredstava	0.00	5,114.22	3.39	-2,216.30	-1.60	0.00	0.00	0.00
Troškovi poslovanja	0.00	659,522.80	659,522.80	389,207.95	389,207.95	389,207.95	389,207.95	389,207.95
Troškovi marketinga	0.00	0.00	0.00	0.00	0.00	0.00	0.00	0.00
Porez na dobit (privrednih organizacija)	0.00	54,047.72	54,047.72	18,079.21	18,079.21	18,079.21	18,079.21	18,079.21
NETO PRIMICI	-2,000,000.00	481,315.26	486,426.09	164,929.15	162,714.45	162,712.84	162,712.84	162,712.84
KUMULATIV NETO NOVÈANIH TO	-2,000,000.00	-1,518,684.74	-1,032,258.65	-867,329.50	-704,615.05	-541,902.21	-379,189.36	-216,476.52
Neto sadašnja vrednost	-2,000,000.00	429,745.77	387,775.90	117,393.31	103,407.97	92,327.64	82,435.39	73,603.03
Kumulativ neto sadašnje vrednosti	-2,000,000.00	-1,570,254.23	-1,182,478.33	-1,065,085.02	-961,677.05	-869,349.41	-786,914.02	-713,310.99
NETO SADAŠNJA VREDNOST	uz 12.00%	32,428.27						
INTERNA STOPA RENTABILNOSTI	12.29%							
MODIFIKOVANA INTERNA STOPA	12.29%							
RAZDOBLJE POVRAÆAJA	uz 0.00%	8.41 godine	= 2029					
RAZDOBLJE POVRAÆAJA - DISKC	uz 12.00%	15.00 godine	= 2035					
ODNOS NETO SADAŠNJE VREDNO	0.02							
Neto sadašnje vrednosti diskontovane n	12/2020							

Figure 11 *Detail of an output form of the software package - Economic flow*

4.4 Profitability

Profitability is the ratio of difference between the total profit and total costs to the total profit. The amount of Profitability is given in the form of an output form of the software package (Figure 12).

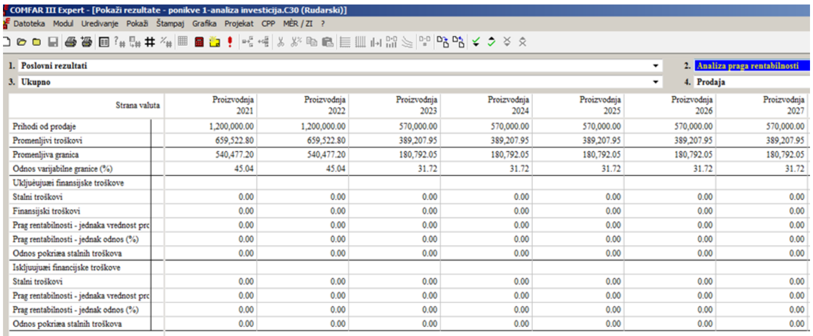

COMFAR III Expert - [Pokaži rezultate - ponikve 1-analiza investicija.C30 (Rudarski)]

Datoteka Modul Uređivanje Pokaži Štampaj Grafika Projekat CPP MÈR / ZI ?

1. Poslovni rezultati
2. Analiza praga rentabilnosti
3. Ukupno
4. Prodaja

Strana valuta	Proizvodnja 2021	Proizvodnja 2022	Proizvodnja 2023	Proizvodnja 2024	Proizvodnja 2025	Proizvodnja 2026	Proizvodnja 2027
Prihodi od prodaje	1,200,000.00	1,200,000.00	570,000.00	570,000.00	570,000.00	570,000.00	570,000.00
Promenljivi troškovi	659,522.80	659,522.80	389,207.95	389,207.95	389,207.95	389,207.95	389,207.95
Promenljiva granica	540,477.20	540,477.20	180,792.05	180,792.05	180,792.05	180,792.05	180,792.05
Odnos varijabilne granice (%)	45.04	45.04	31.72	31.72	31.72	31.72	31.72
Uključujući finansijske troškove							
Stalni troškovi	0.00	0.00	0.00	0.00	0.00	0.00	0.00
Finansijski troškovi	0.00	0.00	0.00	0.00	0.00	0.00	0.00
Prag rentabilnosti - jednaka vrednost prc	0.00	0.00	0.00	0.00	0.00	0.00	0.00
Prag rentabilnosti - jednak odnos (%)	0.00	0.00	0.00	0.00	0.00	0.00	0.00
Odnos pokrića stalnih troškova	0.00	0.00	0.00	0.00	0.00	0.00	0.00
Isključujući financijske troškove							
Stalni troškovi	0.00	0.00	0.00	0.00	0.00	0.00	0.00
Prag rentabilnosti - jednaka vrednost prc	0.00	0.00	0.00	0.00	0.00	0.00	0.00
Prag rentabilnosti - jednak odnos (%)	0.00	0.00	0.00	0.00	0.00	0.00	0.00
Odnos pokrića stalnih troškova	0.00	0.00	0.00	0.00	0.00	0.00	0.00

Figure 12 *Detail of an output form of the COMFAR software package with profitability expressed in %*

4.5 Evaluation of financial efficiency

The results presented in the illustrated financial flow, shown in the previous tables, clearly show the structural share of globally individual components of income, expenditure and periodic results. The dominant structural share of exploitation costs is 26% and earnings of 23% (Figure 13).

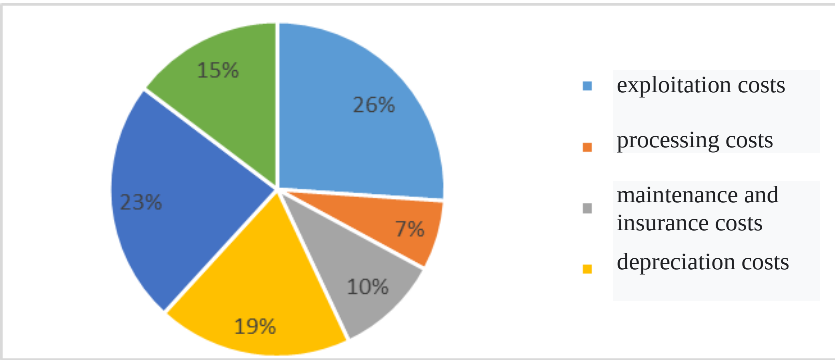

Figure 13 *Cost structure*

4.6 Variation of investments by the sensitivity analysis and investment risk

Sensitivity analysis was performed by changing the following parameters

1. Sales prices (Revenues from sales)
2. Investments - costs of providing the concession right (increase of fixed assets), and

3. Costs of production and processing of limestone (Operating costs)

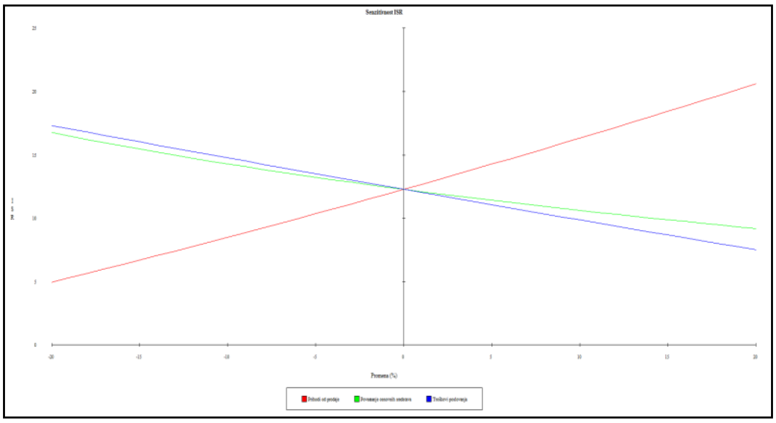

Figure 14 *Output form of the COMFAR 3 software package with sensitivity diagram*

Table 2 *Project sensitivity (%)*

Change (%)	Sales revenues	Increase in fixed assets	Operating expenses
-20.00 %	4.97%	16.77%	17.31%
-16.00 %	6.36%	15.71%	16.29%
-12.00 %	7.78%	14.74%	15.27%
-8.00 %	9.25%	13.86%	14.27%
-4.00 %	10.75%	13.04%	13.27%
0.00 %	12.29%	12.29%	12.29%
4.00 %	13.87%	11.59%	11.32%
8.00 %	15.49%	10.94%	10.36%
12.00 %	17.15%	10.33%	9.40%
16.00 %	18.86%	9.75%	8.46%
20.00 %	20.60%	9.21%	7.54%

Based on the presented values, it can be concluded that the Project is the least sensitive to the changes in investments, and the most sensitive to the changes in selling price of products.

In addition to the sensitivity of the project to the value of input values, the indicators of project economy for different values of investments in providing the concession right were especially considered. The results of the analysis are shown in Table 3 and Figure 15.

Table 3 *Cost-effectiveness indicators for a variable amount of investment*

Investments (€)	Internal rate of return (%)	Time of return (years)	Net present value of the Project (€)
1,250,000	22.03	3.8	628,963
1,500,000	17.45	5.34	430,118
1,750,000	14.42	6.88	231,273
2,000,000	12.29	8.41	22,428
2,040,000	12	8.66	0

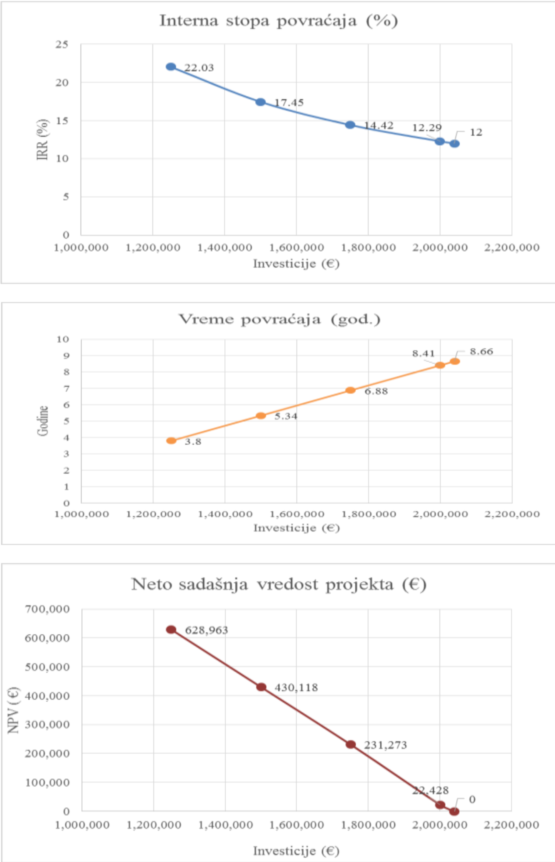

Figure 15 *Diagrams of IRR (%), time of investment return (%) and NPV of the project (€) as a function of investment amount*

5 CONCLUSION

Based on the calculated economic parameters, the provision of the concession right for exploitation of limestone as a construction-technical stone on the Gelja Ljut deposit, under the conditions presented in this Study, can be assessed as economically viable and socially favorable.

The applied methodology of economic evaluation implied an economic analysis taking into account the time factor and is fully in accordance with the methodology recommended by the United Nations Industrial Development Organization (UNDO).

All financial and economic parameters are positive.

The static value of the project is € 401,320, while the net present value of the project is for a period of about 14 years. This net present value of the project is a consequence of strict conditions under which the budget of economic indicators is calculated, a discount rate of 12% and maximized operating costs with limited capacity to the part that represents the direct needs of the Mine and Thermal Power Plant for this mineral resource and its products.

The social effects of the Project expressed through the ecological and general conditions of closure in the conditions of taking over the concession right on the Gelja Ljut deposit are positive.

REFERENCES

[1] N. Stanić, A. Doderović, S. Stepanović, M. Gomilanović, Dynamics of Development the Works of Roof Coal Series of the Open Pit Gacko by the Software Gemcom Gems - Module Cut Evaluation, Mining and Metallurgy Engineering Bor No. 4 2016.

[2] N. Stanić, S. Stepanović, D. Bugarin, M. Gomilanović, Selection the Rational Model of Transport Truck by the Selective Coal Mining at the Open Pit Gacko, Mining and Metallurgy Engineering Bor No.1-2 2017.

[3] S. Stepanović, N. Stanić, M. Šešlija, M. Gomilanović, Analysis of Coal Quality in a Function of Selection Level for Mining at the Open Pit Gacko, Mining and Metallurgy Engineering Bor No.1-2 2017.

[4] N. Stanić, S. Stepanović, D. Govedarica, A. Doderović, Application the Software Solution for Calculation the Capacity of Bucket Wheel Excavators in the Complex Conditions from the Aspect of Resistance to Excavation, Mining and Metallurgy Engineering Bor No.3-4 2017.

[5] COMFAR III EXPERT – Software for Project Appraisal and Analysis, United Nations Industrial Development Organization, Programme Development and Technical Cooperation Division, Investment and Technology Promotion Branch, Vienna, 2009.

[6] Prof. Dr P. Jovanović, Investment Management, Faculty of Organizational Sciences, Belgrade, 2006 (in Serbian)

MINING AND METALLURGY INSTITUTE BOR
UDK: 622

ISSN: 2334-8836 (Štampano izdanje)
ISSN: 2406-1395 (Online)

UDK: 336.7(045)=111

DOI: 10.5937/mmeb2004081M

Nemanja Matić, Boris Siljković**, Marko Savić***

POTENTIALS OF TRADITIONAL CASH METAL COINS VERSUS DIGITAL CONTACTLESS PAYMENT IN THE TIME OF CORONAVIRUS PANDEMIC

Abstract

This paper addresses the challenges associated to the strength of potential for payment with traditional metal cash and paper money versus a non-cash method of payment in the era of the COVID 19 pandemic in the world and our country. The pandemic served to accelerate the contactless method of payment, because payment without contact is now not only a convenience, but a necessity. Before the pandemic in Europe, cash accounted for close to half of the payments, and in just a few weeks of the COVID 19 pandemic, it fell by 10 percent. Concepts that have so far preferred cash were definitely compromised during the pandemic crisis, and the pandemic is actually the strongest marketing of digital contactless payment methods so far, through the dominant contactless style of money exchange in the world and Europe, as shown in the paper we have today.

Some research studies described in the paper in form of the health adventages of mobile wallet payments, as opposed to the proven health-threatening cash and coin-based cash payment model, indicate that the end of the cash era is approaching, being primarily accelerated by the health risk of COVID 19 infection. Particularly interesting is the live study conducted in the area of the northern Kosovo and Metohija, presented in a form of a set of financial services offered by the Postal Savings Bank of the Kosovska Mitrovica branch office, and relation between the contactless and cash payment model, before and after the COVID 19 pandemic. Naturally, all of this is accompanied by significantly limited knowledge related to SARS Cov 2, better known as the current COVID 19 pandemic.

***Keywords**: paper money, metal money, cash, contactless payment, COVID 19, pandemic*

1 INTRODUCTION

The coronavirus pandemic of 2020 promoted digital mobile, network and contactless payment, which means that there are few arguments against application of this model in the post-pandemic period. E-banking involves delivery of banking products and services through the electronic channels that had been previously done through telephone transactions and automatic teller machines (ATMs). Later, with the Internet application, which was considered as the fastest and best channel for delivery of most banking transactions, the job was made easier both for banks and customers. Khalek and Bakri [1] Telephone, Internet and mobile phone have become the main channels of digital banking services making them important for the survival of banks, due to their advantages and practicalities, anytime and anywhere. Sundarraj and Wu, 2005; [2], Daniel, 1999; [3], Mols, 2001. [4] During and after the corona virus pandemic, the banking world, along with the

* *Delikos DOO Sopot, maticnemanja6@gmail.com*
** *Academy of Applied Studies, Department Peć-Leposavić, boris_siljkovic@yahoo.com, savic22@yahoo.com*

ecologically contactless payment everywhere in the world, should become absolute priority. This payment model will almost certainly be present for a long time even after the coronavirus pandemic. The coronavirus pandemic will definitely change everything that was once the norm of traditional banking financial services, especially the cash payment method and the digital payment method. Digital contactless banking enables the development of customer services, reducing the costs associated to face-to-face transactions with customers in branch offices. Dootson et al., 2016. [5]

The model of traditional banking is being tested during this coronavirus pandemic and it has been shown that the traditional cash payment model is currently outdated. The European Central Bank surveys conducted in June 2020 showed a sharp decline in the share of cash payments during the first lockdown of economies across Europe where consumers pay in cash, but much less than before the pandemic.

Knowledge and people who know how to apply that knowledge participate in the development of society nowadays. [23] This has primarily allowed the electronic contactless banking, which represents the application of the new/old technological solutions, and has made possible to the users to perform the money transactions from anywhere and at any time they want using the computer networks. Ilić et al., 2015 [6]

2 HEALTH POTENTIAL OF DIGITAL AND CASH EXCHANGE OF MONEY IN THE AGE OF THE COVID PANDEMIC 19

The time of pandemic has indicated that we have an adaptable so-called a coronavirus environmental bank that has an updated model of digital services including a health strategy of contactless payment methods. The BRIC countries, specifically the Government of India will perform all payments in the futuristic world using the contactless cards, mobile phone applications and other electronic means, while the banknotes and coins will be abolished. [7]

Contactless payment was already on the rise in the U.S.A, but the ongoing coronavirus pandemic has increased the number of Americans using a variety of non-contact payment methods.

In the US, more than 51% of people have opted to use so-called mobile wallets, such as the Apple Pay and other Tap-To-Go credit cards. Consumers mainly use the contactless cards to buy necessities, namely: food: 85%, pharmacy: 39%, retail: 38% fast food restaurants (KSR), fast food: 36%. [8].

Table 1 actually shows the reasons why the health benefits of digital payment in the COVID 19 pandemic era have prevailed over the traditional cash and paper money payments.

China, where coronavirus COVID 19 or Sars Cov 2 first appeared, and its Chinese National Health Commission have classified the new coronavirus as a class A infectious disease, requiring the strictest preventive and control measures, including mandatory patient quarantine and treatment of those who were in a close contact with them [19].

Table 1 *Health potential of using the digital contactless payment versus use of metal and paper money*

Use of metal coins	It is moderately contagious and depends on the composition of the money alloy, its production is more expensive, up to two times of nominal value, and it is harder to protect against counterfeiting.
Use of paper money	Contagious for several days, cheaper to make than coins and easier to protect against a counterfeiting than coins.
Use of contactless card, Master and Visa card. In the USA, cards of the present and the future (Visa Inc., Mastercard Inc., American Express Co., PayPal Holdings Inc.)	Less contagious if contactless, does not change the owners and does not come into contact with sellers and traders. A plastic card costs less than paper money and coins, because it can be used longer — commercial moment. Payment cards have eliminated the need to carry money while reducing the chances of theft or loss of currency.
Mobile applications for payment E banking, Home banking and M banking, so-called digital wallets	The least contagious with the use of hygienic cleaning products for the phone. It requires a mobile phone or computer and an Internet connection.
Cardboard	The virus remains on it for 24 hours. [9]
Stainless steel (banknotes) and plastic cards	Research 1: Materials on which germs and viruses can be minimum kept: Sars Cov 1 and SARS Cov 2 - 5.6 hours on stainless steel and 6.8 hours on plastic. Although the extent of the virus has been significantly reduced, this virus is more stable. Research 2: Even after 72 hours, SARS Cov 2 could be found on plastic and 48 hours on stainless steel [10]
Solid surfaces and materials e.g. ATMs and POS terminals	Sars Cov 2 virus can stay alive for up to two days [11]
Copper alloy for money banknotes	SARS-CoV 2 or Covid 19 virus remain present for 4 hours. It has been proved that copper-containing surfaces show antiviral activity as opposed to polymer surfaces used to make paper banknotes, where the virus could survive for several days. [12] Copper deficiency, although rare, makes people more susceptible to infection. [11] The continuously self-sterilizing form of copper is 99% capable of deactivating SARS-CoV-2 or COVID 19 in 30 seconds. [12]
Metal and glass	Analysis of 22 studies reveals that the human coronaviruses such as the Severe Acute Respiratory Syndrome (SARS), Middle East Respiratory Syndrome (MERS) or Endemic Human Coronaviruses (HCoV) can persist on inanimate surfaces such as metal, glass or plastic for up to 9 days. [13]

3 PRIMATE OF DIGITAL MONEY EXCHANGE AS THE MAIN STYLE IN THE AGE OF THE COVID 19 PANDEMIC IN THE WORLD WITH REFERENCE TO SERBIA

If we use the research and online survey of Accenture NYCE: in 20 countries with 120 bank directors during the pandemic from July to August 2020 as shown in Figure 1 below, it can be seen that the biggest payment disruption was in the USA, followed by the UK, because the consumers have been opting for the new digital payment methods. The surveyed markets include: Australia, Brazil, Canada, China, Denmark, Finland, France, Germany, India, Italy, Japan, the Netherlands, Norway and Singapore. In China, for instance, the mobile wallets are rapidly taking precedence over cash payments - 76% of transactions in 2019 come from mobile wallets, compared to 12% in 2014. For several years now, the consumers in China have been accustomed to use the mobile applications and QR codes to pay in restaurants and stores. Even before the pandemic, China was the second in the global share of payments by mobile wallets and the second market with the fastest growth of payments in the world. In Germany, more than half of card payments in the year of the pandemic were contactless, compared to 35% before the economy was hit by the coronavirus crisis. Since June 2020 in the Netherlands, consumers have paid 20% in cash at their points of sale. This is significantly lower than in January and February 2020, when 30% of their purchases were paid for in cash, but more than immediately after the outbreak of COVID 19. In the Netherlands in April 2020, only 15% of purchases were paid for in cash. In October 2020, the consumers used the contactless payment methods for 67% of their purchases at points of sale, compared to only 50% at the beginning of the year. As it can be seen in Figure 1, the contactless payment in the Netherlands has increased to the detriment of cash payments, and in particular pin-code mobile payment - QR telephone code payment. [22]

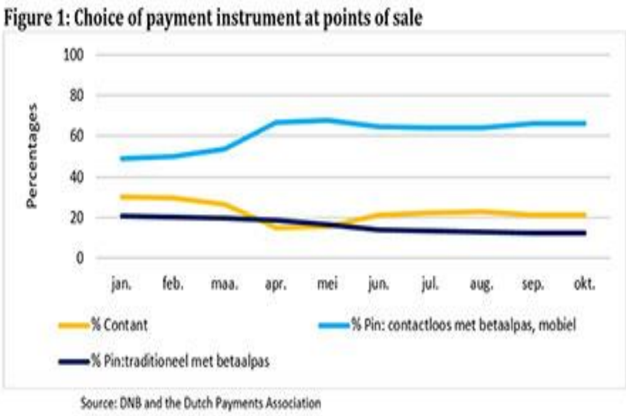

Figure 1 *Choice of payment instruments in the Netherlands at points of sale [22]*

If we look in Figure 2 in the UK in a pandemic year, the "tap and pay" model makes up more than 40% of card payments. In mature markets - such as Western Europe, payments are mostly commodified - only gradual changes are expected to be seen through purchases. The greatest opportunity for contactless payment will be in markets such as Southeast Asia and Latin America, where a cash consumption dominated, and, in some regions, has even increased during the pandemic. The size of a circle in Figure 2 indicates the relative value of transactions in each country. [14] [22] [15]

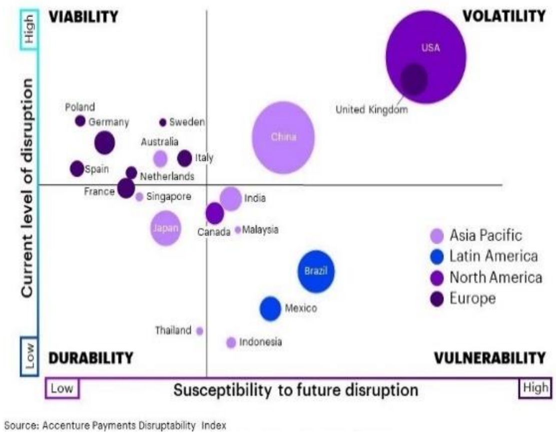

Figure 2 *Increase of digital payments during the COVID 19 pandemic worldwide [14]*

Almost all users of smartphone services will be in the Asia-Pacific region and mainly in China, which will make up the majority of the world's users of direct mobile payments. Mobile payments are also popular among the smartphone users in India, Denmark, Sweden and South Korea. The information in Figure 3 presents an overview of the global proximity payment environment through the mobile applications, including adoption trends in major markets and key players.

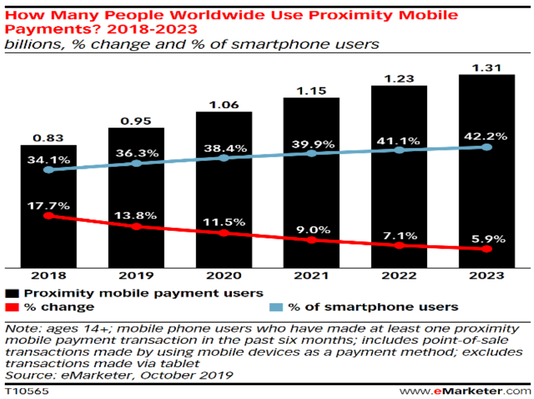

Figure 3 *Predictions of payment services via mobile applications in the world 2018-2023 [16]*

A strong cash payment culture is giving way to the non-cash payment methods mainly due to the COVID 19 pandemic and in order to prevent the spread of coronavirus. For instance, in 2020, there will be 59.3 million mobile payment users in Western Europe, close to 18.7% more than in the previous year. Stable growth is expected until 2023 through the number of service users, when 70.6 million people in the region will have performed at least one proximity mobile payment transaction in the past six months. Sincerily, in numerical terms, the growth of people using mobile applications is predicted, and in percentage terms, there is a noticeable decline in users of contactless mobile payment services as we move away from the base pandemic 2019 in Western Europe, and Figure 4 directly proves it. [17]

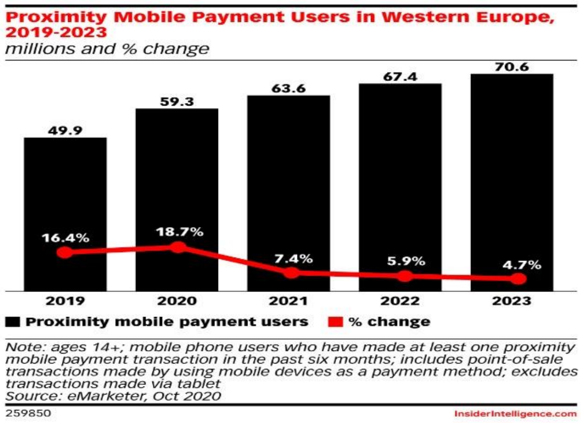

Figure 4 *Rise/fall in mobile phone payments 2019-2023 in the economies of Western Europe [17]*

According to a research conducted by BuyShares.co.uk in June 2020, the global mobile wallet industry is worth $ 1.47 trillion versus $ 405 billion in 2017. The number of people choosing mobile wallets to manage their payments should jump over 29.6% per year by the end of 2020. The data reveals that China is the leading player in the mobile wallet industry, and is predicted to reach a value of 50% of the world's overall market value in 2020. However, the statistics show that the United States, Great Britain and Brazil, as the leading markets for mobile wallets, are expected to grow in 2020. [18]

Serbia is in the early stages of e-banking growth because just over a third of the population is currently active or involved in e-m banking. We had introduced the mobile wallets in Serbia, and it was thought that everyone would immediately pay exclusively by phone. Will the COVID 19 pandemic change that, and indications show that it will continue in 2021, with long term consequences. However, the health progress is certain, but not visible enough for the time being, since the mass immunization just began in January 2021.

When it comes to the wider use of mobile wallets, it is still going slowly both in Serbia and the region, cash is still used a lot. What is being talked about and written about everywhere is reaching the ordinary people and wider population in the region and Serbia more slowly.

4 LIMITATION / DIVERSITY OF PAYMENT METHODS - CASE STUDY POSTAL SAVINGS BANK - KOSOVO MITROVICA

Since the declaration of the state of emergency in Serbia and the proclamation of the COVID pandemic on March 19, 2020, the Postal Savings Bank in Serbia with its branch office in Kosovska Mitrovica has invited its clients to use the electronic banking services as much as possible, i.e., remote access to payment services and transactions. Here, for our needs, and in order to determine the factual situation in the area of the branch office of the Postal Savings Bank in Kosovska Mitrovica, we have made an analysis through an anonymous survey. For this purpose, we have made an overview of the use of contactless versus cash payment methods from the point of view of users-clients and service providers on the example of the Postal Savings Bank of Kosovska Mitrovica and its four municipalities through the branche office in which they operate: Kosovska Mitrovica, Zvecan. Zubin Potok and Leposavic.

At the very beginning of the research, we encountered a crucial limitation in form of impossibility of using electronic payment services in full capacity for the simple reason of unavailability, i.e., relatively small number of POS terminals in retail stores, restaurants, restaurants and other facilities. It is noteworthy that there is still a lack of culture of electronic payment amongst the population of the northern Kosovo and Metohija, although some progress in the use of electronic services is noticeable, especially after the declaration of the pandemic and the use of electronic payment methods.

Due to these facts, all types of electronic services, primarily payment cards and mobile applications offered by the Postal Savings Bank of the Kosovska Mitrovica branch office, have limited practical and application value. Therefore, the bank's client/consumer is prevented from using the so-called mobile wallet and electronic services in full capacity and is mostly oriented towards the cash method of payment and use of services in the territory of the northern Kosovo and Metohija. When it comes to the Posatal Saving Bank, it called on clients to use the electronic banking services as much as possible, i.e., remote access to payment and payment services in the conditions of the state of emergency in the country, declared to prevent spreading of the Covid-19 virus.

Due to these circumstances, we have focused on examining the provision of financial services of the Postal Savings Bank in the north of Kosovo and Metohija, which is registered as a service provider in Serbia, and this bank in Kosovska Mitrovica was officially opened on April 1, 2018 and operates in the payment system of Serbia.

The conducted survey was of an anonymous type, with 100 people of different ages from 25 to 65 and older participated, where both sexes were equally represented. Time period of the survey was March 2020 - August 2020. We received the greatest number of answers from the respondents of young age 35-44, and middle age 45-54. Significantly few participants were very young aged 18-25 and mature over 65-70.

Persons with the high school and faculty degree were equally represented in the answers. Very few people with primary school and high academic degree of master and doctor of science participated.

Based on the answers to the questions asked, it was confirmed that cash withdrawal is the dominant form of using the services of the Post Office in the north of Kosovo and Metohija, with most clients. The survey has shown that the younger population prefers contactless payment methods mainly through mobile applications, but it is insufficiently/very little used. It is noteworthy that all categories of the surveyed population agreed that the following types of electronic payment payments are popular from the health perspective: a). card, b). mobile application, followed by c). check and e) cash. True, it may be stated that the respondents of all ages did not have an aversion for the use of cash as a method of payment and withdrawal of cash during the current pandemic.

Due to these reasons related to the use of cash and the respondents' answers that there were no fears in terms of health security, a new study from the USA in 2020, which proves the opposite, is being analysed. In the appendix below, Table 2 has provided sufficient evidence that there is contamination with the COVID 19 virus (SARS Cov 2) and that paper for money printing may be less contagious with the Coronavirus (Covid 19) than banknotes. However, both this and previous studies have shown that coins and banknotes can be highly transmissible and pathogenic. (Evidence - Table 1). Mobile phones and computers may be reservoirs of infection, primarily due to the material they are made of (glass, plastic and metal). This is also confirmed by the research given in the appendix in Table 2, where it has been proven that SARS Cov 2 (Covid 19) lives the longest on plastic and stainless steel.

Table 2 *Sars Cov 2(Covid 19) lifespan on different materials* [20] [21]

Material	Sars Cov 2(Covid 19) lifespan on different materials
Glass	Measurements of 0 - 3 h, T ½ = 1.3 h 3 h – 2 days, T1/2 = 4.8 hrs
Banknote	Measurements of 0 - 6 h, T1/2 = 0.9 h 6 h – 2 days, T1/2= 7.9 h
Stainless steel	0 -30 min, T1/2 = 0.3 h 30 min – 4 days, T1/2= 14.7 h
Plastic	0 - 6 h, T1/2 = 1.6 h 6 h - 4 days, T1/2= 11.4 hrs)
Paper	0 – 30 min= 4.76 h 30 min - 2 days =1.18 h

Out of respondents who have an open mobile application, which mainly refers to the very young population aged 18-25, and recently the more mature population aged 35 to 45 and over, only 1/3 of the respondents mainly use it to pay for utilities, electricity, water, telephone and other charges.

The dominant way of withdrawing cash by the respondents is from ATMs, while more than 1/3 of respondents decide to withdraw cash directly from the counters at the post office and savings bank, as it is a case with: salaries, pensions, various social benefits, payments for other person's care, social assistance and other forms social benefits.

If we analyze Table 3 in the package of financial services of the Postal Savings Bank of the Kosovska Mitrovica Branch Office, which are the unofficial information gathered by the authors of the paper through interviews with employees of the Bank-Postal Savings Bank, the incrase of contactless payment method has been observed, as opposed to the period before the pandemic. In order to support this claim, the evident growth of e + m and home electronic services through the so-called mobile wallets of the bank-postal savings bank can be used. On the other hand, the number of counters of the Postal Savings Bank branch office in Kosovska Mitrovica for cash withdrawals does not support the affirmation of the contactless method of payment, because it has remained the same before and during the COVID 19 pandemic.

When using the financial services and payment methods, this research recorded a small number of POS terminals, e.g., many small shops that are the dominant type of retail, in the north of Kosovo and Metohija, do not have the POS terminals.

In proportion to these technical limitations, we note elements of insufficient or very low financial literacy of bank/postal savings bank clients regarding the scope and practical application of electronic services using mobile applications. Political and security troubles in the north of Kosovo and Metohija also contribute to this state of modest and timid affirmation and spreading of contactless payment methods.

A certain compensation should be mentioned here - a financial reason for not or insufficiently using POS terminals, both from the point of view of the bank's clients /bank users/ postal savings bank, which limits this payment method in a certain way.

In order to distance the client from the counter cash withdrawal method Bank in favor of contactless payment, the management of the Postal Savings, the above-mentioned financial institution raised the limit for ATMs cash withdraw from 20,000 dinars to 50,000 dinars and thus encouraged this model of financial services during the COVID pandemic.

For this purpose of deterrence from the cash method of payment, we have a certain percentage of commission for withdrawing cash from the counters and ATMs, if you are not a bank client, i.e. you do not have a bank savings bank card. Data related to internet payment were not available to us while the so-called code telephone payment at this branch in Serbia is still in its infancy.

Table 3 *Financial services package of the Postal Savings Bank of the Kosovska Mitrovica branch office**

Type of service / branch office Kind of financial services-payment method / branch office	Branch office K. Mitrovica-total Before during pandemic	Zvečan Before during pandemic	Z. Potok Before during pandemic	Leposavić Before during pandemic
Number of counters	5 5	2 2	2 2	2 2
Number of ATMs	2 5	2 2	1 1	1 1
Number of cards	22,000 36,000	4,500 7,000	1,000 1,500	2,500 3,300
Number of POS terminals	41 out of which K. Mitrovica 31 Before and during pandemic	5 5	3 3	2 2
e bank services for legal entities-number e transaction	2,400 9,600	700 3,800	1,200 6,400	300 1,700
m bank services + home services for individuals-number of m and h transactions	600 3,000	400 2,100	500 2,600	300 1,900
Internet payment - purpose defined visa -master card -electron visa	No data	No data	No data	No data
QR payment-so-called telephone. code payment	It is still developing in the north of Kosovo and Metohija and in Serbia			

* ***Note***: *The financial services package refers to the period shortly before the pandemic of March 2020 to December 2020.*

Source: *Author's overview based on data collected through interviews and on information from the Postal Savings Bank of the Kosovska Mitrovica Branch Office*

Figure 5 *Postal Savings Bank of the Kosovska Mitrovica*

5 CONCLUSION

From the point of writing a paper on contactless payment via cards, mobile wallets and other models of electronic payments, the need for cash has been forgotten. We have proven that by the use of contactless payment, you pay from a secured, and especially healthly safe distance, along with what the contactless method of payment provides the most: speed, security, simplicity and convenience from any location. Research conducted in the first two studies has shown that the toxicity and transmissibility of SARS Cov 2 or COVID 19 in the use of cash and paper money is great, but there are also the other materials from which ATM and POS terminals are made of, primarily due to metal, glass and plastic. It has been proven that, primarily due to these circumstances, mobile applications as a payment model are the most secure and thus the safest method for the health aspect and the most practical from anywhere. Contactless payment is today, in time of the pandemic, the main style in all the economies of the world and Europe, which can be regarded as leaders, but there are exceptions. After all, COVID 19 only accelerated the "death" of the cash method of payment in the developed Europe with the components of the so-called commodity variety of payment methods, especially in the so-called countries of the new Europe, Bulgaria and Romania. The contactless payment model is still in its infancy, but also in development in the Balkans region and Serbia. People pay more often by a card in Luxembourg and France. The Scandinavian countries are at the very top of the scale. There, many hotels, bars or shops do not want to accept payment with coins and banknotes at all. In Sweden, 82% of people pay non-cash. We have shown in the paper that the greatest opportunity for contactless payment will be in the future in markets such as Southeast Asia and Latin America, where cash consumption dominated in the previous period. China, through the form of contactless payment methods, has been dominating on a global level for many years, and with the pandemic, it has only confirmed its first place in the world in that respect. Finally, it is evident that the growth of e-commerce and payments is expanding, even more so during the COVID 19 pandemic. A practical live study in form of a survey and field interviews about the diversity/limitations of various modalities of financial services of the Postal Savings Bank of Kosovska Mitrovica, only showed a growing trend of contactless payment method versus cash payment, with all the weaknesses and limitations that accompany the development of various payment methods at this branch office. From a health point of view, this means that a trend or choice of a safer payment model is growing, but that is still in its infancy. This only leaves a question for some further research on that topic in perspective.

REFERENCES

[1] Khalek Y.A., and Bakri A. (November 2017): The E Banking in Emerging Markets, International Journal of Development Research, Vol 07, Issue 11, pp.17186-17192, downloaded: https://www.journalijdr.com/sites/default/files/issue-pdf/11192.pdf Date of access: 20/05/2020

[2] Sundarraj R.P and Wu J. (2005), "Using Information - Systems Constructs to Study Online - and Telephone-Banking Technologies", Electronic Commerce Research and Applications, Vol.4 No.4, pp.427-443.

[3] Daniel, E. (1999), "Provision of Electronic Banking in the UK and the Republic of Ireland", International Journal of Bank Marketing, Vol.17 No.2, pp.72-82.

[4] Mols N.P. (2001), "Organizing for the Effective Introduction of New Distribution Channels in Retail Banking", European Journal of Marketing, Vol.35 No.5-6, pp.661-686.

[5] Dootson, P., Beatson A. and Drennan, J. (february 2016), "Financial Institutions Using Social Media – Do Consumers Perceive Value?", International Journal of Bank Marketing, Vol. 34 No.1, Emerald publishing, pp.9-36

[6] Ilić, N. M., Spalević, Ž. and Veinović, Mladen. (november 2015). E - Banking Application and Security, Conference: Sinergija, in Bijeljina, Bjeljina, Vol. 16 No. 1, pp.113 downloaded: https://www.researchgate.net/publication/289525272_Elektronsko_bankarstvo_-Primena_i_Sigurnost, Date of access: 20/08/2020

[7] Samonagesh, V., Ganesh, S., M. Sathish, M. T. (Avgust-October 2020). Impact of Covid-19 Outbreak in Digital Payments, International Journal for Innovative Research in Multidisciplinary Feld, Volume 6, Issue 8, pp.159 downloaded: (PDF) Impact of Covid-19 Outbreak in Digital Payments (researchgate.net) Date of access: 24/08/2020

[8] https://www.cnbc.com/select/mastercard-survey-contactless-payments/

[9] https://newsroom.ucla.edu/releases/covid-19-through-air-contaminated-objects Date of access: 05/06/2020

[10] Doremalen, V. N., Bushmaker, T., Morris, H. D., Holbrook, G. M., Gamble, A., Williamson, N. B. (March 2017, 2020). Aerosol and Surface Stability of SARS-CoV-2 as Compared with SARS-CoV-The New England Journal of Medicine downloaded: https://www.nejm.org/doi/pdf/10.1056/NEJMc2004973, Date of access: 24/04/2020

[11] https://www.newindianexpress.com/states/kerala/2020/mar/22/atms-pos-machines-remain-hotspots-of-virus-transmission-2120098.html, (Date of access: 10/08/2020)

[12] https://www.wunc.org/post/new-coronavirus-can-live-surfaces-2-3-days-heres-how-clean-them (Date of access: 05/04/2020)

[13] G. Kampf, D. Todt, S. Pfaender, E. Steinmann, (February 6, 2020) "Persistence of Coronaviruses on Inanimate Surfaces and Their Inactivation with Biocidal Agents", Journal of Hospital Infection, Vol. 104, Issue 3, pp. 246–251. DOI: https://doi.org/10.1016/j.jhin.2020.01.022

[14] https://www.businesswire.com/news/home/20201124005256/en/COVID-19-Increases-Urgency-for-Banks-to-Transform-Payment-Systems-as-Digital-Payments-Soar-Finds-Research-from-Accenture (Date of access: 10/12/2020)

[15] https://www.thalesgroup.com/en/markets/digital-identity-and-security/banking-payment/cards/contactless (Date of access: 10/11/2020)

[16] https://www.emarketer.com/content/global-mobile-payment-users-2019 (Date of access: 05/03/2020)

[17] https://www.emarketer.com/chart/240924/proximity-mobile-payment-users-western-europe-2019-2023-millions-change (Date of access: 01/01/2021)

[18] https://thepaypers.com/mobile-payments/mobile-wallet-payments-to-surge-by-50-percent-in-2020--1242730 (Date of access: 05/09/2020)

[19] Annoor Awadasseid1, Yanling Wu, Yoshimasa Tanaka Wen ZhangInitial, Intial Success in the Identification and Management of the Coronavirus Disease 2019 (COVID-19) Indicateshuman – to - Human Transmission in Wuhan, China, International Yournal of Biological Sciences, 2020; 16(11), Reviev, IVYSPRING, International publisher, doi: 10.7150/ijbs.45018 pp.1856 https://www.ijbs.com/v16p1846.pdf, (Date of access: 05.06.2020.).

[20] Chin, A. W H., Chu, J. T. S., Perera, M. R.A. et al. Stability of SARS-CoV-2 in Different Environmental Conditions. Lancet Microbe, Volume1, Issue 1, (May 2020); published online April 2, pp.411 https://doi.org/10.1016/S2666-5247(20)30003-3 (Date of access: 10/07/2020)

[21] https://www.thelancet.com/cms/10.1016/S2666-5247(20)30003-3/attachment/bfda5654-ca06-42d3-8beb-5f3aa5fc2df0/mmc1.pdf, Date of access:11/05/2020, pp. 1-8

[22] https://www.dnb.nl/en/news/news-and-archive/dnbulletin-2020/dnb391390.jsp

[23] V. Radovanović, Lj. Savić, Knowledge and Innovations –Key Factors of Development and Emloyment in the Mining Companies, Mining and Metallurgy, N1, 2014, Institute Bor, https://irmbor.co.rs/wp-content/uploads/2016/12/mmebor1_14.pdf, pp.154

INSTRUCTIONS FOR THE AUTHORS

Journal **MINING AND METALLURGY ENGINEERING BOR** is published four times per a year and publishes the scientific, technical and review paper works. Only original works, not previously published and not simultaneously submitted for publication elsewhere, are accepted for publication in the journal. The papers should be submitted in both, Serbian and English language. The papers are anonymously reviewed by the reviewers after that the editors decided to publish. The submitted work for publication should be prepared according to the instructions below as to be included in the procedure of reviewing. Inadequate prepared manuscripts will be returned to the author for finishing.

Volume and Font size. The work needs to be written on A4 paper (210x297 mm), margins (left, right, upper and bottom) with each 25 mm, in the Microsoft Word later version, font Times New Roman, size 12, with 1.5 line spacing, justified to the left and right margins. It is recommended that the entire manuscript cannot be less than 5 pages and not exceed 10 pages.

Title of Work should be written in capital letters, bold, in Serbian and English. Under the title, the names of authors and institutions where they work are written under the title. The author of work, responsible for correspondence with the editorial staff, must provide his/her e-mail address for contact in a footnote.

Abstract is at the beginning of work and should be up to 200 words, include the aim of the work, the applied methods, the main results and conclusions. The font size is 10, italic.

Key words are listed below abstract. They should be minimum 3 and maximum of 6. The font size is 10, italic.

Basic text. The papers should be written concisely, in understandable style and logical order that, as a rule, including the introductory section with a definition of the aim or problem, a description of the methodology, presentation of the results as well as a discussion of the results with conclusions and implications.

Main titles should be done with the font size 12, bold, all capital letters and aligned with the left margin.

Subtitles are written with the font size 12, bold, aligned to the left margin, large and small letters.

Figure and Tables. Each figure and table must be understandable without reading the text, i.e., must have a serial number, title and legend (explanation of marks, codes, abbreviations, etc.). The text is stated below the figure and above the table. Serial numbers of figures and tables are given in Arabic numbers.

References in the text are referred to in angle brackets, exp. [1, 3]. References are enclosed at the end in the following way:

[1] Willis B. A., Mineral Procesing Technology, Oxford, Pergamon Press, 1979, pg. 35. (for the chapter in a book)

[2] Ernst H., Research Policy, 30 (2001) 143–157. (for the article in a journal)

[3] www: http://www.vanguard.edu/psychology/apa.pdf (for web document)

Specifying the unpublished works is not desirable and, if it is necessary, as much as possible data on the source should be listed.

Acknowledgement is given where appropriate, at the end of the work and should include the name of institution that funded the given results in the work, with the name and number of project, or if the work is derived from the master theses or doctoral dissertation, it should give the name of thesis / dissertation, place, year and faculty where it was defended. Font size is 10, italic.

The paper works are primarily sent by e-mail or in other electronic form.

Editorial address : Journal MINING AND METALLURGY ENGINEERING BOR
Mining and Metallurgy Institute
35 Zeleni bulevar, 19210 Bor
E-mail: nti@irmbor.co.rs; milenko.ljubojev@irmbor.co.rs
Telephone: +381 (0) 30/435-164; +381 (0) 30/454-110

We are thankful for all authors on cooperation

CIP - Каталогизација у публикацији
Народна библиотека Србије, Београд

622

MINING and Metallurgy Engineering Bor / editor-in-chief Milenko Ljubojev. - 2013, no. 2- . - Bor : Mining and Metallurgy Institute Bor, 2013- (Bor : Grafomedtrade). - 24 cm

Tromesečno. - Je nastavak: Rudarski radovi = ISSN 1451-0162
ISSN 2334-8836 = Mining and Metallurgy Engineering Bor
COBISS.SR-ID 201387788